Manufacturing of single and multilayer tablets: influence of material properties and process parameters on die filling and layer adhesion

Inaugural-Dissertation
to obtain the academic degree
Doctor rerum naturalium (Dr. rer. nat.)

submitted to the Department of Biology, Chemistry, and Pharmacy
of Freie Universität Berlin

by

MARCO BELLINI
from Garbagnate Milanese, Italy

2018

Die vorliegende Arbeit wurde von Mai 2014 bis April 2018 unter der Leitung von Prof. Dr. Roland Bodmeier im Institut für Pharmazie angefertigt.

1. Gutachter: Prof. Dr. Roland Bodmeier
2. Gutachter: Prof. Dr. Philippe Maincent

Disputation am 08.06.2018

Acknowledgements

First of all, I thank Prof. Dr. Roland Bodmeier for giving me the opportunity to be part of his research group. I am very grateful to him for the valuable support and interesting conversations we have had in these 4 years. His advice allowed me to gain valuable experience and grow both personally and as a scientist.

I am very grateful to Prof. Dr. Philippe Maincent for reviewing and evaluating my thesis.

My thanks also go to Dr. Andriy Dashevskiy, Dr. Martin Körber, Dr. Fitsum Sahle and Dr. Mathias Walther for the inspiring scientific discussions, valid suggestions and inputs along my Ph.D., which helped me to progress even in moments of standstill.

A special thank you goes to Dr. Sven Staufenbiel, Marina, Marius and Miriam for correcting parts of this thesis and providing important feedbacks and suggestions.

I thank all the present and former members of the research group with whom I spent fun moments, in particular Frederike, Marina, Marius, Miriam, Prutha and Reza for their lovely friendship and infinite support, and Luisa for having been an amazing lab-mate, a pleasant discussion partner and a valuable advisor.

I thank Mrs. Eva Ewest, Ms. Gabriela Karsubke, Mr. Andreas Krause and Mr. Stefan Walter for the great support and generous assistance in numerous issues related to the laboratory.

I am infinitely grateful to my girlfriend Faustine for her love, the immense patience and support in all the difficult moments of these 4 long years.
My sincere thanks go to Andrea, Davide and Massimiliano for having been wonderful and supporting friends despite the distance, and to Antonio and Francesco for creating a friendly atmosphere and being great confidants.

Finally, my gratitude goes to my parents and to my family who have given me the great opportunity to achieve this academic qualification; their endless support and advice helped me through these years. Grazie!

Table of contents

1. Introduction

1.1. Tablet manufacturing

Tableting is the densification process, in which a loose powder is turned into a coherent mass (*i.e.* tablet), by molding or compaction. This manufacturing process is vastly used in the pharmaceutical industry, accounting almost 70% of the oral dosage forms produced for human use [1] (Fig. 1). Tablets popularity is ascribed to the inexpensive and simple manufacturing process, longer stability, ease in dispensation and administration, compared to other dosage forms [2]. Furthermore, tablets have great versatility in formulation design, allowing the achievement of immediate or modified release profiles. A combination of immediate and modified release patterns is also possible, but it requires a multilayer design. This approach grants therapeutic advantages, such as the achievement of optimal drug blood concentration, the effective treatment of local diseases and the reduction of daily administrations, hence an improvements in efficacy, safety and patient compliance [3,4].

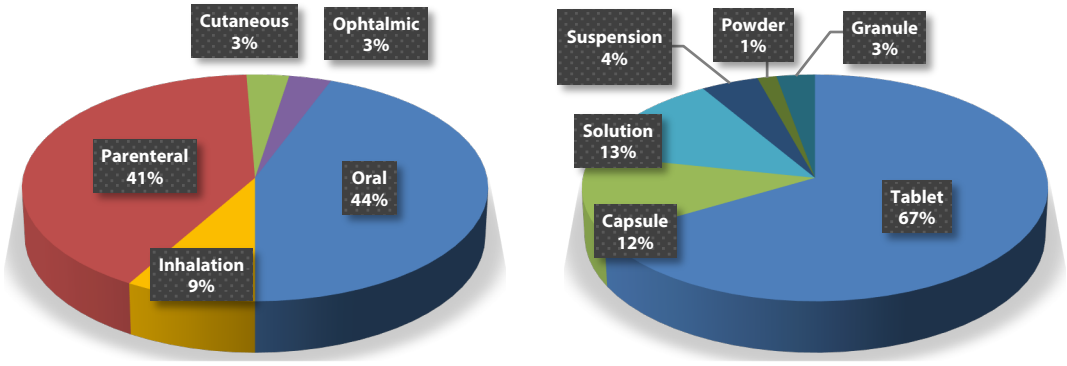

Figure 1. Route of administration of new drug approved by FDA in 2017 [5].

1.2. Physics of tablet manufacturing

1.2.1. Mechanism of particle consolidation

Tablet compaction is the most common manufacturing technique and involves the use of tablet presses, in which a normal force or pressure is applied on loose powder in a confined space. Different stages have been identified in this process [6,7]:

- Rearrangement
- Particle deformation/fragmentation
- Compaction
- Relaxation

As the pressure is increased, powder particles move within the die to occupy existing particle voids, and results in a close packing structure, causing a volume reduction. Once no more space is available for rearrangement, particles undergo to reversible elastic deformations and particles suffer permanent deformations, as the elastic limit of the material is exceeded, the deformation become permanent.

Depending on the plastic or brittle nature of the material or blend, plastic deformation or particle fragmentation may occur (Fig. 2) [8,9].

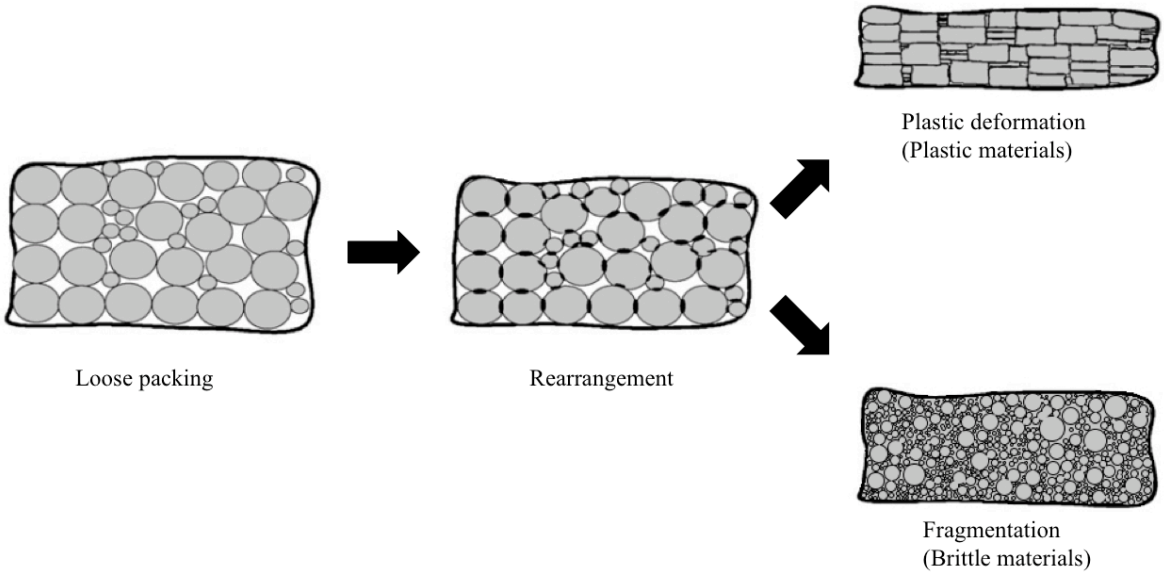

Figure 2. Stages of the consolidation mechanism for plastic and brittle material tablets (adapted from [10]).

As the densification progresses, particles are tightly packed and new surfaces are formed through fragmentation or plastic flow, resulting in an increase of contacts between particles. At this stage,

inter-particular bonds are formed through interatomic forces, local fusion bonding and particle interlocking [11]. At the end of the compaction cycle, pressure is removed and the tablet is subjected to elastic relaxation [12,13].

1.2.2. Plasticity and brittleness

The physical from of a material, whether amorphous or crystalline state, have a strong impact on tableting process [14]. Amorphous materials have a plastic behavior [15], behave elastically and linearly as long as the stress does not overcome the yield point (or elastic limit). Once the material is compressed above its elastic limit, particles undergo to permanent deformations [16]. In contrast, crystalline materials have a brittle behavior, characterized by particle fragmentation without any significant plastic deformation, once subjected to compressive stress [16]. Crack propagation and fracture mechanics promote the generation of new bonding surfaces, which improves the tablet strength [17]. Therefore the original particle size of brittle materials has less importance towards tablet consolidation, compared to low fragmenting plastic materials [18].

The minimum stress level required by a material to deform plastically is defined yield stress (*i.e.* pressure, in case of the tableting process) and represents the material resistance to densification [19]. The measurement of this value is the most common method to characterize material plasticity and brittleness and it is calculated as the reciprocal of the slope K in the Heckel equation:

$$Eq.1 \qquad \frac{1}{1-E} = KlogP + A$$

where E is the tablet porosity, K and A are constants specific for the material under compaction and P is the compaction pressure in MPa [20].

Studies have vastly reported that the yield pressure of plastic materials falls in the range 40-135 MPa. Above this range, the main consolidation mechanism is particle fragmentation and materials are considered as brittle [21–23].

1.2.3. Powder flow properties

Powder flow is the relative movement of bulk particles among loose powders or along the container wall surface [24] and depends on the equilibrium between forces promoting and preventing the flow itself [25]. Gravitational and external mechanical forces promote the powder flow and are affected by several factors, such as inclination of the powder bed, particle mass and true density. In contrast, surface interactions and frictions, adhesive and cohesive forces prevent the particle flow. The extent of these forces depends on both chemical and physical particle properties, *i.e.* particle size and surface, size distribution and shape [26,27], moisture content [28], surface energy and chemical composition [29].

The flowing behavior has a critical role in tablet manufacturing during powder mixing, blend transfer and die filling, and each step have influence on the quality of the final product [2]. In literature, several flow characterization techniques are available and have been successfully employed to evaluate powders and formulations, *i.e.* static and dynamic angle of repose [30], Hausner ratio [31], flow through an orifice [30], ring shear tester [32] and powder rheology [33]. Most of these techniques focus on specific aspects of the powder flowability and correlations between tapped density measurement, orifice flow, angle of repose and avalanching behavior have been reported in literature [34–36]. These methods can predict the powder behavior during mixing and tableting [27] and some attempts have been conducted to correlate the powder flow to die filling on industrial rotary presses [37]. Among these methods, the characterization through a powder rheometer is a recent and uprising technique. The powder rheology is measured by spinning a metal blade along a helical path through the test sample in a glass cylinder (Fig. 3).

Figure 3. Schematic diagram of the powder rheology measurement technique (adapted from [33]).

Samples are conditioned to a constant rheological state by gently spinning the metal blade through the powder and a reproducible packing density is achieved [27]. Afterwards, cycles of conditioning-test sequence are performed moving swiftly the blade through the powder sample to disturb the rheological state. Torque and force needed to displace the blade are recorded and employed to calculate rheological properties, correlated to powder flowing behavior.

1.3. Tablet manufacturing

1.3.1. Eccentric presses

Eccentric tablet presses are single punch machines employed in development and manufacturing, widely in use before the introduction of rotary presses in mid-1980 [38]. These presses are still in use in early formulation development and for low-volume production of complex multilayer tablets [2]. The press is equipped with stainless steel tooling (*i.e.* die, upper and lower punches) coupled with an eccentric mechanism and driven by an electrical motor. The production cycle consists of die filling, compaction and ejection steps (Fig. 4).

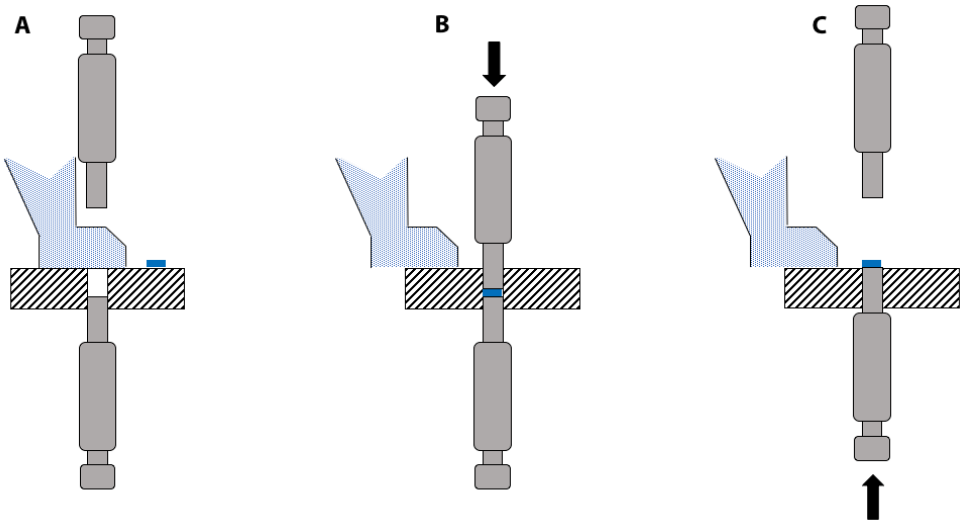

Figure 4. Operating cycle of an eccentric tablet press:(A) die filling, (B) compaction and (C) ejection steps (adapted from [2]).

As the feed shoe moves across the die opening, the die is filled with the powder blend by gravitational force (Fig. 4 A). Afterwards, the feed shoe is retracted and the upper punch penetrates into the die to compact the powder, while the lower punch stays stationary (Fig. 4 B). After compaction, the upper punch is retracted and the lower punch is raised to perform the ejection (Fig. 4 C). As a new cycle starts, the tablet is moved away from the feed shoe.

1.3.2. Rotary presses

Rotary presses are modern and fast machines, which allow high-volume production up to 1 million tablets per hour, depending on complexity of the product, size and number of equipped tooling [39,40]. Die and punches are mounted on a rotating turret and pass through four stations: filling, pre-compaction, main compaction and ejection (Fig. 5).

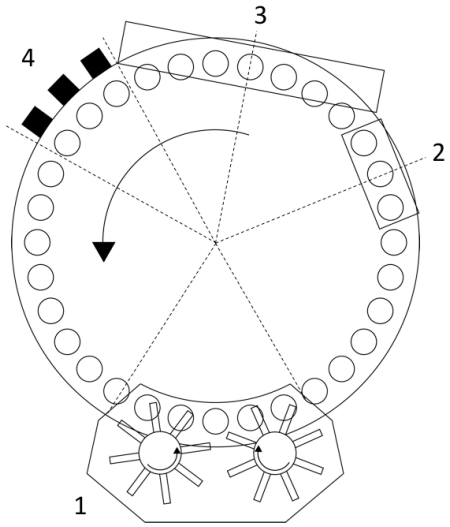

Figure 5. Rotary tablet press (top view): (1) Feeding, (2) pre-compaction, (3) main compaction and (4) ejection stations (adapted from [2]).

The die filling is performed by a feed frame, connected to a mass flow hopper: the lower punch reaches its lowest position prior the filling station and the filling process occurs as the dies moves across the feed frame. This process is promoted by gravity or forced with a single or double rotating impeller [37,41]. To promote the powder motion, the punch can be lowered during the movement across the feed frame to generate vacuum (*i.e.* suction fill technique) [42]. The success of the filling process depends on the feed frame geometry, the turret rotation speed and the fill technique in use [43–45]. To achieve the desired weight and improve the completeness of die filling, the die could be overfilled via lowering the punch further then needed. Before leaving the feed frame, the punch is raised by a dosing cam, to expel the excess of powder and achieve the desired weight.

The compaction phase is performed in two steps: pre-compaction and main compaction. At first, a low compaction pressure (*i.e.* pre-compaction) is applied to reduce the powder volume and remove the excess of air within the particles. As the punches travel through the compaction rollers, the main compaction pressure is applied to consolidate the powder into a coherent tablet. In contrast to the eccentric press mechanism, both punches of a rotary tablet press exert the

compaction pressure, resulting in a more homogeneous pressure application and tablet density [46]. Eventually, the lower punch is raised to eject the tablet out of the die.

On a standard rotary press, each tooling produces a single tablet per each revolution and the press production rate depends solely on press speed. This process is defined "single-sided production operation" and is often directly connected to in-line packaging machines. However, most of the modern machines have a double-sided production configuration and are equipped with two filling and compaction station (Fig. 6 A) [39,40].

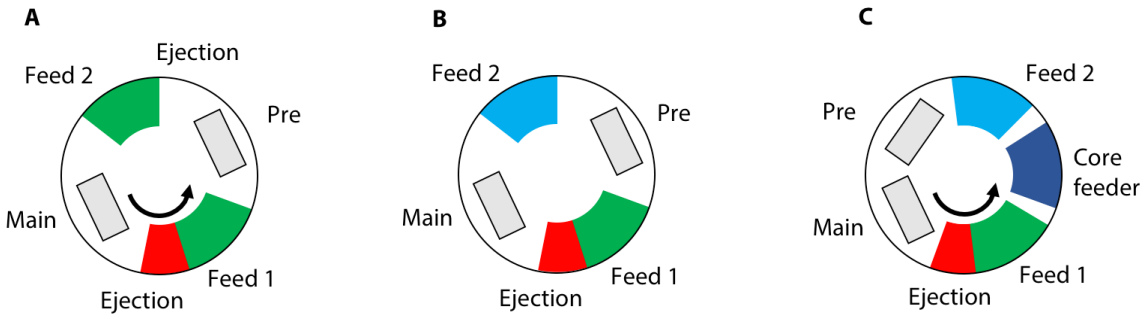

Figure 6. Schematic representation of (A) double-sided production operation, (B) bilayer production operation and (C) press coating production operation: feeding (Feed 1 and 2), pre-compaction (Pre), main compaction (Main), and ejection stations (adapted from [2]).

This configuration doubles the production rate for each revolution, for constant press speed and number of installed tooling. Furthermore, this press design versatility allows more complex manufacturing processes, such as multilayer tablets (Fig. 6 B) and press-coated tablets (Fig. 6 C), at the cost of a lower production rate.

1.3.3. Multilayer technology

In the last two decades, FDA and EMA approved several multilayer tablets as drug combination or as controlled drug delivery system (Table 1). The great rise of interest in this technology is ascribed to multiple advantages these systems grant, such as the combination of incompatible APIs to avoid undesired APIs degradation [47–49] and the association of multiple APIs in a single dosage unit, thereby improving patient compliance and efficacy [50,51], due to their synergistic effect [48]. Furthermore, a multilayer design allows the combination of different release profile patterns, thereby improving the efficacy (*i.e.* IR/ER) [52–55] with potential extension of patent protection through reformulation [56].

Beside the aforementioned advantages, the multilayer technology presents several challenges that formulation scientists have to overcome to deliver a safe product and a robust manufacturing process. The major problem occurring in formulation development is the tendency of multilayer systems to delaminate [55]: tablets without a sufficient layer adhesion tend to separate into individual layers during manufacturing or packaging processes [57]. Moreover, temperature and humidity during storage have a strong impact on long term physical stability [58]. The current manufacturing technology have some technical limitations concerning potential layers cross contamination [59,60], inaccurate individual layer weight control [61] and large tablet size, which can impact the swallowability of the dosage unit.

Table 1. FDA- and EMA-approved products with multilayer technology (1998-2018).

Trade name (Company)	Therapeutic agent	Therapeutic area	Rational for bilayer technology
Actoplus MET XR (Takeda)	Pioglitazone/Metformin hydrochloride	Type 2 diabetes	IR/ER
Aerinase (MSD)	Desloratadine/Pseudoephedrine sulphate	Allergic rhinitis	IR/ER
Amaryl M SR (Sanofi)	Glimepiride/Metformin hydrochloride	Type 2 diabetes	IR/ER
Atripla (Gilead Sciences)	Efavirenz/Emtricitabine/ Tenofovir disoproxil fumarate	HIV/AIDS	Incompatibility
Cardura XL (Pfizer)	Doxazosin mesylate	Benign prostatic hyperplasia	Osmotic pump (push-pull)
Cipro XR (Bayer)	Ciprofloxacin	Urinary tract infections	IR/ER
Clarinex-D (MSD)	Desloratadine/Pseudoephedrine sulphate	Allergic rhinitis	IR/ER
Cokiera (AbbVie)	Dasabuvir/Ombitasvir/Paritaprevir/Ritonavir	Chronic Hepatitis C	IR/ER
DuoPlavin (Sanofi)	Clopidogrel/Acetylsalicylic acid	Acute Coronary Syndrome	Incompatibility
Duetact (Takeda)	Glimepiride/Pioglitazone hydrochloride	Type 2 diabetes	Incompatibility
Euratesim (Alfasigma)	Piperaquine tetraphosphate/Artenimol/ dihydroartemisinin	Malaria	Incompatibility
Glucotrol XL (Pfizer)	Glipizide	Type 2 diabetes	Osmotic pump (push-pull)
Incresync (Takeda)	Alogliptin/Pioglitazone	Type 2 diabetes	Incompatibility
Janumet XR (MSD)	Sitagliptin/Metformin hydrochloride	Type 2 diabetes	IR/ER press-coated
Juvisync (MSD)	Sitagliptin/Simvastatin	Type 2 diabetes	Incompatibility
Kinzalkomb (Bayer)	Telmisartan/Hydrochlorothiazide	Hypertension	Incompatibility
Lexxel (AstraZeneca)	Enalapril maleate/Felodipine	Hypertension	Press-coating
Lodotra (MSD)	Prednisone	Rheumatoid Arthritis	Press-coating
Mucinex D (Adams Laboratories)	Guaifenesin/Pseudoephedrine	Expectorant	IR/ER
Pritor Plus (Boehringer-Ingelheim)	Telmisartan/Hydrochlorothiazide	Hypertension	Incompatibility
Procardia XL (Pfizer)	Nifedipine	Hypertension	Osmotic pump (push-pull)
Tredaptive* (MSD)	Laropirant/Niacin	Atherosclerosis	IR/ER
Treximet (Pernix Therapeutics)	Sumatriptan/Naproxen sodium	Migraine	Incompatibility

*withdrawn from the market

1.3.4. Problems occurring in manufacturing

Tablet defects are a major problem in tablet manufacturing and occur as visual cracks on the tablet surface, resulting in a potential product failure [2]. Beside cosmetic rationales, cracks can undermine the efficacy and stability of the dosage form, in particular for modified-release tablets with multilayer or press-coated design. These defects ranges from horizontal detachment of the tablet upper portion, defined "capping" (Fig. 7 A) [62], to cracks formation within the body of the tablet, in a process called "delamination" (Fig. 7 B) [63,64].

A **B**

Figure 7. Tablet presenting (A) capping or (B) delamination [65].

Multilayer tablets are particular susceptible to the latter since they are prone to separate in two individual layers. Elasticity is suggested as the main cause of tablet defects. Indeed, the elastic recovery occurring after compaction has a remarkable negative effect on the formed bonds: the stored elastic strain causes internal stresses and promote the bonding rupture, leading to a strong decrease in tablet mechanical strength [66,67]. This phenomenon is enhanced by air entrapment in the die during the compaction phase. Indeed, large residual air pockets can store enough elastic energy to promote cracks formation during decompression [68].

Capping occurrence is reported as proportional to the press speed, because the increase in press speed is often followed by a remarkable increase in elastic energy [69]. Furthermore, the punch shape has an important role on the occurrence of tablets defects and convex tablets are more prone to capping [62].

1.4. Process parameters in tablet manufacturing

1.4.1. Single layer tablets

The optimization of manufacturing parameters is critical to achieve a successful manufacturing process and to ensure a high-quality product. Modern presses allow precise adjustment of fill volume, punch gap during the compaction phase and press speed [2].
The fill volume is the volume of powder filled during each cycle. It influences the tablet mass and depends on the position of the lower punch during filling step. Since this process depends on powder bulk volume, flow properties have a large impact on the final tablet mass value and variability. Fill volume optimization takes in account material bulk density and powder flow properties to constantly achieve the desired tablet weight.

The punch gap is the distance between the punch tips at the maximum compaction pressure and is adjusted as penetration depth in the die of both upper and lower punches. It determines the final tablet thickness, porosity and hardness [70], therefore the optimization of this parameter is critical to achieve the desired physical properties and release profile. The compaction process is often subdivided in two steps: pre-compaction and main compaction. The extent of the pre-compaction is generally 10-20% of the main compaction and it is used to remove air pockets in the loose powder, reducing lamination and capping occurrence [70]. Instead, the main compression is responsible of the formation of a coherent mass and has direct effect on porosity hardness and friability.

The press speed represents the number of revolution executed within one minute and it has an impact on both production rate and final quality of the product. The bonding mechanism of plastic materials involve particle deformations (or plastic flow) and requires time to create enough contact surfaces and bonds for a strong and coherent tablet [71,72]. In contrast, materials which consolidate by brittle fracture have high yield pressures and offer the same resistance to deformation at any press speed. Indeed, the particle fracture is not a time-dependent process and it occurs at the same extent during each compaction cycle, irrespective of the press speed [23,69]. The main challenge encountered during the production scale up of tablet formulations is the increase of rotation speed. Due to experimental constraints, this topic has been investigated in separate tests to evaluate the effect of press speed on die filling and dwell time. The filling process can be directly evaluated on a commercial tablet press [73] or simulated on a model-shoe system [74], which allows the study of complex pattern of feeder motion through shakings and vibrations. This technique simulates the gravity fill as the feeder shoe moves across the die opening, and other filling techniques are available *e.g.* agitation filling or suction fill.

In contrast, compaction simulators can replicate the punch movement of industrial tablet presses at any manufacturing condition [75]. The tests are performed on small batches to reduce the material consumed and screen several different formulations. However, to date no attempt to evaluate the effect of press speed on die filling and compaction properties was combined on a compaction simulator.

1.4.2. Multilayer layer process parameters

The consolidation of single layer tablets occurs through the generation of interatomic forces, local fusion bonding and particle interlocking [11]. The same mechanisms are also responsible for the consolidation of multi-layered tablets, but this process requires enough surface area to build a strong interaction between the particles of different materials.

As previously discussed (cf. 1.4.1.), pre-compaction has a potential effect to prevent the delamination occurrence and its use is recommended in multilayer tableting before the die filling of the second layer. However, an excessive first layer compaction pressure determines an insufficient interface roughness for the layers interaction and leads consequently to process failure [47,59,76]. The optimization of pre-compaction pressure is therefore critical to promote the interfacial adhesion through particle interlocking and surface bonding [77]. The occurrence of insufficient surface roughness of the first layer is particularly pronounced for high compactible materials, such as microcrystalline cellulose [78,79]. Indeed, a high compaction pressure applied on the first layer of these materials results in a remarkable decrease in available nesting sites for the particles of the second layer. Despite the negative effect of first layer compaction, a minimum tamping pressure is strongly recommended to avoid any uncontrolled mixing during the second filling and the formation of uneven interfaces at high production speed, due to centrifugal forces [60].

Therefore, the layer sequence has to be optimized based on material properties and layer ratio. Bilayer tablet formulation with layer ratio of 1:3 or higher did not present a significant impact of layer weight disproportion on the layer adhesion [80]. However, due to mechanical limitations, current available bilayer presses do not offer the possibility to produce tablets with a first layer smaller than the second one [61].

The main compaction pressure has a primary role towards tablet hardness [70] and layer adhesion [47]. Higher compaction pressures provide greater energy available for particle interaction, particle fracture and surface bonding. This effect is suggested to be dependent on the layer materials: the increase of main compaction pressure determines a linear increase of the interfacial

adhesion when plastic materials constitute the first layer of the tablets [77]. The retained plasticity allows the second layer to penetrate into the first one, and mechanical interlocking increases the bonding. An opposite trend is observed when the first layer is constituted of brittle materials.
The transmission of the compaction pressure through the powder changes depending on the material properties: particles deformation occurs at greater extent in the lower central region of the die than at the outer radial areas. The stress in compaction acts primarily in a downward central direction, due to the presence of wall frictions, which reduces the vertical movement of the particles in contact with the die. A region with lower density was observed at the outmost part of the layers interface, hence resulting in a lower layer adhesion. The combination of radial stress concentration and lower adhesion results in higher delamination tendency [81].

The effect of press rotation speed on the consolidation mechanism of single layered tablets has been extensively investigated [22,78,82]: a lower rotation speed determines a longer dwell time and results in a better consolidation. However, no remarkable changes in layer bonding strength were reported during testing of multilayer tablets, in particular when the second layer material was plastic [77]. This process parameter was, however, investigated in the range of 10-20 RPM, therefore not representative of the standard conditions at industrial scale, where speed may become a critical factor on larger tablet presses.

1.5. Delamination characterization

Insufficient layer adhesion is the cause of delamination in multilayer tablets, which occur as separation of the tablet into individual layers. This problem represents the main challenge to obtain a reliable manufacturing process for multilayer tablets and have great impact on product efficacy and safety. Therefore, the characterization of delamination tendency is the first important step for the mechanistic understanding of layer adhesion and its evolution over the time, which is critical towards the optimization of formulation and manufacturing process [83].

To date, few methods have been proposed for this measurement and they are categorized depending on the degree of sample alteration, whether permanent or not. Destructive methods are carried out to the specimen failure and they differ mainly in the direction of force application, *i.e.* normal stress or shear stress. This difference consequently leads to unequal results. Hence, a standardized method is currently missing. In contrast, non-destructive methods rely on various imaging techniques to investigate the state of the bilayer interface and identify cracks, but they require specific equipment and expertise to process and explain the results. Furthermore, the indirect nature of the tablet measurement requires a correlation to physical properties to give data relevant in bilayer tablet characterization.

1.5.1. Destructive methods

1.5.1.1. Tensile stress test

The test is performed through the application of a tensile stress to sample failure [79]. Each tablet is beforehand attached to metal plates with a cyanoacrylate-based super glue and the sample is mounted on a dynamometer. A constant tensile stress is applied and the resulting resistance (or force needed to separate the tablet in two layers) is measured (Fig. 8).

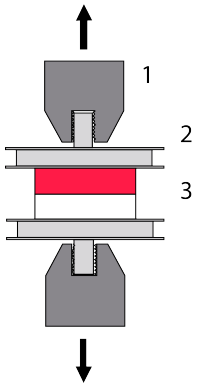

Figure 8. Tensile stress test: (1) clamps, (2) metal stubs and (3) bilayer tablet.

This type of measurement is easy to perform and yields unambiguous results, because the tensile stress is uniformly distributed on the layer interface. However, it requires a long setup time compared to other methods and it may result in an incomplete layer separation [83], if the adhesion between layers is stronger than the intra-layer cohesion.

1.5.1.2. Shear stress test

In this test, the stress is applied parallel to the layer interface to sample failure. The sample is fixed with two metal screws on a modified hardness tester and a shear stress is applied sideways on the protruding layer (Fig. 9) [84,85]. The force application allows a closer simulation of the stresses on tablets during production, packaging and transportation. Although the shear force is more relevant towards the real tablets behavior, the poor understanding of stress distribution at the interface during the test make the test result explanation complex [83]. Furthermore, the results of this method are biased by the friction exerted by the metal screws.

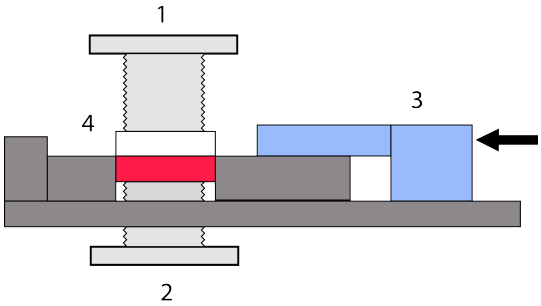

Figure 9. Shear stress test: (1) fixing screw, (2) adjusting screw, (3) Monsanto hardness tester and (4) bilayer tablet.

1.5.1.3. V-shape punch breaking test

The sample is positioned on a V-shaped metal support with an opening angle of 90° and depth of 6 mm. A punch with a round-shaped tip applies a normal stress at the layers interface to sample failure and the breaking force is measured as peak of the force-displacement curve (Fig. 10) [86].

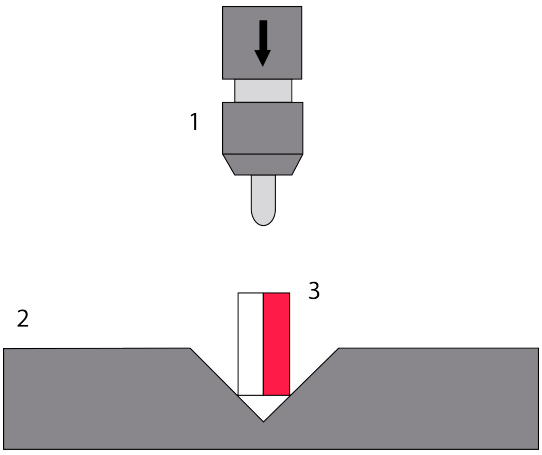

Figure 10. V-shape breaking test: (1) punch, (2) V-shaped support and (3) bilayer tablet.

This test has similar advantages and disadvantages of the shear stress test, but the different design provides a measurement without friction. Furthermore, the application of the stress directly at the layer interface promotes the delamination rather than an incomplete layer separation. However, this test does not simulate stresses and vibration typical of manufacturing, handling and packaging processes and requires a correlation to give data relevant in bilayer tablet characterization.

1.5.1.4. Three-point bending test

This test requires the preparation of specific bilayer rectangular specimens, with large dimensions. The sample is positioned on two cylindrical supports and a round-shaped punch applies a constant normal stress at the layers interface causing sample bending and complete separation in two layers (Fig. 11) [87,88].

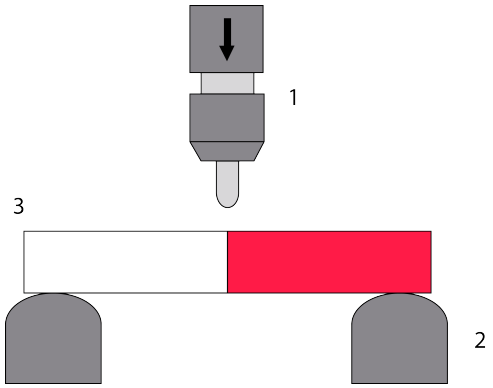

Figure 11. Three-point bending test: (1) punch, (2) cylindrical supports and (3) bilayer specimen.

This method measures the maximal normal stress needed to separate the sample in half. However, the method requires large size specimen, therefore not suitable for expensive materials.

1.5.2. Non-destructive methods

1.5.2.1. Air-coupled acoustic measurement

This method is a non-destructive imaging technique to characterize tablet surfaces and interface, applying vibrations through acoustic stimuli. A bilayer tablet is positioned between an air-coupled transducer and a laser interferometer. The transducer provides out-of-plane acoustic vibrations to excite the sample in several vibration modes (or harmonics). Sample oscillations are acquired by a laser interferometer, digitalized and processed by spectral analysis, using the fast Fourier transform algorithm [57].

This technique is able to identify mechanical defects (*i.e.* cracks, lamination, and capping) and is applicable to different tablet shapes and types.

1.5.2.2. Terahertz pulsed imaging

This technique is a non-invasive imaging technique, which employs terahertz radiations in the range 3-100 cm^{-1} to characterize material properties of multi-layered structures. A laser unit generates impulses with extremely short duration (130 fs) and the laser beam is split into two parts by a polarizing cubic beam splitter. One beam is directed against the sample and the scattered radiation is reflected by a mirror to combine with the not-scattered beam. Eventually, the radiation is detected, digitalized and processed [89–91]. The technique is able to identify different interfaces in the tablet and eventual mechanical defects.

1.5.2.3. X-ray micro-computed tomography

X-ray μCT is a volumetric imaging technique used to determine the material density, based on the intensity attenuation of a radiation as is passes through the specimen. The sample is positioned on a rotating support, between a micro-focal energetic source and a charge couple detector. The tablet is targeted with X-rays and a detector measures the local intensity of the diverging radiations transmitted through the specimen. The X-ray attenuation is calculated based on the Lambert-Beer law and the radiographs (or projection images) are used to reconstruct a 3D-representation of the sample structure [63,79,92].

1.6. Compaction simulators

The compaction simulator is a single-station press, specifically designed to reproduce the cycle of any tableting process in real time and to record the relevant process parameters [75]. A stainless-steel frame ensures stiffness and robustness at high load compaction. The punches are mounted on two actuators (*i.e.* upper and lower) and are equipped with high accurate piezoelectric load cells and linear variable displacement transducers (LVDT) to measure force and displacement, respectively (Fig. 12).

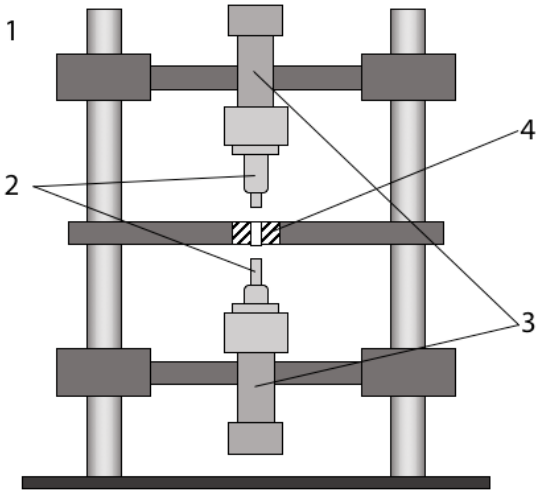

Figure 12. Schematic diagram of a compaction simulator: (1) loading frame, (2) upper and lower punches, (3) upper and lower actuators and (4) die (adapted from [93]).

Recorded data are sent to a control unit, which elaborates the output signal and drives the punches accordingly to the requested profile. Depending on the machine type, the actuators are powered by an electrical motor or by a hydraulic pump.

The press simulation is achieved either by position or by load control. In the first mode, punches are driven to simulate the real punch displacement of any given tablet press. The displacement-time profile is calculated based on the angles between the press stations (*i.e.* die filling, compaction and ejection) and the Rippie-Danielson equation:

$$Eq.2 \qquad z = \sqrt{[(r_1 + r_2)^2 - (r_3 sin\omega t - x)^2]}$$

where z is the vertical punch displacement, r_1 is the radius of the compaction roller, r_2 is the radius the vertical curvature of the punch head rim, r_3 is the radial distance between the turret

center and punch center, x is the horizontal distance between the center of the upper punch and the center of vertical curvature of the punch head rim, t is the time and w is the turret angular velocity [94].

Instead, in load control mode the punch movement follows a custom force-time profile, which rarely replicates a real press profile [95]. This mode is largely used in material testing to determine the physical and mechanical properties of raw materials, such as compactability, compressibility, elastic recovery and Yield pressure [78].

The understanding of the compaction mechanism and powder behavior is important to promote a faster formulation development [2]. The use of a compaction simulator allows, on the same device, optimization of process parameters, scale-up and trouble-shooting of batch problems [96]. Furthermore, robust tablet formulations for phase I studies can be developed with a small amount of drug and material [23].

High cost of device and maintenance, and the required high expertise to operate the machine and explain the results are main disadvantages of the compaction simulator use.

1.6.1. Mechanical compaction simulators

In mechanical simulators, a single punch is driven by a planetary roller screw, an electro-mechanical actuator, which comprises a screw shaft, a nut and a variable number of rollers (Fig. 13).

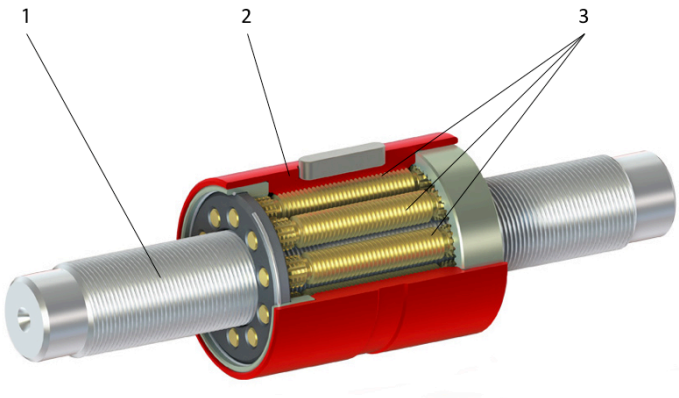

Figure 13. Schematic diagram of a planetary roller screw: (1) screw shaft, (2) nut and (3) rollers (adapted from [97]).

This actuator is positioned under the lower punch and converts the rotational motion in linear displacement (*i.e.* vertical displacement) through a rotation or a sideway displacement of the screw, which results in travel of nut-planetary roller assembly. Despite its design complexity, this

electro-mechanical actuator has large use due to high-precision, high-speed and heavy-load applications.

Mechanical simulators are generally cheaper, require less maintenance and the tablet production rate is faster (up to 25 tablets/min), compared to hydraulic systems. The maximum output of 1200 tablets/hour, make these machines are suitable for the manufacturing of clinical batches. However, the use of an electro-mechanical actuator allows a lower maximal load (50 kN) and lower punch speed limit (380 mm/s), compared to hydraulic compaction simulators.

1.6.2. Hydraulic compaction simulators

In these simulators, two hydraulic cylinders provide a unidirectional travel to punches through the use of high-pressure hydraulic fluid (*i.e.* mineral oil). An electrohydraulic servo valve transfers the fluid to the cylinders, at a pressure proportional to an electrical input signal. The variation of hydraulic pressure in the barrel results in a proportional piston travel (Fig.14).

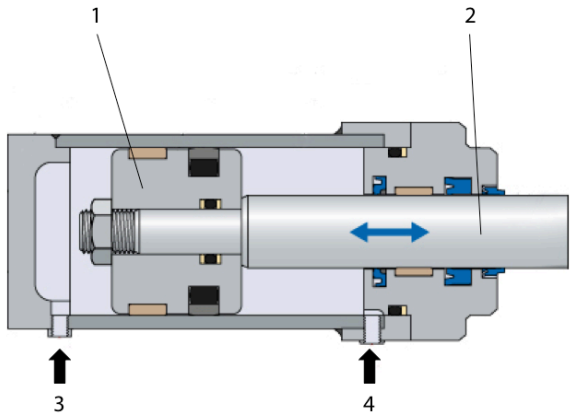

Figure 14. Schematic diagram of a hydraulic cylinder: (1) piston, (2) piston rod, (3) extend flow port and (4) retract flow port (Adapted from [98]).

Two hydraulic cylinders are connected to upper and lower punches, converting oil pressure in linear displacement. This design provides precise control of position, velocity and force at any given condition within the machine structural limit. Furthermore, it provides higher maximal force (100kN) and punch speed limit (2000 mm/s), compared to mechanical simulators. However, hydraulic systems have high cost, requires frequent maintenance and have a slow tablet production rate (up to 5 tablets/min), which is not optimal for the production of small clinical batches [23].

1.7. Research objectives

Parameters involved in the manufacturing of single layer tablets have been extensively investigated to ensure product safety and efficacy through the optimization of the tableting process. However, the achievement of a complete die filling has a great impact on the uniformity of content, in particular at high speed. To date, die filling has been investigated on a model-shoe system, which simulates the powder behavior but it is difficult to correlate with industrial scale process parameters. Only few studies have been conducted on standard rotary presses due to the high material consumption.

Process parameters of multilayer tablets manufacturing have been investigated only in separated experiments, hence the effect of process parameters interactions and material properties on layer adhesion is still unknown.

Therefore, the objectives of this study were:

- the investigation of die filling behavior on an industrial tablet press with excipients commonly used in tableting, through the replication of manufacturing process on a compaction simulator;
- the modelling of die filling process in correlation to physical and flow properties and prediction of the powder behavior in die filling;
- the development of a frictionless shear test to evaluate layer adhesion of bilayer tablets;
- the investigation on the impact of material properties, process parameters and their interactions on layer adhesion of multilayer tablets.

2. Materials and methods

2.1. Materials

Microcrystalline cellulose (Avicel PH-112 and Avicel PH-200, FMC Corp., Philadelphia, PA, USA), hydroxypropyl methylcellulose (Methocel K15M, Colorcon Ltd., Dartford, UK), lactose (Tablettose 80, Meggle GmbH, Wasserburg, Germany), spray-dried lactose (Flowlac 90, Meggle GmbH, Wasserburg, Germany), calcium phosphate dehydrate (Emcompress, JRS Pharma LP, Rosenberg, Germany), pregelatinized starch (Starch 1500, Colorcon Ltd., Dartford, UK), polyvinyl acetate/polyvinylpyrrolidone (Kollidon SR, BASF SE, Ludwigshafen, Germany), microcrystalline cellulose pellets (Cellphere CP-102, Asahi Kasei Corp., Tokyo, Japan), mannitol (Pearlitol 200 SD, Roquette SA, Lestrem, France) and magnesium stearate (Baerlocher GmbH, Unterschleissheim, Germany).

2.2. Material characterization

2.2.1. Powder particle properties

Particle size distribution of each powder was evaluated with a laser diffractometer (Helios Magic, Sympatech GmbH, Clausthal-Zellerfeld, Germany) in the range 4.5-875 μm. The particle shape was estimated by particle roundness. Pictures of particles for each powder (n > 20) were taken with an optical microscope (Axioskop, Carl Zeiss AG, Oberkochen, Germany) and digitally processed (ImageJ, NIH, Rockville, MA, US) to calculate the particle roundness as follows:

$$Eq.3 \qquad R = \frac{4A}{\pi l_{Max}^2}$$

where A is the projected area and l_{Max} is the maximum length of the single particle.

2.2.2. Powder flow properties

Flow properties of powders were determined through the Hausner ratio on a tap density tester (Erweka Tap Density Tester, Erweka GmbH, Heusenstamm, Germany), according to European Pharmacopoeia method [99]. Moisture content was measured gravimetrically with a thermal balance (Mettler Toledo LLC, HB43-s Halogen, Columbus, OH, USA). Scanning electron microscopy (Quanta 200 SEM, FEI Corporate, Hillsboro, OR, USA) was used to evaluate the morphology and roughness surface of particles.

2.2.3. Powder rheology

The rheology of powders was measured with a powder rheometer (FT3, Freeman Technology, Tewkesbury, UK), equipped with a borosilicate test vessel (Ø = 25 mm) and a metal blade (Ø = 23.5 mm). The vessel was filled with about 30 ml of powder and a preliminary cycle was performed to condition the sample to a uniform rheological state. Afterwards, the powder exceeding 25 ml was removed and 7 identical cycles of test and conditioning were performed at 100 mm/s blade speed
(n = 3)**.** Torque and force needed to spin the metal blade through the sample were measured as a function of displacement either during the upward or downward movement. The sum of these values was integrated to calculate the total energy needed to overcome the powder resistance to flow [100]. Depending on the blade speed and direction of movement, three rheological properties were measured:

1. the Basic Flowability Energy (BFE) represents the total energy measured moving the blade downward during the 7th cycle at constant speed and it was calculated as follows:

$$Eq.4 \qquad BFE = \int_0^H \left(\frac{T_d}{Rtan\alpha} + F_d\right) dH$$

where H is the blade penetration depth, R is the impeller radius, α is the helix angle formed by the impeller during its movement, T_d is the torque requested to spin the blade and F_d is the force needed to displace the blade in the sample during a downward movement [101]. This property represents the behavior of the powder in a confined space, therefore under stress;

2. the Specific Energy (SE) represents the total energy needed to move the blade upward during the 7th cycle at constant speed, normalized on the sample mass and calculated as follows:

$$Eq.5 \qquad SE = \frac{\int_0^H (\frac{T_u}{Rtan\alpha} + F_u) dH}{m}$$

where m is the mass of the sample, T_u is the energy needed to spin the blade and F_u is the force needed to displace the blade in the sample during an upward movement [102]. This property represents the behavior of the powder in an unconfined space;

3. the Flow Rate Index (FRI) is the ratio between the total energy needed to displace the metal blade at different rotation speeds. The energy is measured during the downward movement of the blade and is calculated as follows:

$$Eq.6 \qquad FRI = \frac{BFE_{\frac{10mm}{s}}}{BFE_{\frac{100mm}{s}}}$$

where $BFE_{10mm/s}$ and $BFE_{100mm/s}$ are the Basic Flowability Energy values measured after 7 cycles at 10 mm/s and 100 mm/s blade speed, respectively [102]. This property represents the powder sensitivity to a change in blade speed.

2.2.4. Elastic recovery and yield pressure measurements

Elastic recovery and yield pressure were measured on a compaction simulator (HB50, Huxley Bertram Engineering Ltd, Cambridge, UK) equipped with an 11 mm flat-faced B-type tooling. Pure excipients were compacted at 300 MPa with a force-controlled compaction profile (V-shape profile) and the increase of compaction pressure was set at 20 MPa/s. The elastic recovery was calculated as follows:

$$Eq.7 \qquad E_R\% = 100\frac{(V_f - V_{min})}{V_{min}}$$

where V_f and V_{min} are the final volume and the minimum volume of the tablets during compaction, respectively. The minimum volume was calculated from the compaction data recorded by the instrument, as punch gap measured at maximum load. These values were compensated by press- and tooling-elasticity corrections. To ensure the complete material relaxation, the tablets dimensions were measured 72 h after preparation (n = 3) with a digital micrometer (DIGI-MET, Helios-Preisser GmbH, Germany). Elastic and plastic works were directly measured on the instrument during the same compaction profiles as area under the curve on a force-displacement profile and the relative work contributions were calculated as follows:

$$Eq.8 \qquad W_P\% = 100\left(\frac{W_P}{W_T}\right)$$

$$Eq.9 \qquad W_E\% = 100\left(\frac{W_E}{W_T}\right)$$

where W_P is the plastic work, W_P is the elastic work and W_T is the total work.
The in-die Heckel plot method was applied to measure the yield pressure of each material in use [20,103].

2.2.5. Evaluation of difference in elastic recovery

Bilayer tablets were prepared on a compaction simulator (HB50, Huxley Bertram Engineering Ltd, Cambridge, UK) equipped with an 11 mm flat-faced B-type tooling, applying 15 MPa as first layer compression and a main compression ranging from 100 MPa to 300 MPa. The compression was performed as simulation of an industrial tablet press profile (Fette 3200i) at 40 RPM. The difference in elastic recovery was calculated as follows:

$$Eq.10 \qquad \Delta E_R\% = |E_R^1\% - E_R^2\%|$$

where $E_R^1\%$ and $E_R^2\%$ are the elastic recovery of first and second layer, respectively [104].

2.3. Simulation of die filling on an industrial tablet press

The simulation of the die filling on an industrial tablet press (Korsch XL800, Korsch AG, Berlin, Germany) was performed with a compaction simulator (HB50, Huxley Bertram Engineering Ltd, Cambridge, UK) equipped with 11 mm flat-faced B-type tooling. The filling process was performed with a powder feeder, refilled after the preparation of each batch to keep constant the powder height in the feeder. The filling depth was set to an arbitrary value of 10 mm and powders were compacted at 100 MPa with the purpose to obtain tablets possessing sufficient hardness to be handled and weighed. The simulation was performed at 5 different press speeds, ranging from 5 to 90 RPM, and adjusting the displacement velocity of the feeder at increasing values (Table 2).

Table 2. Calculated feeder residence time over the die and feeder velocity at different press rotation speeds.

Press speed (RPM)	Feeder residence time (ms)	Feeder velocity (mm/s)
5	1502	20
15	500	60
40	187	158
65	115	261
90	83	375

The velocity to match the feeder residence time over the die was calculated as follows:

$$Eq.11 \qquad v = \frac{2l_p}{t}$$

where l_p is the internal diameter of the powder feeder and t is the feeder residence time over the die (Fig. 15).

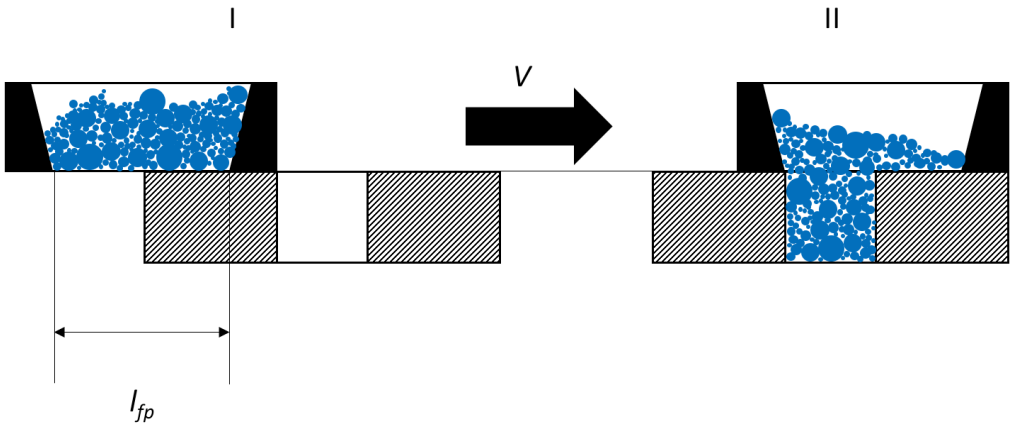

Figure 15. Die filling diagram with feeder in *I)* starting position and *II)* filling position.

The latter was calculated from the angular velocity in the uniform circular motion:

$$Eq.12 \qquad \omega = \frac{2\pi}{T} = \frac{\theta}{t}$$

where T is the period of one rotation and θ is the angle, expressed in radian, swept out in time t.

Equation 12 can be written as function of time assuming 45° as angle of filling, which is a typical value of an industrial scale tablet press (Fig. 16):

$$Eq.13 \qquad t = \frac{\theta T}{2\pi}$$

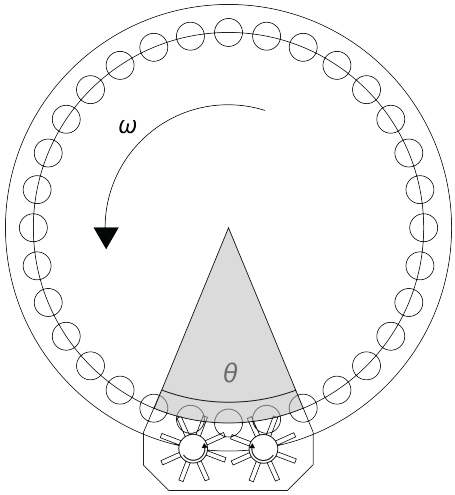

Figure 16. Vertical view diagram of a generic tablet press.

The simulation of die filling was performed with three different techniques: gravity, forced and suction fill. The completeness of die filling was evaluated as mass ratio, calculated as follows:

$$Eq.14 \qquad \Delta m = \frac{m_i}{m_{5RPM}}$$

where m_i is the average mass of 10 tablets at given press speed and m_{5RPM} is the average mass of 10 tablets prepared at the press speed of 5 RPM. A slow rotation speed was assumed as not remarkably influencing the die filling. Furthermore, the filling density was calculated as follows:

$$Eq.15 \qquad \rho = \frac{m}{V}$$

where m is the average mass of 10 tablets prepared at given press speed and V is the die volume.

2.4. Bilayer tablets preparation

The bilayer tablets were prepared on a compaction simulator (HB50, Huxley Bertram Engineering Ltd., Cambridge, UK) equipped with an 11 mm flat-faced B-type tooling, running a simulation profile of an industrial bilayer tablet press (Fette 3200i). Pure excipients were beforehand blended with 0.5% magnesium stearate for 10 min at 42 RPM in Turbula mixer (Turbula®, Willy A. Bachofen AG Maschinenfabrik, Muttenz, Switzerland). The mixing shell was filled to 33% of the total 250 mL volume, based on the bulk density of each powder, to ensure a reproducible blending through the whole set of batches. The tablets were conditioned overnight at room temperature and 40% RH and were tested 24 h after their production (n = 10). This procedure was adopted to reduce the impact of environmental conditions on mechanical properties and thereby obtaining good reproducibility of the results.

2.5. Evaluation of the shear test

2.5.1. Characterization of bilayer tablets

The layer adhesion of each tablet was measured with a custom-made shear test device (Fig. 17).

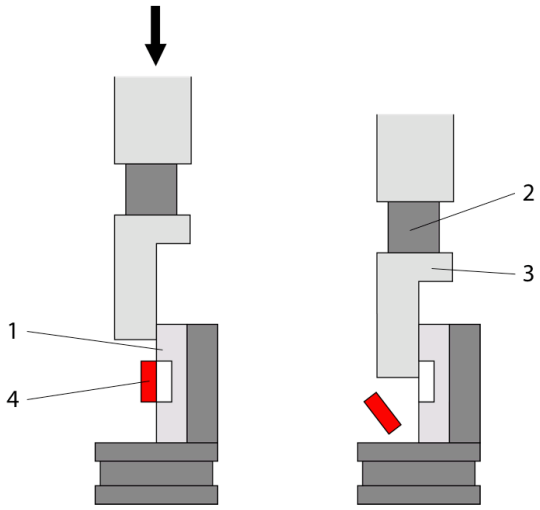

Figure 17. Shear test used to characterize the layer adhesion: (1) tablet holder, (2) load cell, (3) upper punch and (4) bilayer tablet.

The tablet was positioned in a tablet holder by means of a micrometer, so that the first layer was exposed to the custom-shaped upper punch. The tablet position was maintained fixed with a screw and slightly tightened (0.1 Nm) by means of a torque screw driver (TorqueVario-S ESD 0.1-0.6 Nm, Wiha GmbH, Schonach, Germany), avoiding undesired radial stress at the tablet interface

(Fig. 18 A). The device was then installed on the compaction simulator. The shear stress was slowly applied to specimen failure (1 mm/s rate) by a specifically designed upper punch equipped with a 1 kN load cell (Fig. 18 B). The layer adhesion value was measured as peak on the force-displacement profile.

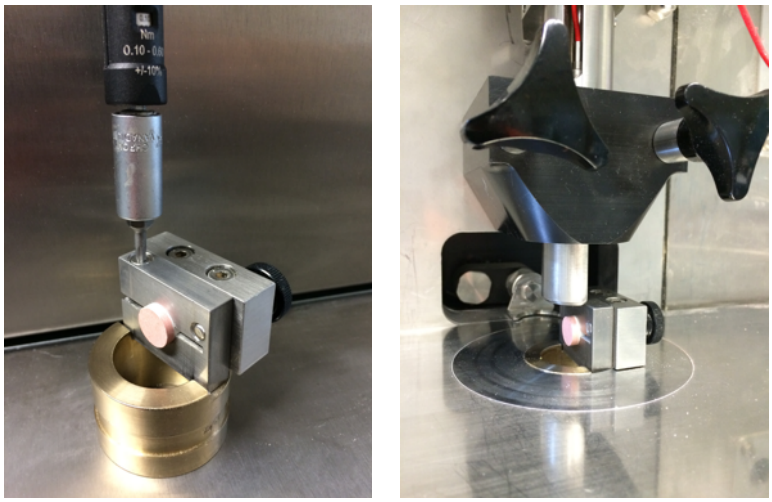

A B

Figure 18. Shear test (A) tablet holder with torque screw driver during test setup and (B) installed on the compaction simulator during a test run.

2.5.2. Excipient differentiation and test variability

In order to evaluate the feasibility of the novel method for the assessment of layer adhesion and its capability to discriminate differences due to excipients and variability between measurements, Avicel PH-200, Methocel K15M, Tablettose 80, Emcompress and Starch 1500 were selected and paired in all possible layer combinations, *i.e.* 25 batches. Lubricated powders were compacted, applying a pressure of 250 MPa and extending the dwell time to 10 s in order to reduce any potential compression speed effect (n = 10). The tablets batches were tested as described in 2.5.1.

2.5.3. Compaction pressure differentiation

To evaluate the test sensitivity to detect differences in layer adhesion on tablets produced with various compaction pressures, 4 combinations were selected: Tablettose 80-Methocel K15M, Tablettose 80-Starch 1500, Methocel K15M-Starch 1500 and Avicel PH-200-Tablettose 80. Lubricated powders were compressed at pressures ranging from 50 to 400 MPa with 100 ms dwell time and the tablet batches were tested as described in 2.5.1.

2.6. Stability Study

Avicel PH-200-Methocel K15M and Ethocel 4- Emcompress were selected as material combinations for the stability study, representing hygroscopic and non-hygroscopic combinations, respectively. Lubricated powders were compacted at 250 MPa and stored 30 days at different temperature and moisture conditions (Table 3).

Table 3. temperature and moisture storage conditions of the stability study.

Temperature	Moisture	Experimental conditions	
5°C	1%	Fridge	Desiccator with silica beads
5°C	75%	Fridge	Desiccator with NaCl saturated solution
25°C	40%	Climate chamber	
40°C	1%	Climate chamber	Desiccator with silica beads
40°C	75%	Climate chamber	Desiccator with K_2CO_3 saturated solution

The storage conditions were monitored during the experiment with a temperature and humidity logger (iButton Hygrochron DS1923, Maxim Integrated Inc., San Jose, CA, USA). Layer adhesion was measured (cf. 2.5.1.) on tablet samples (n = 5) after 1 day and every 7 days, for 5 total time-points.

2.7. Design of Experiment: effect evaluation of process parameters

The influence of pre-compression pressure (*Pre*), main compression pressure (*Main*) and turret rotation speed (*Rtn*) on layer adhesion was assessed on different excipient combinations through a 3-factors 3-level central composite Design of Experiment (Table 4).

Table 4. Central Composite Design of Experiment levels for each factor.

Parameter		-1	0	+1
Pre-compression	(MPa)	0	15	30
Main compression	(MPa)	100	200	300
Turret rotation Speed	(RPM)	20	40	60

The layer adhesion of each tablet was measured with the shear test device (cf. 2.5.1.) and the average values were used as response in the statistical analysis (n = 5). The experimental design and statistical analysis were performed with JMP® Pro 13 (SAS Institute Inc., Cary, NC, USA). The significance of the models was assessed with an ANOVA test, and the goodness of fit was evaluated through the coefficient of determination R^2.

The relationship between factors and the response variable was modelled with the following polynomial equation:

$$Eq.16 \qquad y = b + b_1x_1 + b_2x_2 + b_3x_3 + b_{12}x_1x_2 + b_{23}x_2x_3 + b_{13}x_1x_3 + b_{11}x_1^2 + b_{22}x_2^2 + b_{33}x_3^2$$

where y is the response variable (layer adhesion), x_1, x_2 and x_3 are the process parameters in dimensionless form and b, b_1, b_2, b_3, b_{12}, b_{23}, b_{13}, b_{11}, b_{22} and b_{33} are the regression coefficients.

2.8. Strain rate calculation

The movement of both punches was recorded during the compaction cycles of each Design of Experiment at low and high speed (20 RPM and 60 RPM, respectively) and used to calculate the strain on the powder material, as follows:

$$Eq.17 \qquad \varepsilon = \frac{l_0 - l}{l_0}$$

where l_0 is the initial punch gap and l is the final punch gap [16].
The strain rate was calculated as the change in strain with respect of time, as follows:

$$Eq.18 \qquad \varepsilon_{rate} = \frac{d\varepsilon}{dt}$$

where ε is the strain due to the movement of both punches and t is the time.

3. Results and discussion

3.1. Establishment of a new model to predict die filling on a compaction simulator through powder rheological properties

The progress in the technology of tablet presses during the last two decades allowed the design of rotary machines capable of large volume throughput, up to 1 million tablets per hour [105]. The high production rate requires presses equipped with large round die table (or turret) to hold several dies (usually 80 to 90) and operated at high rotation speed (up to 90 RPM). As the size of turret and tablet press increase, the punch has a longer distance to sweep, leading to a decrease in dwell time and tablet consolidation [17].

The effect of high press speed on tablet consolidation has been extensively investigated [22,77,78,82], causing low hardness and high friability, in particular for plastic materials. In fact, during the compaction of these excipients, the consolidation occurs mainly through plastic deformation, which needs a sufficient time to build inter-particular bonds and form hard tablets [106]. Mass variability due to incomplete die filling is another challenge, caused by the increase of press rotation speed [107] and results in poor content uniformity [73]. As the turret rotates faster, the feeder resides a shorter time over the die and the filling process is not complete. Therefore, powder flow properties and feeder residence time over the die become critical parameters to achieve content uniformity at high production speed [37].

As the turret rotates faster, the feeder resides a shorter time over the die and the die filling process tends to be incomplete [37]. The effect of press speed on die filling is critical in particular for poorly-flowing materials and has been investigated in separate tests. The standard approach consists in the evaluation directly on commercial tablet presses [73] or simulated on a model-shoe system [74]. This last technique allows the study of complex pattern of feeder motion through shakings and vibrations, simulating the gravity fill as the feeder shoe moves across the die opening. Alternatively, other filling techniques are available e.g. agitation filling or suction fill.
In the present study, the die filling of 9 excipients commonly used in tableting was investigated. The powders were characterized by residual moisture content, Hausner ratio, particle shape and size distribution. Rheological properties were evaluated with a powder rheometer and compared

to the particle properties. Afterwards, the die filling of an industrial tablet press was replicated with a compaction simulator at different press speeds and the impact of powder flow properties on the die filling process was evaluated. The die filling simulation was correlated to the powder rheological properties and the model equations were validated through the prediction of die filling of spray-dried mannitol (Pearlitol SD 200) and subsequent experimental confirmation.

3.1.1. Powder characterization and powder rheology

Mean particle size, particle roundness, residual moisture content and Hausner ratio were measured for 9 excipients commonly used in direct compression (Table 5).

Table 5. Hausner ratio (H_R), loss on drying (LOD%), physical and rheological properties of the excipients in use (mean ± SD, n = 3).

Excipient	H_R	BFE (mJ)	SE (mJ/g)	FRI	d_{50} (µm)	Roundness	LOD%
CP-102	1.11	149.67 ± 11.59	6.63 ± 0.87	1.306	171.07	0.849 ± 0.115	3.63
Flowlac 90	1.13	74.5 ± 1.54	6.50 ± 0.07	1.164	130.99	0.846 ± 0.147	0.77
Kollidon SR	1.13	27.13 ± 0.80	5.02 ± 0.11	1.420	60.30	0.786 ± 0.202	3.16
Tablettose 80	1.18	94.40 ± 1.92	7.71 ± 0.58	1.250	143.70	0.672 ± 0.142	0.57
Emcompress	1.21	235.00 ± 11.00	9.23 ± 0.36	1.332	219.98	0.720 ± 0.122	3.38
Avicel PH-112	1.26	53.90 ± 12.85	8.22 ± 0.72	1.334	108.91	0.663 ± 0.233	3.57
Avicel PH-200	1.33	100.03 ± 8.42	11.13 ± 0.20	1.350	283.02	0.490 ± 0.193	4.63
Starch1500	1.40	62.10 ± 2.80	5.04 ± 0.12	1.526	73.72	0.676 ±0.143	7.73
Methocel K15M	1.45	105.77 ± 8.97	13.46 ± 0.54	1.065	65.97	0.498 ± 0.200	3.90

BFE = Basic Flowability Energy, SE = Specific Energy, FRI = Flow Rate Index

Excipients with large particle size, round particle shape (roundness ≥ 0.7) and low moisture content had good flow properties [28,108,109], as confirmed by Hausner Ratio values lower than 1.25 for Kollidon SR, Cellphere CP-102, Flowlac 90, Tablettose 80 and Emcompress [110]. The rheological properties of the investigated materials were measured, as comparison to the characterization with Hausner ratio (Table 2). As previously reported, good flowing excipients had values of Basic Flowability Energy (BFE) higher than ≃ 90 mJ and Specific Energy (SE) lower than 10 mJ/g, requiring higher energy to spin the blade in the sample, compared to poor flowing materials. This counter-intuitive trend was observed for powders with high bulk density: as the sample was poured in the vessel, a great number of particles was efficiently packed in the volume directly in front of the blade and air pockets were not present. Therefore, the zone of stress transmission became relatively extended and required high flow energy for the blade displacement [33]. In contrast, poor-flowing materials were characterized by a low bulk density

and air pockets reduced the number of particle in front of the blade. Cellphere CP-102, Tablettose 80 and Emcompress had values of Basic Flowability Energy higher than 90 mJ. And were identified as good flowing excipients.

In contrast, Avicel PH-200 and Methocel K15M had a Basic Flowability Energy value lower than ≃ 90 mJ and Specific Energy value higher than 10 mJ/g. Therefore, they were identified as bad flowing materials. The flow pattern established during the Specific Energy measurement was an upward motion and the powder flowed in a low stress condition. Therefore, bulk compressibility had no remarkable impact on the measured flow energy, and the Specific Energy was mostly related to cohesion and other physical properties, such as particle size, shape and texture [100]. However, the characterization of powder flowability obtained through the Hausner ratio was discordant with the Basic Flowability Energy measurements of Kollidon SR (low value), Avicel PH-200 and Methocel K15M (high values). Despite the round particle shape (0.786) and the smooth surface (Fig. 19 A), which probably reduced the particle-particle friction, Kollidon SR have a small particle size, causing high cohesiveness. In contrast, the rod-like particle shape of Methocel K15M (Fig. 19 B) and the surface roughness of Avicel PH-200 (Fig. 19 C) determine severe particle friction and interlocking during the blade displacement in the sample, increasing the powder stiffness [101] and eventually causing high energy consumption to promote the powder flow.

Figure 19. SEM picture of (A) Kollidon SR, (B) Methocel K15M and (C) Avicel PH-200.

The Flow Rate Index (FRI) measured the powder sensitivity to change in blade speed and it was used as estimation of the powder cohesiveness. Powder sensitivity to blade rotation at lower speed was caused by greater demand in energy to fluidize the sample and to promote the escape of entrained air. As previously reported, the increase in blade speed promoted less air removal from the sample and the material became easier to flow (FRI>1). In contrast, non-cohesive powders

were much less sensitive to flow rate. The amount of air entrained in the powder remained constant and the force transmission was unaffected by the change in blade speed (FRI ≃ 1) [102]. Cellphere CP-102, Flowlac 90 and Tablettose 80 presented the lowest Flow Rate Index because of the round shape and large particle size, which resulted in low cohesiveness. As expected, materials with a small particle size, such as Starch 1500 and Kollidon SR had high cohesiveness caused by the high surface area and confirmed by high values of Flow Rate Index. These results were in accordance with the Hausner ratio values equal or higher than 1.4, expected for cohesive powders [111]. Moreover, a low Flow Rate Index was observed for Methocel K15M probably caused by the irregular particle shape. At low speed, particles were closer to each other and a severe particle interlocking could occur, having a negative impact on Flow Rate Index values [102]. Therefore, the material required less energy for the blade to promote the powder flow.

3.1.2. Simulation of die filling

3.1.2.1. Evaluation with gravity fill

Die filling simulation was performed for all the investigated excipients with gravity fill. Although tablet formulations are not comprised by a single component, the die filling evaluation was performed on pure excipients. It was assumed that a powder mixture would present an average filling behavior of the respective pure materials, depending on their content in the mixture. Good flowing material, such as Emcompress, Cellphere CP-102, Tablettose 80 and Flowlac 90 were expected to have excellent die filling due to their optimal particle properties (cf. 3.1.1.). In contrast, a complete die filling of these excipients was reached only up to 15 RPM, and at higher press speeds the completeness of filling process was remarkably reduced to filling ratios of 0.5-0.7 of the die volume (Fig. 20 A).

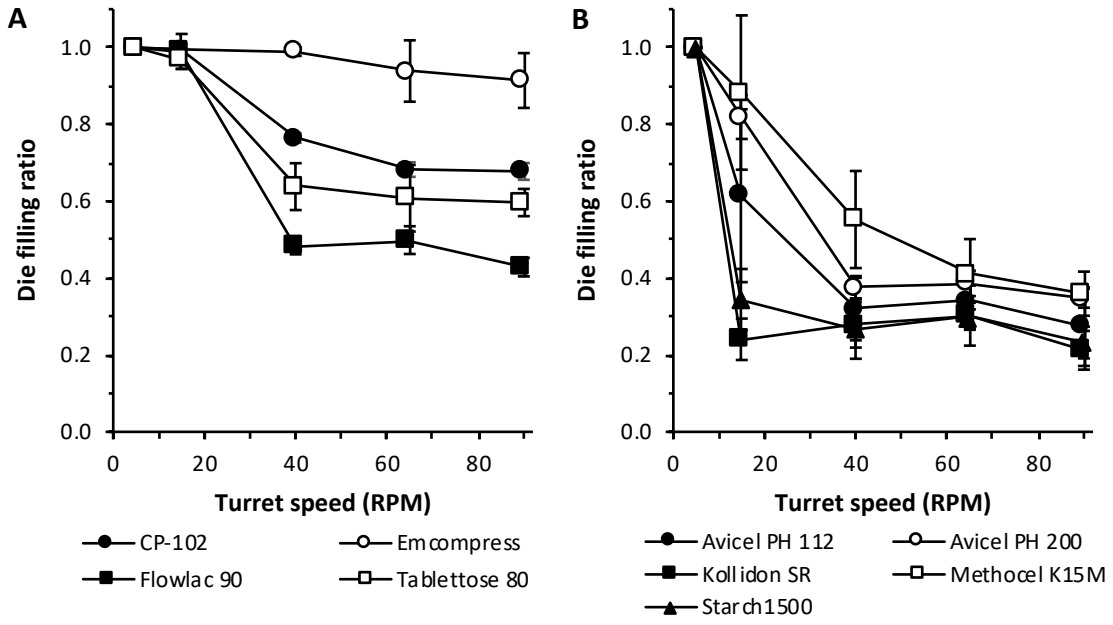

Figure 20. Die filling simulation of an industrial tablet press with gravity fill: (A) good flowing and (B) poor flowing excipients, according to rheological properties.

Emcompress was the only excipient to reach a complete die filling even at 90 RPM (die filling ratio 0.9 or higher). In contrast, the ratio of die filling for all other excipients was negatively affected by the press speed, and a complete filling was not achieved even at low speed (Fig. 20 B).

According to the characterization of flow properties with Hausner ratio, Kollidon SR was among the materials possessing the best flow behavior. However, this excipient had a strong incompleteness of die filling (0.25 die filling ratio) already at 15 RPM. Probably, the particle

cohesiveness of Kollidon SR had an impact on the die filling properties, despite the flow improvement determined by spherical particle shape and smooth surface (cf. 3.1.1.).

The effect of press speed on die filling variability was evaluated as function of the coefficient of variation (CV%). Good-flowing materials were not remarkably affected by the increase in press speed. In fact, the CV% of all these excipients was lower than 10% and press speeds higher than 15 RPM did not determine further increase in die filling variability, with the sole exception of Tablettose 80 (Fig. 21 A).

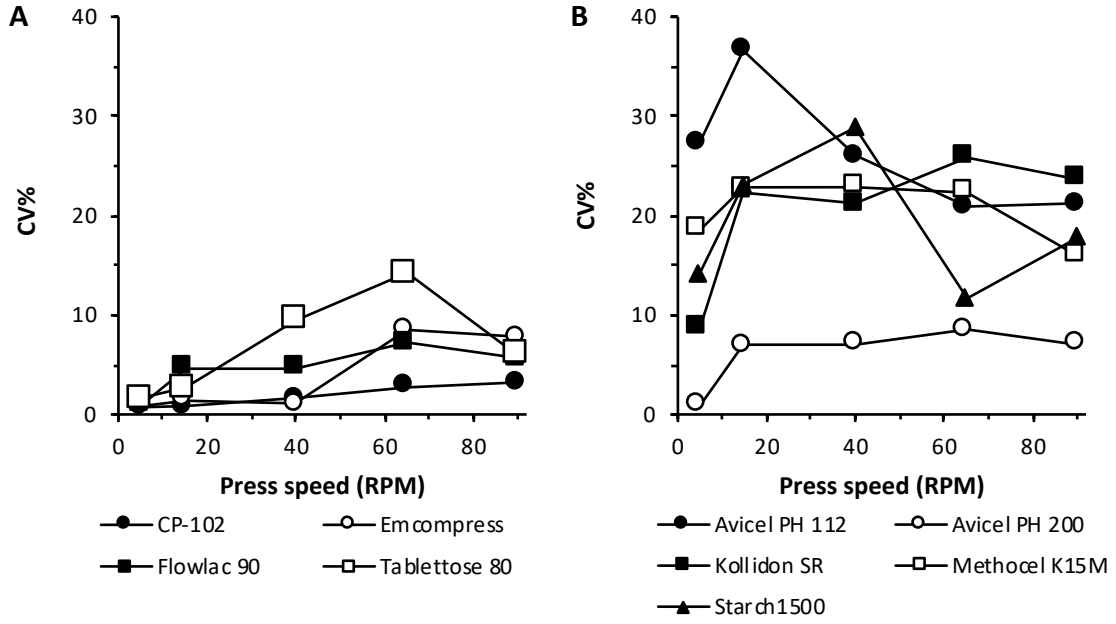

Figure 21. Effect of press speed on die filling variability, during simulation of an industrial tablet press with gravity fill: (A) good flowing and (B) poor flowing excipients, according to rheological properties.

In contrast, poorly-flowing materials had higher variability in die filling already at low press speed (Fig. 21 B) since the bad flow properties promoted the formation of powder bridges in the feeder. However, a decrease in die filling variability was observed for Avicel PH-112, Starch 1500 and Methocel K15M as the press speed increased. Probably, the swift change of the feeder movement direction during simulation at high rotation speed determined enough mechanical stresses to reduce powder bridges formation and promoted the powder flow. Furthermore, Avicel PH-200 represented an exception with a variability in die filling comparable to excipients with better flowing properties.

3.1.2.2. Evaluation with forced fill

The powder feeder was equipped with a metal stirrer to perform the die filling simulation with forced fill. The stirring speed was set to 50 RPM. This setup improved the powder motion in the feeder, and enhanced the die filling for all excipients. The effect was noticed on good flowing excipients, such as Flowlac 90 and Tablettose 80 (Fig. 22 A), which had an incomplete filling at low press speed with gravity fill. Remarkable improvements were also obtained for all materials with poor-flowing properties (Fig. 22 B).

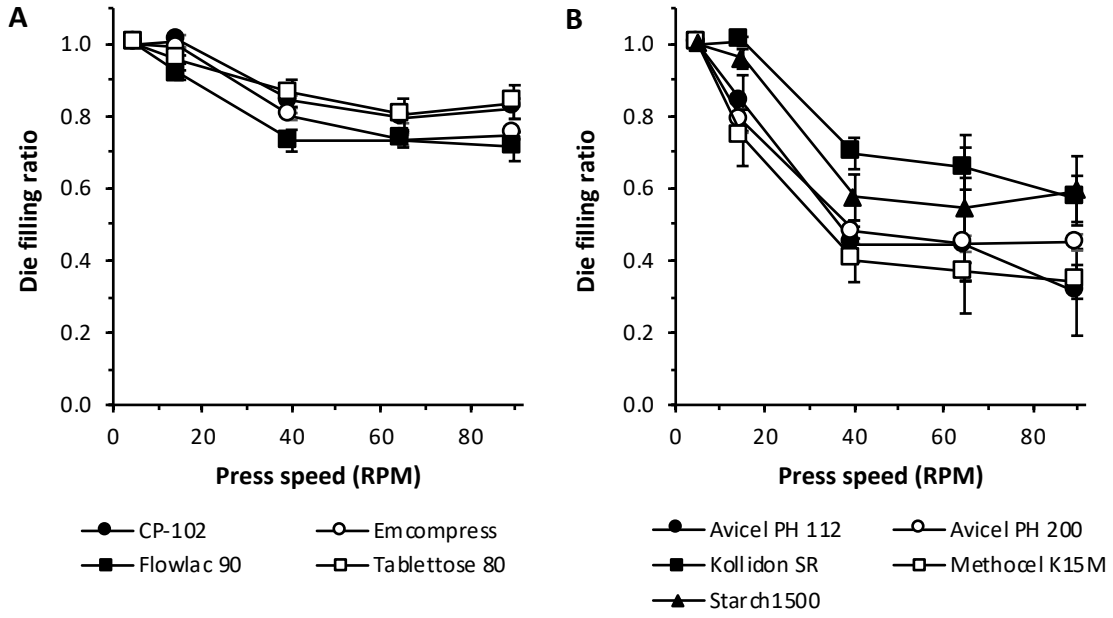

Figure 22. Die filling simulation of an industrial tablet press with forced fill: (A) good flowing and (B) poor flowing excipients, according to rheological properties.

However, Emcompress presented an unexpected reduction in the ratio of die filling. Probably, this effect was caused by higher sensitivity to the change in blade speed, compared to other good flowing materials (cf. 3.1.1.). Indeed, the blade movement caused air entrapment and impaired the flowing properties of these powders.

The investigation of die filling variability was performed as evaluation of press speed effect on the coefficient of variation. Good-flowing excipients presented a low fluctuation in the completeness of die filling (CV% < 5%), even at high press speed (Fig. 23 A).

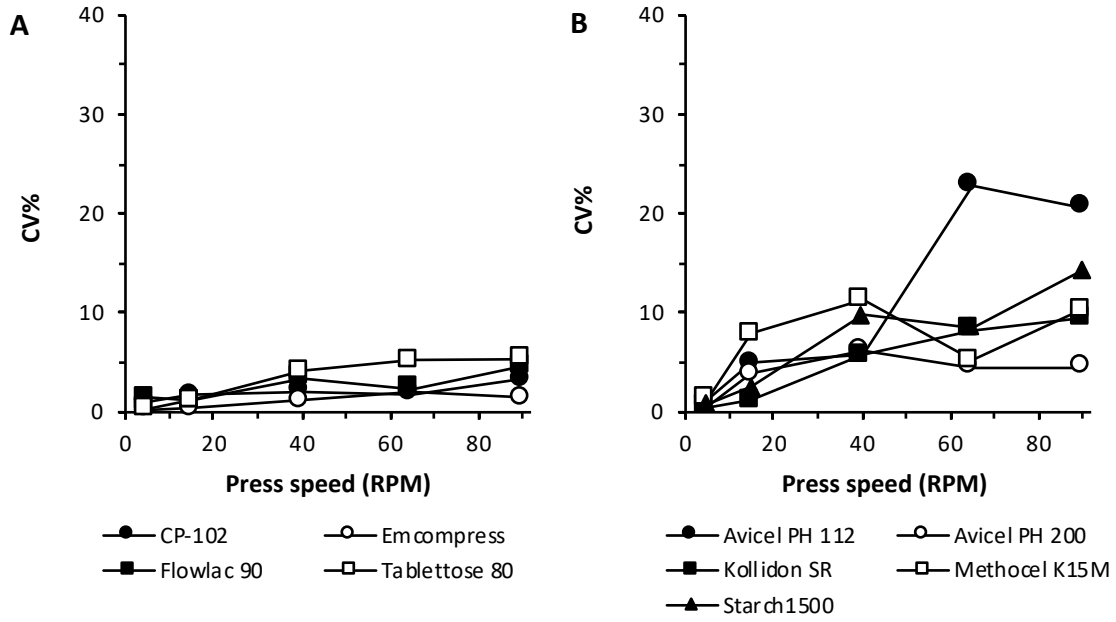

Figure 23. Effect of press speed on die filling variability, during simulation of an industrial tablet press with forced fill: good-flowing (A) and (B) poorly-flowing excipients, according to rheological properties.

Similarly, a remarkable reduction in filling variability, compared to the gravity fill technique, was observed for poorly-flowing excipients during the simulation with forced fill (Fig. 23 B). Indeed, the rotation of the metal stirrer promoted a reproducible filling process and prevented the formation of powder bridges in the feeder. Furthermore, the filling variability increased accordingly with the press speed, probably, due to the sole effect of the decrease in feeder residence time over the die. Despite an overall enhancement with forced fill technique, a complete filling process was not achieved for all investigated materials.

3.1.2.3. Evaluation with suction fill

During the simulation with suction fill, the movement of the lower punch was synchronized with the feeder displacement. As the feeder crossed the die opening, the lower punch was swiftly moved downward. The punch displacement generated vacuum, which promoted the flow of powder particles in the die and improved the particle packing [42]. Moreover, this technique reduced the air entrapment during the filling process, a critical factor for cohesive materials. As expected, the suction fill determined an enhancement in die filling for good flowing excipients (Fig. 24 A).

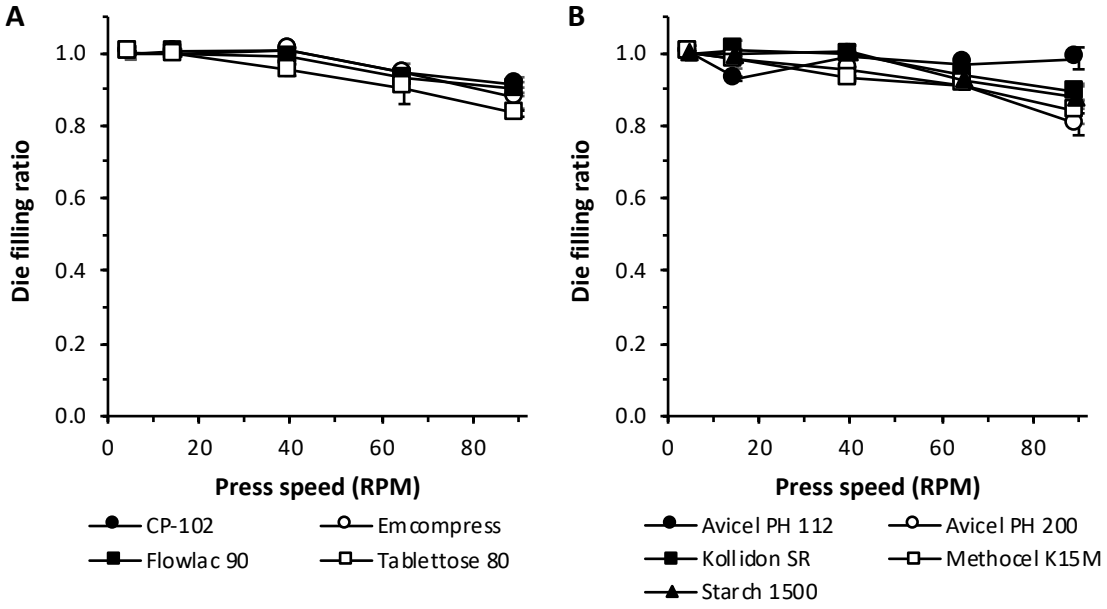

Figure 24. Die filling simulation of an industrial tablet press with suction fill: (A) good flowing and (B) poor flowing excipients, according to rheological properties.

Furthermore, a remarkable improvement of filling process was observed in particular for poorly-flowing excipients, probably due to less air entrained in the powder (Fig. 24 B), reaching a complete die filling (0.8-1.0 die filling ratio). In fact, the use of the suction fill technique greatly reduced the amount of air entrained in cohesive powders, promoting a better particle packing in the die [74].

In contrast to the filling techniques previously investigated, the variability of die filling was low for all excipients in all tested conditions. The effect of press speed on die filling variability was evaluated as function of the coefficient of process were low (CV%<5%) for all excipients in every tested condition (Fig. 25 A and B). Indeed, the mechanical stress generated by the vacuum was

sufficient to prevent the formation of powder bridges in the feeder and no remarkable filling variability was noticed for poor-flowing excipients.

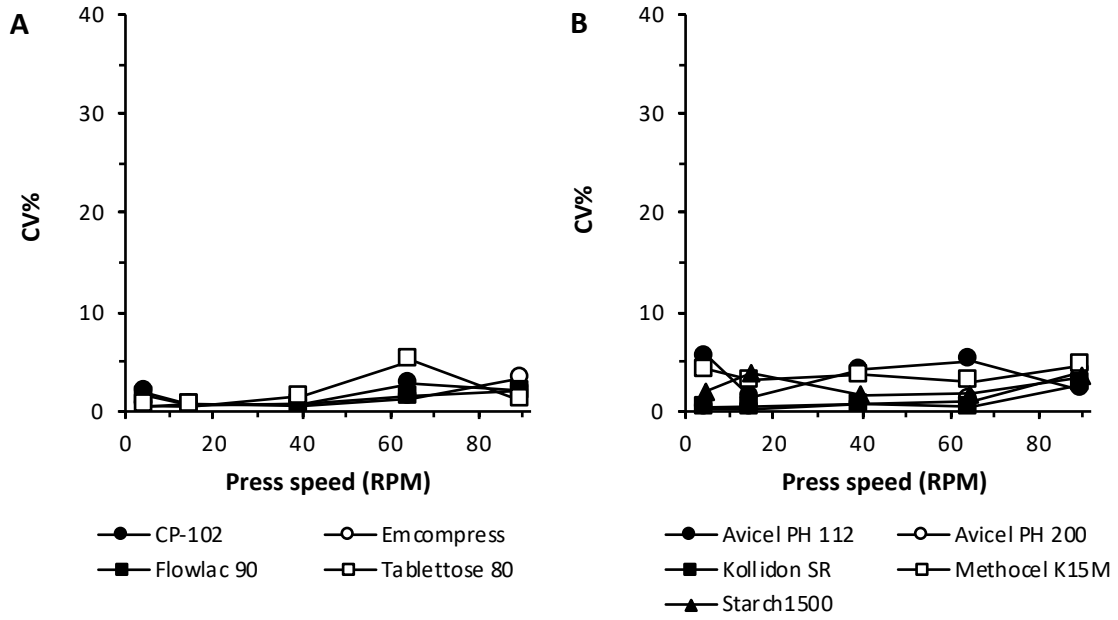

Figure 25. Effect of press speed on die filling variability, during simulation of an industrial tablet press with suction fill: (A) good flowing and (B) poor flowing excipients, according to rheological properties.

3.1.2.4. Evaluation of filling density

The particle packing inside the die depends on the flow properties of each material and it determined the filling density [107]. As the speed of tablet press increased, a reduction in filling density was expected, in particular for poor-flowing materials [37]. Instead, good flowing excipients were expected to have a lower reduction in die filling density.

According to a visual assessment, the filling process with gravity fill was complete for all tested excipients at low speed. However, poor-flowing materials presented a filling density lower than the bulk density (Table 6).

Table 6. Bulk density and filling density achieved with gravity, forced and suction fill at 5 and 90 RPM.

Excipient	ρ_{bulk} (g/ml)	$\rho_{gravity}$ (g/ml)		ρ_{forced} (g/ml)		$\rho_{suction}$ (g/ml)	
		5 RPM	90 RPM	5 RPM	90 RPM	5 RPM	90 RPM
Avicel PH-112	0.360	0.218	0.060	0.407	0.127	0.366	0.361
Avicel PH-200	0.390	0.384	0.134	0.419	0.189	0.417	0.335
CP-102	0.873	1.021	0.692	1.025	0.842	1.070	0.976
Emcompress	0.860	0.978	0.894	0.996	0.745	1.084	0.950
Flowlac 90	0.640	0.632	0.271	0.762	0.545	0.716	0.645
Kollidon SR	0.540	0.502	0.115	0.541	0.309	0.619	0.552
Methocel K15M	0.310	0.249	0.090	0.332	0.133	0.345	0.289
Starch1500	0.720	0.699	0.175	0.790	0.469	0.754	0.720
Tablettose 80	0.510	0.735	0.439	3.90	1.45	0.726	0.640

Probably, air entrapment and the formation of powder bridges in the feeder could have reduced the pressure of the overlying powder, leading to lower particle packing in the die. This assumption was confirmed by the values of filling density obtained during forced fill, which were higher than the respective bulk density for all excipient investigated. The metal stirrer prevented the formation of powder bridges and improved the powder motion in the feeder.

Cellphere CP-102, Emcompress and Tablettose 80 presented a filling density higher than the bulk density. This effect was particularly remarkable at low turret rotation speeds, where the longer residence time over the die and the pressure of the overlying powder in the feeder increased the particle packaging. At higher speed, most materials presented a filling density with gravity and forced fill remarkably lower than the bulk density due to incomplete die filling.

Instead, during the filling process with suction fill, all materials presented a filling density higher or comparable to the bulk density even at 90 RPM. A complete die filling for all materials was achieved only with this technique.

3.1.3. Mathematical modelling

3.1.3.1. Correlation of die filling with rheological properties

The increase in rotation speed of the tablet press had a negative effect on the die filling and the reduction in feeder residence time over the die prevented a complete filling with gravity fill (cf. 3.2.1.1.). This effect occurred between 5 and 65 RPM, reaching eventually a plateau at 90 RPM. Therefore, this range was selected for the mathematical modelling.

The ratio of die filling was described by a semi-log function of turret speed, as in the following equation:

$$Eq.19 \qquad \Delta m = a_s \ln(V_{turr}) + q$$

where Δm is the ratio of die filling, a_s is the slope in the semi-log plot, V_{turr} is the turret speed and q is the intercept. The slope a_s represented the excipient sensitivity to the press speed: as the feeder residence time decreased, materials with optimal flow properties still performed a complete filling process, therefore the profile in the semi-log plot had a low value slope (Fig. 26 A).

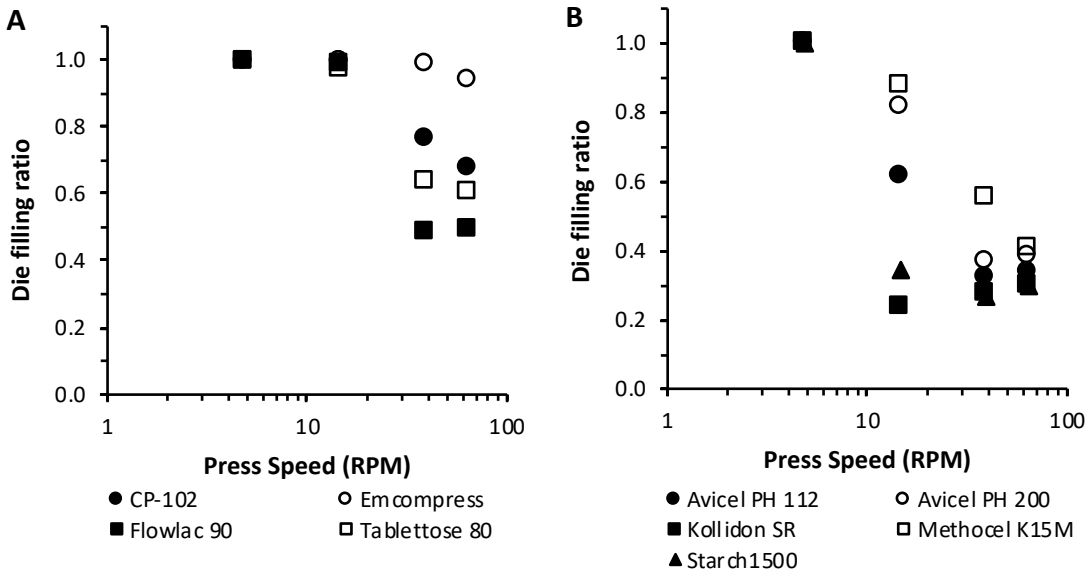

Figure 26. Semi-log plot of the ratio of die filling as a function of the turret speed in gravity fill: (A) good flowing and (B) poor flowing excipients, according to rheological properties.

In contrast, poor-flowing excipients, characterized by incomplete die filling profile already at low press speed, presented a higher value of the slope a_s, as for Avicel PH-112, Avicel PH-200 and Methocel K15M. Moreover, due to their bad flowing properties, Kollidon SR and Starch 1500 presented an abrupt decrease in the profile of die filling (Fig. 25 B) and the equation predicted

the material behavior with less accuracy, as confirmed by the poor correlation coefficient R^2 (Table 7).

Table 7. Slope and intercept values of the die filling simulation with gravity and forced fill techniques.

Excipient	Gravity fill			Forced fill		
	a_s	q	R^2	a_s	q	R^2
Avicel PH-112	- 0.272	1.398	0.9501	- 0.241	1.416	0.9417
Avicel PH-200	- 0.268	1.4604	0.9341	- 0.230	1.3785	0.9785
CP-102	- 0.131	1.2603	0.8548	- 0.087	1.1763	0.8202
Emcompress	- 0.019	1.0392	0.9578	- 0.110	1.2153	0.8697
Flowlac 90	- 0.231	1.448	0.8164	- 0.115	1.1944	0.9461
Kollidon SR	- 0.262	1.2486	0.6585	- 0.152	1.3025	0.8234
Methocel K15M	- 0.237	1.4322	0.9464	- 0.262	1.4247	0.9804
Starch1500	- 0.269	1.2978	0.7648	- 0.200	1.3784	0.8729
Tablettose 80	- 0.169	1.3246	0.8752	- 0.076	1.1377	0.9505

The semi-log plot of filling completeness during forced fill presented remarkable linearity for all investigated excipient (Fig. 27 A and B), as confirmed by the high values of correlation coefficients R^2.

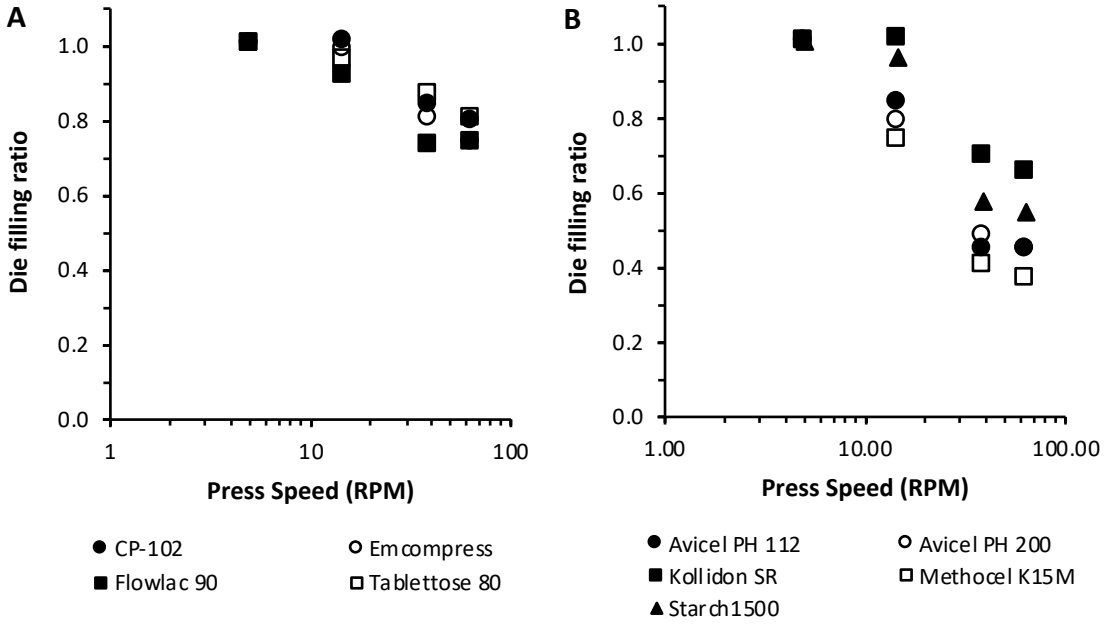

Figure 27. Semi-log plot of the ratio of die filling as a function of the turret speed in forced fill: good flowing (A) and poorly-flowing (B) excipients, according to rheological properties.

Die filling with suction fill presented similar profiles for all investigated excipients. Therefore, no differentiation was possible and no modelling for this technique was performed.

The excipient sensitivity to press speed (a_s) (Table 7) was evaluated as function of the rheological properties for each excipient in use. The slopes used in the model were converted to the respective absolute values for ease of comprehension.

A strong correlation was found between $|a_s|$, calculated during the die filling simulation with gravity fill, and the Basic Flowability Energy, as confirmed by the good correlation coefficient $R^2 = 0.9024$ (Fig. 28).

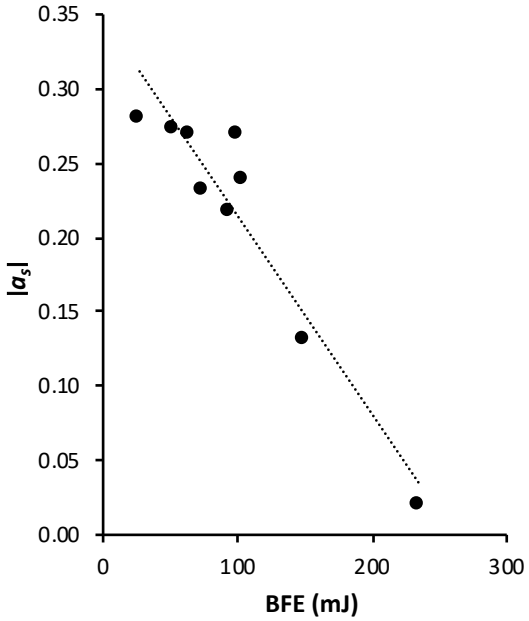

Figure 28. Relationship between the material sensitivity to the press speed a_s during gravity fill and Basic Flowability Energy.

Emcompress and CP-102 were the only excipients reaching a complete die filling process with gravity fill and the model was able to discriminate them from less flowing excipients. The dotted line represents the linear regression of the Basic Flowability Energy values and the calculated values of the slope a_s. Ideally, all values should be located on the linear regression fit and the deviations were attributed to the over- and under-estimation of the model, during the linearization process.

The following model equation was obtained:

$$Eq.20 \qquad |a_s| = -0.0013BFE + 0.3478$$

where $|a_s|$ is the excipient sensitivity to press speed, measured during die filling simulation with gravity fill and BFE is the Basic Flowability Energy.

In contrast, no correlation was found between $|a_s|$, calculated during the die filling simulation with gravity fill, and the Specific Energy, confirmed by the low correlation coefficient (R^2 = 0.0108). It was noticed that the normalization on the sample mass determined a lack of correlation, driven by the values of good-flowing excipients, which had a low $|a_s|$ value (CP-102, Emcompress, Flowlac 90 and Tablettose 80). Indeed, these materials had higher particle packing inside the sample vessel of the powder rheometer, due to a lower compressibility, therefore a higher bulk density.

In contrast, a strong correlation was found between $|a_s|$, calculated during the die filling simulation with gravity fill, and the Specific Energy not normalized on the sample mass (SE^*), as confirmed by the good correlation coefficient R^2 = 0.931 (Fig. 29).

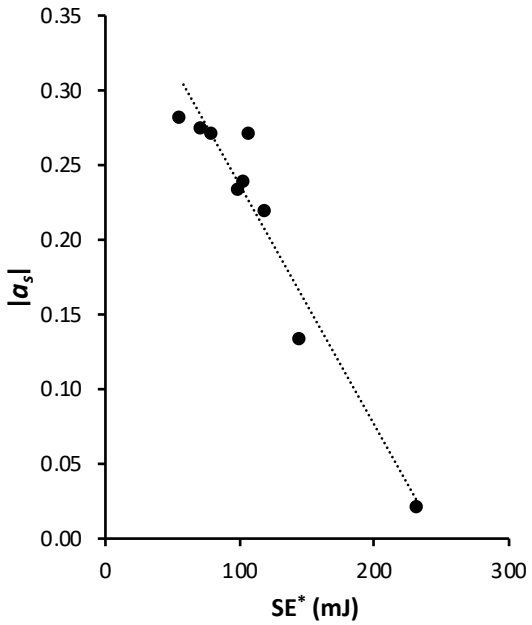

Figure 29. Relationship between the material sensitivity to the press speed a_s during gravity fill and Specific Energy, not normalized on sample mass.

The following model equation was obtained:

$$Eq.21 \qquad |a_s| = -0.0016SE^* + 0.3968$$

where $|a_s|$ is the excipient sensitivity to press speed, measured during die filling simulation with gravity fill and SE^* is the Specific Energy, not normalized on sample mass.

Although a trend was noticed, no correlation was found between Basic Flowability Energy or Specific Energy and $|a_s|$, calculated during the die filling simulation with forced fill technique (R^2 = 0.0134, R^2 = 0.2164, respectively). Indeed, the forced fill technique determined mechanical stresses and had a remarkable effect in promoting the powder flowing of the investigated excipients. Therefore, the powder rheology could not simulate or predict the powder behavior, under stress conditions.

3.1.3.2. Model validation

Among the material not included in the initial selection, spray-dried mannitol (Pearlitol SD 200) was selected to validate the model as excipient with low Hausner Ratio and its physical and rheological properties were measured (Table 8).

Table 8. Hausner ratio (H_R), loss on drying (LOD%), physical and rheological properties for Pearlitol 200 SD (mean ± SD, n = 3).

Excipient	H_R	BFE (mJ)		SE (mJ)		FRI	d_{50} (µm)		Roundness		LOD%
		Mean	SD	Mean	SD		Mean	SD	Mean	SD	
Pearlitol 200 SD	1.11	82.83	6.01	8.93	0.12	1.526	150.97	0.941	0.669	0.173	0.28

The values of Basic Flowability Energy lower than 90 mJ and Specific Energy lower than 10mJ/g suggested the material not having optimal flowing properties. This assumption was in contrast with the low value of Hausner ratio. Large particle size and low moisture content had a remarkable impact to promote the powder flow. However, the measurement of Flow Rate Index was remarkably high, compared to excipients with similar properties as Tablettose 80. This high value was supposed to be dependent to the irregular particle shape (0.669), causing blade speed sensitivity and a cohesiveness higher than other tested excipients.

Die filling simulation with Pearlitol 200 SD was performed using gravity, forced and suction fill techniques. According to the properties similar to other investigated materials (cf. 3.1.1.), Pearlitol 200 SD was expected to possess an incomplete die filling during gravity fill from 40 RPM and a remarkable improvement with forced fill. Moreover, a complete die filling was

expected during suction fill. Instead, the investigated material presented a strong decrease in die filling ratio (0.3 die filling ratio at 90 RPM) even during forced fill (Fig. 30).

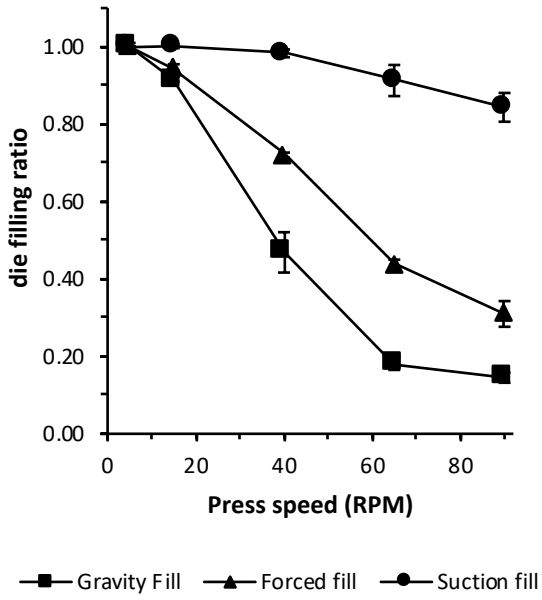

Figure 30. Simulation with gravity, forced and suction fill of Pearlitol 200 SD.

Despite similar particle properties and powder rheology, Pearlitol 200 SD presented higher cohesiveness compared to Tablettose 80, confirmed by the higher values of Flow Rate Index and Specific Energy. However, similarly to other excipients, the suction fill technique provided remarkable improvements and determined a complete filling process at 90 RPM (Table 9).

Table 9. Bulk density and filling density achieved with gravity, forced and suction fill at 5 and 90 RPM for Pearlitol 200 SD.

Excipient	ρ_{bulk} (g/ml)	$\rho_{gravity}$ (g/ml)		ρ_{forced} (g/ml)		$\rho_{suction}$ (g/ml)	
		5 RPM	**90 RPM**	**5 RPM**	**90 RPM**	**5 RPM**	**90 RPM**
Pearlitol 200 SD	0.510	0.504	0.088	0.564	0.175	0.564	0.460

To confirm the goodness of predictions with the model equations, the expected material sensitivity to press speed (a_s) was estimated from the measured values of Basic Flowability Energy (a_{BFE} = 0.240) and Specific Energy (a_{SE*} = 0.205). These were compared with the values obtained from semi-log plot of die filling simulation of Pearlitol 200 SD during gravity fill (a_s =

0.241). Hence, a good prediction of the die filling was obtained with the model equations, in particular the estimation from Basic Flowability Energy (Fig. 31 A).

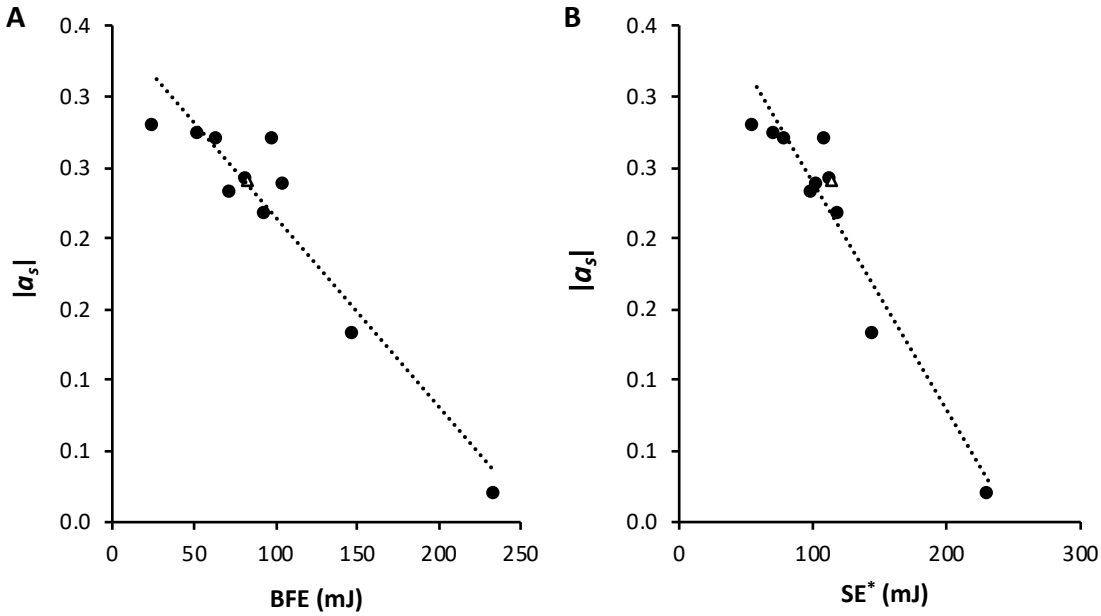

Figure 31. Relationship between the excipient sensitivity to the press speed (a_s) during gravity fill and (A) Basic Flowability Energy or (B) Specific Energy, not normalized on sample mass (∆ represents Pearlitol 200 SD).

3.2. Development and evaluation of a novel method to test layer adhesion of bilayer tablets

Multilayer tablets have become a successful technology over the last 50 years, and several products have been commercialized with tis design [56]. The growing tendency in manufacturing of bilayer tablets is ascribed to the versatility this dosage form offers, for example as combination of incompatible APIs [49] and different drug release profiles [52,54]. Product life extension can also be achieved through reformulation into multi-layered dosage forms [61]. Tablet delamination represents the main manufacturing challenge, which may occur during handling and packaging processes or during long-term storage [85]. The failure is generally observed at the interface between layers as a result of an insufficient layer adhesion [112].
To date, few methods have been proposed for this measurement [79,84,88]. They differ mainly in the direction of stress application, *i.e.* normal stress or shear stress and the difference consequently leads to unequal results. Hence a standardized method is currently missing. Long setup time and high friction developed during the run are further critical aspects to consider using these techniques.

In the present work, a novel method to evaluate layer adhesion on bilayer tablets was developed and evaluated. Based on the challenges offered by the methods already in literature, the following 4 test requirements were identified: short setup time, reproducibility, the ability to discriminate differences in formulation and compression pressure. The initial design was modified to fulfil the aforementioned requirements in the final version. The influence of test speed and tablet positioning was evaluated to identify the optimal test parameters. Furthermore, the effect of temperature, moisture and storage time was evaluated and the optimal storage conditions were assessed.

3.2.1. Shear test development

3.2.1.1. Test requirements

The main challenge affecting multilayer tablets production is the delamination, which occurs as a separation localized at the layers interface. In literature, the lack of sufficient layer adhesion is reported to be the principal cause leading to tablet failure and vary depending on the materials comprised in the layers [61]. Therefore, the characterization of layer adhesion is of primary importance to assess the formulation tendency to delaminate and its suitability for the manufacturing process of each formulation.

The investigation on the causes leading to the failure of a bilayer tablet production process required a suitable method to characterize tablets prepared with different excipients and process parameters. On the basis of methods present in literature, the following test requirements were identified:

1. Short setup time;
2. Ability to differentiate tablets prepared with different excipients;
3. Ability to differentiate tablets prepared with different compaction pressures;
4. Reproducibility.

Firstly, the time required for sample preparation and test run had to be short, to analyze in a reasonable time several batches of multiple tablets each. Indeed, some of the tests in use requires the bilayer tablets to be glued on small metal plates and afterwards tested on a dynamometer [79]. Despite this method could reduce the stress applied on the tablets during sample handling, it was time consuming, requiring at least 1 h to ensure a complete drying of the glue.
In the tableting process, a linear increase of the layer adhesion is expected accordingly to the increase in compaction pressure, due to higher formation of particle bonds [47]. Furthermore, material physical characteristics have a critical role on bilayer tablet adhesion properties, depending on the intra- and inter-layer combinations. Therefore, the test required sufficient sensitivity to reliable differentiate tablets prepared with different excipients and compaction pressures.
At last, the test must grant reliable and reproducible results, even during the evaluation independent batches prepared with the same formulation.

3.2.1.2. Shear device (version 1)

Based on the aforementioned test requirements, the first version of the shear device was designed. Two Teflon blocks were machined to fit in the clamp of a dynamometer (Ta.XTplus, Stable Micro

Systems, Surrey, UK). An 11 mm slot was drilled to hold the tablet in position and a single metal screw was added to allow a fine alignment of the layer interface with the sliding plane of the two blocks (Fig. 32 A).

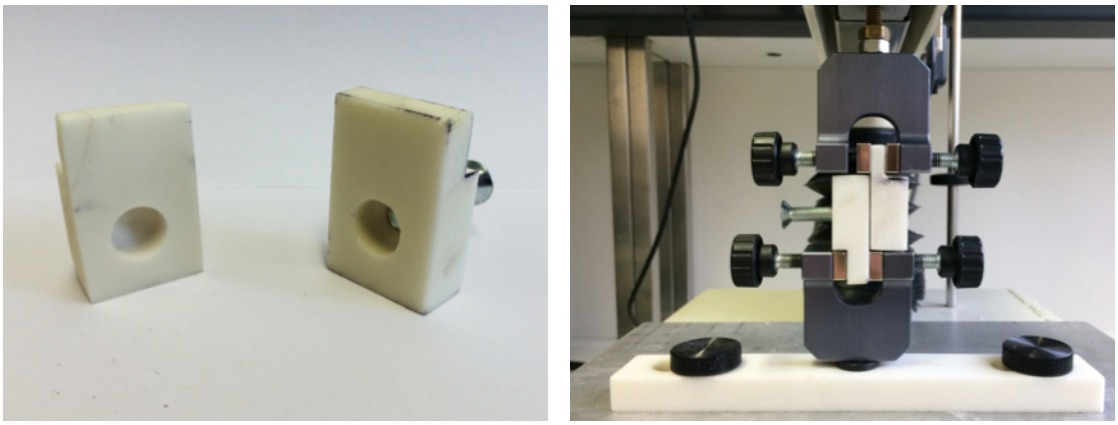

A B

Figure 32. Version 1 of (A) shear device and (B) device installed on the Ta.XTplus.

4 batches (n = 5) of bilayer tablets combination Avicel PH-200-Emcompress were prepared at different compaction pressures ranging from 50 to 250 MPa and tested with the shear test, applying a tensile stress until rupture. A good correlation was observed between compaction pressure and measured layer adhesion (Fig. 33).

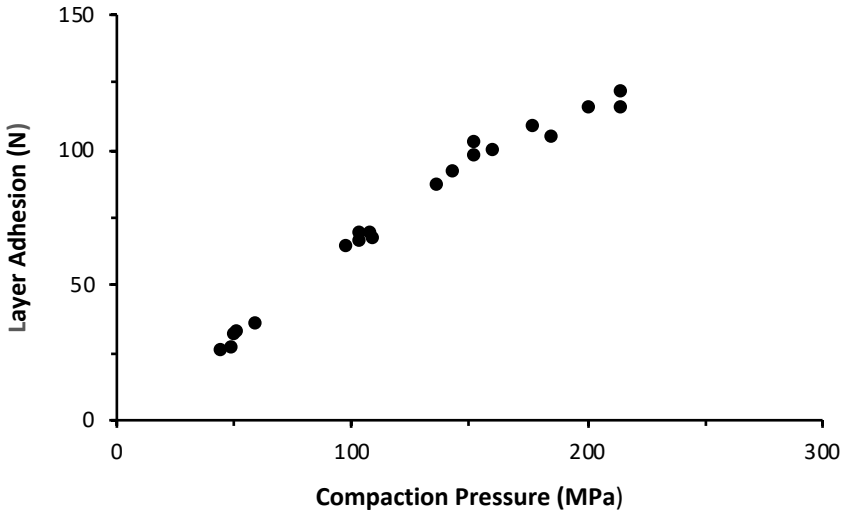

Figure 33. Effect of compaction pressure on layer adhesion, evaluated with shear device (version 1).

All batches were tested in about 1 h and the test was able to differentiate tablets prepared with different compaction pressures. However, a sideways movement of the upper clamp was detected

during each run. It was observed that the 4 mm screw connecting the clamp to the instrument was subjected to a remarkable bending during the test. A deformation of the Teflon block could not be excluded as well. The extent of this effect was linearly proportional to the applied tensile stress, therefore depending on the resistance offered by the tested tablet and causing a bias on the measured values at high layer adhesion (Fig. 32). The bending occurrence was supposed to be caused by the material choice and block design, which did not allow a perfect alignment of the clamps. In addition, the tablet fitting in the slot was loose and a misalignment often occurred during the run. Indeed, the slot was mechanically drilled and the diameter of the hole was slightly greater than 11 mm.

3.2.1.2. Shear device (version 2)

To overcome the aforementioned design flaws, an improved design was prepared in aluminum, a stiffer material compared to Teflon, but relatively easy to machine (Fig. 34 A). The metal blocks were shaped to allow a better alignment of the fixing clamps, therefore of the stress along the tablet layers interface (Fig. 34 B).

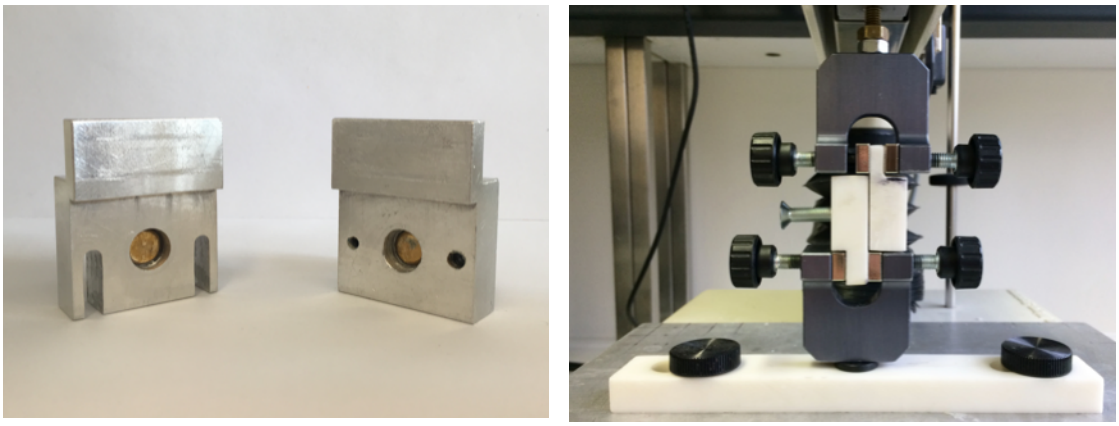

A **B**

Figure 34. Version 2 of (A) shear device and (B) device installed on the Ta.XTplus.

The stress application was changed from tensile to compressive, to ease the tablet positioning during test setup. The screw connecting the upper clamp to the instrument was replaced with a shorter one, to reduce the tablet movement during a test run.

Tablettose 80-Methocel K15M, Tablettose 80-Stach and Avicel PH-200-Tablettose 80 combinations were selected and 7 batches of bilayer tablets (n = 10) were prepared at compaction pressure ranging from 50 to 400 MPa (Fig. 35).

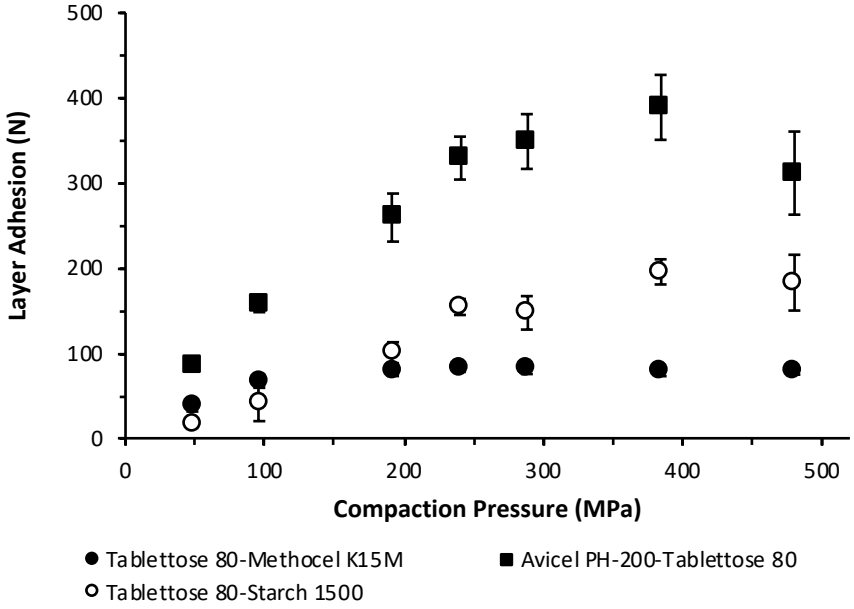

Figure 35. Effect of compaction pressure on layer adhesion, evaluated with shear device (version 2).

The shear device presented comparable setup time and discrimination capability of the version 1. Despite the attempt to overcome the bend tendency, a sideways movement of the device was noticed at high layer adhesion (>250 N), probably caused by elastic deformation of the instrument and device. The variability of layer adhesion measurement, calculated as coefficient of variation (CV%), was lower than 10% for almost all combinations in the investigated range of compaction pressures. Higher values of CV% were observed at layer adhesion values greater than 250 N. This variability was probably caused by the elastic deformations and a lack of sufficient speed in data acquisition. Indeed, as the tablet failed, the Texture Analyzer was not able to record the abrupt decrease in layer adhesion, due to the speed limitation of the data acquisition system to 1 sample/s.

3.2.1.3. Shear device (version 3)

To overcome the aforementioned technical limitations the device design was adapted to fit into a compaction simulator (Fig. 36).

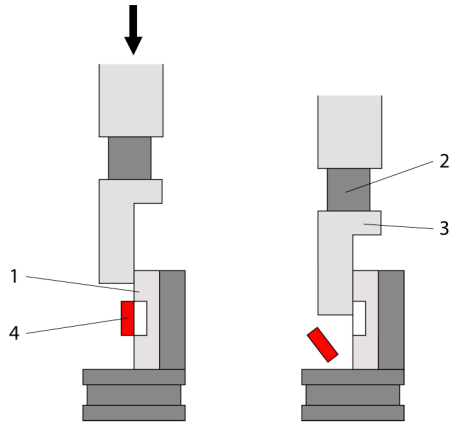

Figure 36. Version 3 of the shear device to be installed on the compaction simulator: (1) tablet holder, (2) load cell, (3) upper punch and (4) bilayer tablet.

The instrument bigger size and higher stiffness compared to the dynamometer, reduced the impact of elastic deformation at the forces in use. Moreover, it was equipped with a faster data acquisition system (5000 samples/s), which provided an accurate analysis. The upper punch was equipped with a piezoelectric load cell of maximal force 1kN (Fig 37 A) and it was shaped to penetrate in the tablet holder without friction (Fig. 37 B). The tablet was positioned in a tablet holder by means of a micrometer (Fig. 37 C), so that the first layer was exposed to the upper punch.

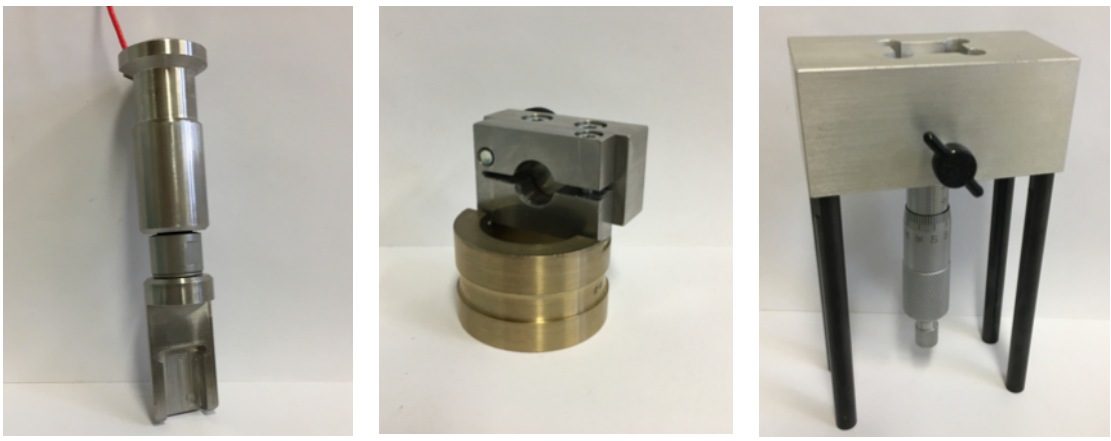

A **B** **C**

Figure 37 Custom-shaped upper punch (A), tablet holder (B) and micrometer (C).

The tablet was fixed in position with a clamp and slightly tightened by means of a torque screw driver, to avoid undesired radial stress at the tablet interface. The device was afterwards installed

on the compaction simulator and a shear stress was applied to measure the bilayer tablet resistance to delamination.

At first, the speed of stress application was investigated at different upper punch velocity. The combination Avicel PH-200-Tablettose 80 was selected and a large batch of tablets was prepared at 250 MPa. The tablets were tested (n = 10) at 4 punch speeds, then standard deviation (SD) and coefficient of variation (CV%) were compared to identify the optimal velocity (Table 10).

Table 10. Effect of the test speed on variability of layer adhesion for the combination Avicel PH-200-Tablettose 80.

	0.01 mm/s	**0.1 mm/s**	**1 mm/s**	**10 mm/s**
SD	16.70	24.10	10.50	49.61
CV%	8.73	10.22	3.30	20.38

The lowest variability in layer adhesion was obtained at 1 mm/s, therefore this velocity was selected as the standard punch speed.

3.2.2. Evaluation of the test requirements

3.2.2.1. Excipient differentiation

Avicel PH-200, Methocel K15M, Tablettose 80, Emcompress and Starch 1500 were selected and the tablets prepared with all layer combinations were tested in order to evaluate the variability among the measurements and the capability of the test to identify formulation differences (Fig. 38).

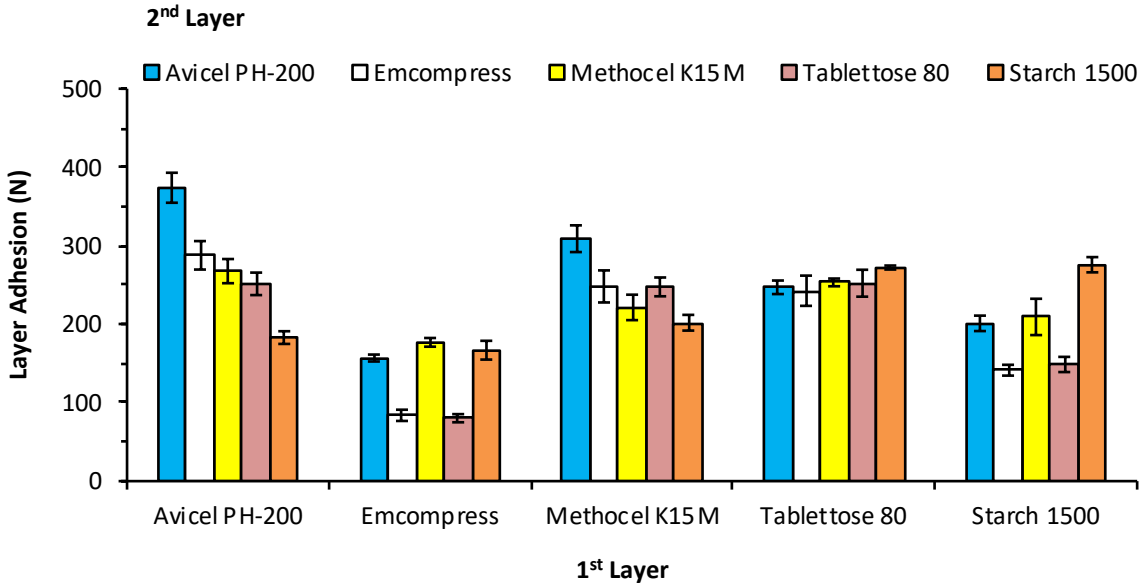

Figure 38. Layer adhesion measured for combinations of different excipients as first and second layer.

The evaluation of all 25 combinations was performed in about 6 h (approximately 15 min per batch). The layer adhesion of tablets prepared with Emcompress and Tablettose 80 in the second layer was generally constant, independently of the excipient constituting the first layer. These materials are described as brittle [22] and the particle fracture during compaction generates a high surface for layer interactions, reducing the variability determined by different materials in the first layer. Vice versa, tablets prepared with plastic materials (as Methocel K15M and Starch 1500) in the second layer presented similar layer adhesion patterns, depending on the first layer composition: combinations with plastic materials in the first layer had a higher layer adhesion than with brittle materials. However, the same tendency was not evident for Avicel PH-200. Furthermore, the inversion of the two excipients layers had a remarkable impact on the layer adhesion, in particular when brittle materials were combined with plastic excipients. The test allowed the differentiation of tablets prepared with excipients and the overall variability of the measurements, evaluated as coefficient of variation (CV%), was lower than 10% in all cases, suggesting test reliability and reproducibility.

3.2.2.2. Compaction pressures differentiation

From the previous evaluation, four combinations of excipients were selected based on increasing layer adhesion: Tablettose 80-Methocel K15M, Tablettose 80-Starch 1500, Methocel K15M-Starch 1500 and Avicel PH-200-Tablettose. These formulations were compressed into tablets at compaction pressures ranging from 50 to 500 MPa and the layer adhesion was evaluated (Fig. 39).

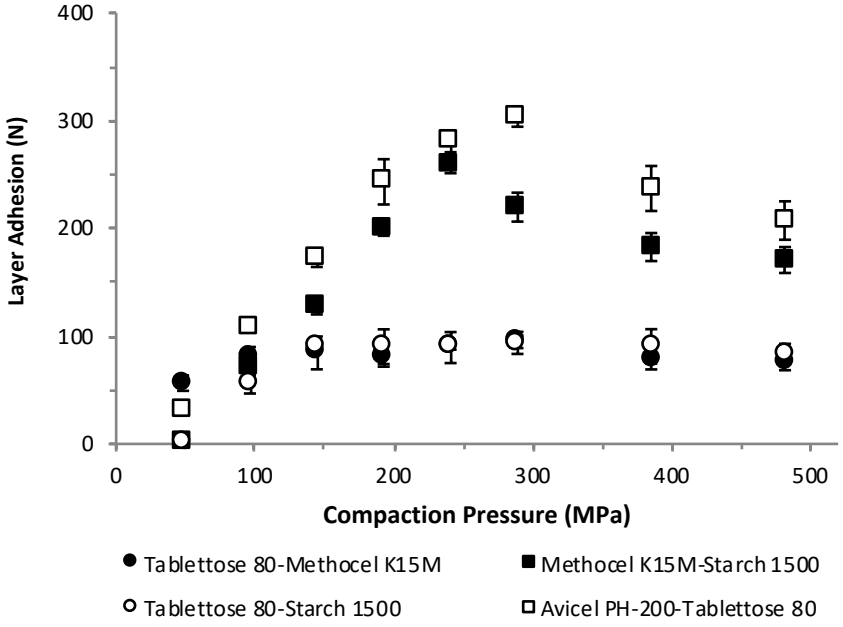

Figure 39. Layer adhesion measured for different layer combinations prepared at increasing compaction pressures.

A direct correlation between compaction pressure and layer adhesion was detected, and the coefficient of variation was lower than 10% for all material combinations. The layer adhesion of Methocel K15M-Starch 1500 and Avicel PH-200-Tabettose 80 constantly increased with increasing compaction pressure up to 300 MPa, where it started to decrease. In contrast, the adhesion of tablets prepared with the combinations Tablettose 80-Methocel K15M and Tablettose 80-Starch 1500 reached a plateau while at low compaction pressure, and no further improvement was obtained.

3.2.2.3. Reproducibility

Three independent powder blends of the combination Methocel K15M-Emcompress were lubricated with 0.5% Mg stearate in Turbula mixer for 10 minutes and compressed to tablets at 250 MPa. The samples (n = 10) were stored in climate chamber at 25°C and 40% RH, to avoid any temperature and moisture effect, and the layer adhesion was tested after 1 day and 5 days (Fig. 40).

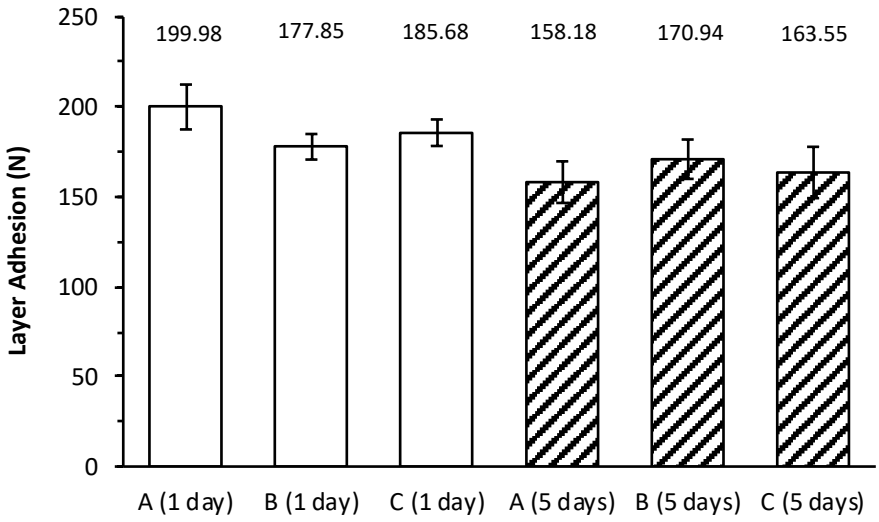

Figure 40. Layer adhesion measured for the same layer combinations prepared in independent batches and tested at different time-points.

A slight variation in layer adhesion was observed within the batches tested the same day, but the difference was reported not significant by means of a two-ways ANOVA (p = 0.056). Instead, this variability was caused by small differences in preparation of the powder blend (in particular during lubrication and mixing steps) and the intrinsic variability of the consolidation mechanism in compression process. In contrast, the time elapsed between tablet preparations and testing was reported as the significant factor leading to layer adhesion difference (p < 0.001).

3.2.2.4. Evaluation of tablet positioning during the test

To assess the influence of tablet positioning in the testing device, a large batch of Tablettose 80-Starch 1500 combination tablets was prepared at 250 MPa and tested at 5 different positions (Fig. 41).

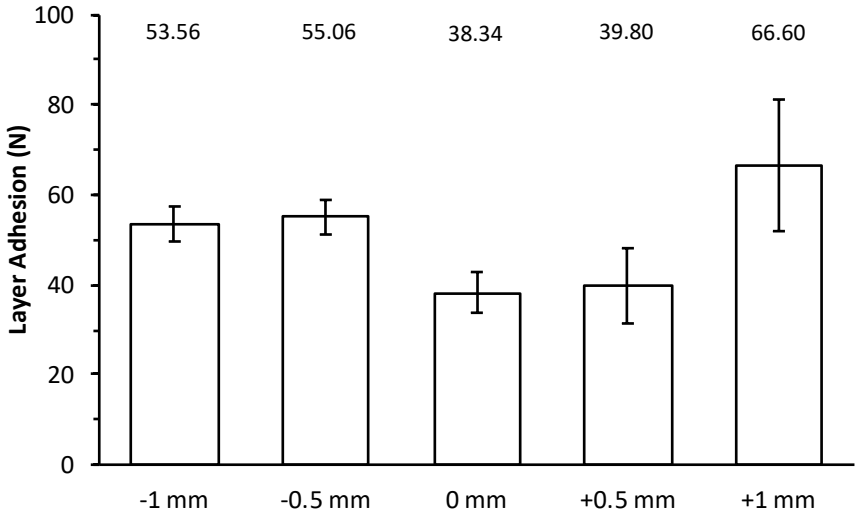

Figure 41. Effect of tablet misplacement on layer adhesion, evaluated with shear device (version 3): "0 mm" refers to the correct alignment of layer interface and shear device; a positive deviation refers to a protruding tablet position.

The zero position (0 mm) was selected as the position were the layer interface was perfectly aligned with the tablet holder interface. From this position, an incremental variation of 0.5 mm was imposed up to +/- 1 mm. A small misplacement was considered negligible if the tablet interface was positioned slightly above the device surface (< 0.5mm).

3.2.3. Evaluation of storage conditions on layer adhesion

3.2.3.1. Experimental setup

Previous experiments (cf. 3.2.2.3.) reported a time-dependent decay of layer adhesion. However, the impact of the time elapsed between preparation and testing changes depending on moisture and temperature conditions during storage.

The evaluation of the effect of storage time and conditions on layer adhesion was performed on two excipient formulations: Methocel K15M-Avicel PH-200 was selected as combination of hygroscopic materials [113,114] and a remarkable impact of moisture on layer adhesion was expected; Vice versa, Ethocel 4-Emcompress was selected as non-hygroscopic combination [115,116], with lower impact of moisture on layer adhesion.

The powders were lubricated with 0.5% Mg Stearate in Turbula Mixer and a single large batch for each formulation was prepared at 250 MPa compaction pressure. Afterwards, samples for each batch were stored for 30 days under the following conditions:

A. 5°C, 1% RH
B. 5°C, 75% RH
C. 25°C, 40% RH
D. 40°C, 1% RH
E. 40°C, 75% RH

The condition C represents the standard conditions in which handling, packaging and storage are normally performed. The other conditions were selected to evaluate the change in layer adhesion under thermal stress or exposition to unconventional humidity levels, during a storage period of 30 days.

3.2.3.2. Stability of hygroscopic combination

Layer adhesion for Methocel K15M-Avicel PH-200 combination stored in standard conditions (25°C, 40% RH) presented a slight decrease in layer adhesion (Fig. 42).

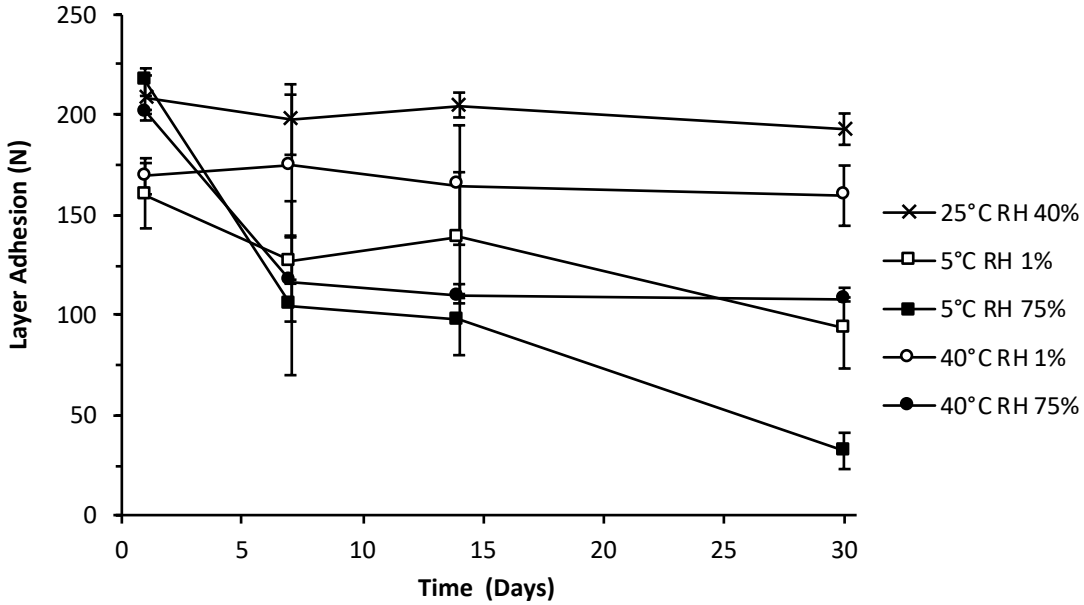

Figure 42. Effect of storage time and conditions on layer adhesion of Methocel K15M-Avicel PH-200 combinations.

As expected, a remarkable reduction in layer adhesion was observed already after 7 days (~ 50%) on tablets stored at high moisture level (75% RH), and a larger decrease was obtained after 30 days (~ 85%). In contrast, the tablets stored at low humidity (1% RH) presented an initial decrease in layer adhesion (~ 20%), but an overall lower reduction over the time, compared to high moisture conditions. The hygroscopic nature of Avicel PH-200 and Methocel K15M caused a remarkable variation on layer diameter of stored tablets, proportional to the change in moisture level compared to the standard storage conditions (25°C, 40%) (Table 11).

Table 11. Layer diameter and relative change from the standard conditions (25°C, 40% RH) of Avicel PH-200-Methocel K15M combination after 30 days.

Batch	d_1 (mm)	d_2 (mm)	Δd_1%	Δd_2%
25°C, 40% RH	10.931	10.983		
5°C, 1% RH	10.828	10.914	-0.94	-0.63
5°C, 75% RH	11.166	11.190	2.15	1.88
40°C, 1% RH	10.904	10.963	-0.25	-0.18
40°C, 75% RH	11.058	11.027	1.16	0.40

Tablets prepared with hygroscopic materials and stored at high moisture conditions presented higher change in layer diameter, compared to low moisture storage conditions. The different expansion or contraction of each layer caused a radial strain, with consequent reduction in layer adhesion [85]. This expansive phenomenon was remarkable for tablets stored at high moisture conditions, weather the contraction at low humidity levels had no remarkable impact on layer adhesion.

A negative effect of storage temperature on layer adhesion was detected, but up to 14 days it had a low impact than the moisture effect. Tablets stored at low temperature (5°C) presented a lower layer adhesion compared to the batches stored at higher temperature (40°C), at same humidity conditions (Fig. 42). Low temperature storage conditions promoted a remarkable reduction on layer adhesion after 30 days (~ 85.18%), compared to the higher temperature condition. Similarly, to the moisture effect, a change in storage temperature caused thermal expansion or contraction of tablet layers, and consequent generation of radial stresses (Table 11). Therefore, 25°C and 40% RH was selected as standard storage conditions for the test.

3.2.3.3. Stability of non-hygroscopic combination

Layer adhesion for Ethocel 4-Emcompress combination presented no sensitivity to temperature or moisture conditions (Fig. 43), compared to the previously tested combinations (cf. 3.2.3.2.).

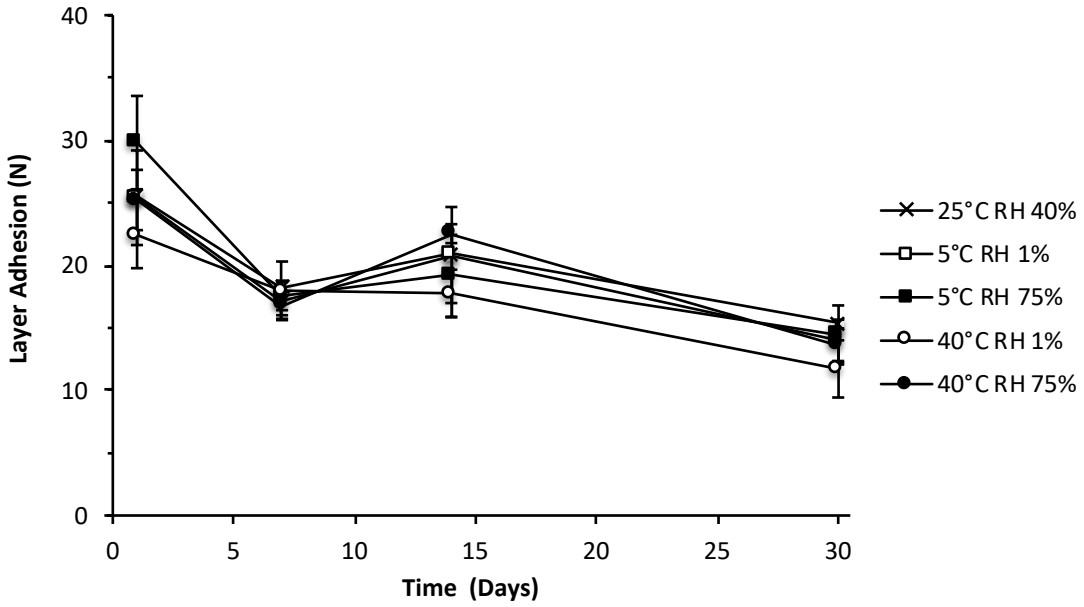

Figure 43. Effect of storage time and conditions on layer adhesion of Ethocel 4-Emcompress combinations.

The low impact of moisture on layer adhesion for this combination is determined by the non-hygroscopic nature of the materials in use. Similarly, no remarkable effect of temperature on layer adhesion was identified. However, the overall decline of layer adhesion (~ 50%) was attributed to the effect of the elapsed time between production and testing. The expansion and contraction of layer diameter due to humidity adsorption was not remarkable for this combination, due to the non-hygroscopic nature of the excipients in use (Table 12).

Table 12. Layer diameter and relative change from the standard conditions (25°C, 40% RH) of Ethocel 4-Emcompress combination after 30 days.

Batch	d_1 (mm)	d_2 (mm)	Δd_1%	Δd_2%
25°C, 40% RH	11.046	10.958		
5°C, 1% RH	11.034	10.940	-0.11	-0.16
5°C, 75% RH	11.023	11.051	-0.20	0.85
40°C, 1% RH	10.989	10.968	-0.52	0.09
40°C, 75% RH	11.010	11.020	-0.33	0.57

3.3. Evaluation of manufacturing process parameters leading to delamination of multilayer tablets

The main challenge encountered in manufacturing of bilayer tablets is the occurrence of delamination, as layer separation at the layer interface [112]. This may cause the tablet to lack of necessary layer adhesion to stand handling, packaging and storage processes, leading to the product failure. Therefore, beside standard requirements of hardness and friability, layer adhesion of multilayer tablets is measured as resistance offered to stress application.
Young's modulus [61,64,117,118] and the difference in elastic recovery of excipients comprised in the layers [88] are suggested as reasons leading to delamination of bilayer tablets. A great difference in elastic modulus between layers causes an unequal expansion during decompression: this generates radial stresses at the interface, which subsequently weaken layer bonds and lead to delamination [117]. Moreover, the layers may relax at different rates, thus contributing to the increase of radial stresses.

In the present study, the influence of process parameters on layer adhesion was investigated. Since material properties strongly affect tablet delamination, mixtures of three excipients were selected to simulate potential pharmaceutical formulations as combinations of immediate (calcium phosphate dehydrate and microcrystalline cellulose) and sustained (calcium phosphate dehydrate and hydroxypropyl methylcellulose) drug releases. The elasticity of these excipients was estimated by mean of their elastic recovery. A novel shear stress test was developed and evaluated for the measurement of tablet layer adhesion, where a custom-made device was used in combination with a compaction simulator (cf. 3.2.). Moreover, a central composite design of experiment was performed with the mentioned excipients combinations. Three process parameters affecting tablet delamination were investigated pre-compaction, main compaction and turret rotation speed. So far, these process parameters have been studied only as independent factors. Hence, the interaction of process parameters has been evaluated during this study as an additional reason for bilayer tablet delamination.

3.3.1. Characterization of material properties

3.3.1.1. Plasticity and elasticity evaluation

Plastic materials are characterized by low yield pressure and high elasticity [22]. These properties are critical to understand the behavior of the material during compaction under different process conditions, therefore yield pressure, elastic recovery, elastic and plastic work were measured for all the excipient in use (Table 13).

Table 13. Yield Pressure (P_y), elastic recovery (E_R%), plastic work (W_P) and elastic work (W_E) measurements for different excipients (n = 3).

Material	P_y (MPa)		E_R%		W_E (J)		W_P (J)		W_E %	W_P %
	Mean	SD	Mean	SD	Mean	SD	Mean	SD		
Avicel PH-112	85.81	5.41	7.01	0.20	0.65	0.03	9.74	0.09	6.28	93.71
Emcompress	286.87	4.71	4.41	0.27	0.51	0.04	15.01	0.24	3.30	96.70
Ethocel STD 4	22.42	0.31	10.91	0.01	3.05	0.85	7.40	0.16	29.14	70.86
Kollidon SR	50.20	1.95	8.38	0.20	2.19	0.06	11.53	0.19	15.95	84.05
Methocel K15M	33.94	1.58	13.71	0.92	1.30	0.04	6.70	0.25	16.28	83.72

Microcrystalline cellulose, ethylcellulose, polyvinylpyrrolidone and hydroxypropyl methylcellulose fell in the category of plastic materials because of their yield pressure values smaller than 135 MPa [21,22]. The elastic recovery was used as an estimation of the material elasticity. As expected, excipients defined as plastic materials had high elastic recovery (ER% > 8-10%) and high elastic work after compaction (W_E%), measured as ratio on the total work. A low value of elastic work was measured for Avicel PH-112 (6.28%), in contrast with the observed high elastic recovery. This suggested that, during decompression, the expansion of microcrystalline cellulose tablets was slower than other excipients, resulting in an elastic work lower than expected. In contrast, brittle excipients like Emcompress do not present a strong expansion after decompression. The lack of elasticity of Emcompress was confirmed also by the elastic work measured during compaction (3.30%). Most of the energy was used in fragmentation and bond formation therefore, mostly retained in the tablet [119].

3.3.1.2. Analysis of differences in elastic recovery

In order to evaluate the effect of increasing difference in elastic recovery on layer adhesion, tablets comprising plastic and brittle excipient combinations were prepared at different compaction pressures and tested by layer adhesion. The lowest adhesion values were observed for plastic-plastic formulations characterized by a high difference in elasticity (Fig. 43 A).

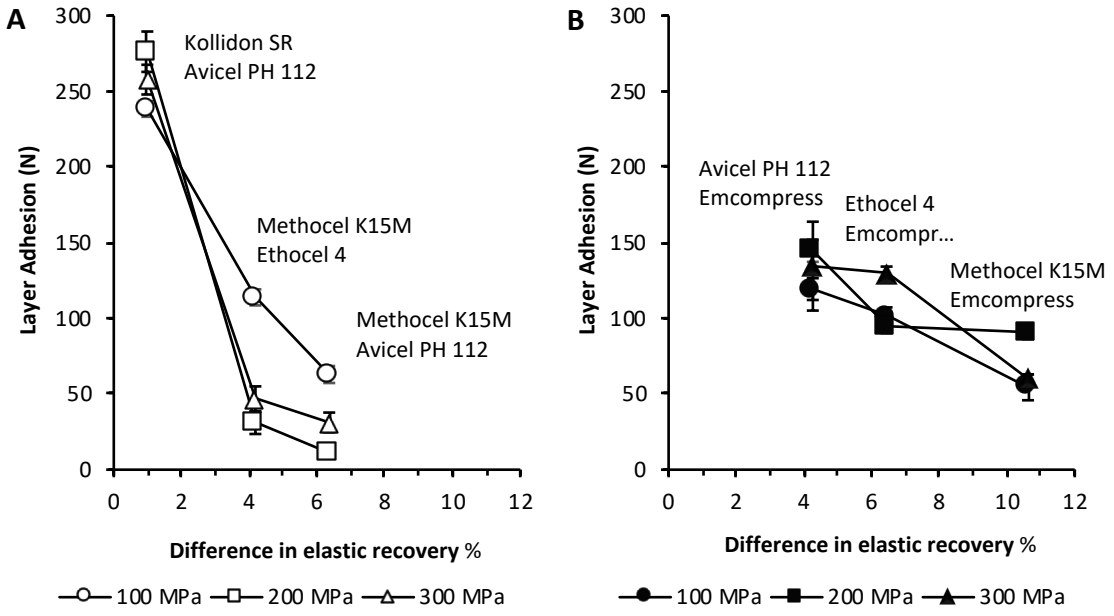

Figure 43. Effect of difference in elastic recovery on layer adhesion for (A) plastic-plastic and (B) plastic-brittle combinations.

The difference in elastic recovery caused the weakening of the bonds between layers (Busignies et al., 2013; Podczeck and Al-Muti, 2010), probably due to high stresses in radial and axial directions generated during decompression and ejection, resulting in a lower layer adhesion [117]. Furthermore, the second layer compaction pressure had a strong effect on layer detachment: as the pressure increased from 100 to 300 MPa, combinations with high elasticity difference exhibited a greater reduction in layer adhesion. In contrast, the layer adhesion of formulations with plastic-brittle materials was not remarkably affected by the compaction pressure and difference in elastic recovery, although a variation was present (Fig. 43 B).

In order to evaluate formulations with different elastic recovery, plastic-plastic (Methocel K15M-Avicel PH-112) and plastic-brittle (Avicel PH-112-Emcompress) combinations with the highest difference in elasticity were selected and investigated with a Design of Experiments, evaluating the effect of manufacturing process parameters towards the layer adhesion. The brittle-brittle material combination (Emcompress-Emcompress) was selected as reference with no difference in elastic recovery.

3.3.2. Experimental design

The evaluation of the effect of process parameters on layer adhesion was performed with a Design of Experiment, which provided coefficients (or estimates) of the model equation for each factor. These values indicated the extent, the trend (positive or negative) and, if applicable, the non-linearity (as factor squared) of each parameter. The most significant factors were identified as a function of the *p*-value ($p < 0.05$). Furthermore, the significance of the obtained models was assessed with an ANOVA test, and the goodness of fit was evaluated through the coefficient of regression R^2.

3.3.2.1. Effect of process parameters on layer adhesion of brittle-brittle combination

The difference in elastic recovery of two layers resulted in a negative effect of the compaction pressure on layer adhesion (cf. 3.3.1.2.). By definition, the difference in elastic recovery between layers of the same material is equal to zero. Therefore, the brittle-brittle combination was selected as a reference formulation, not affected by the difference in the elastic properties of the layers. No negative effect of the compaction pressure on the layer adhesion was expected, even at high pressures (>200 MPa). Furthermore, brittle materials are known to be insensitive to strain rate [23]. Hence, the turret rotation speed was not expected to be a significant factor in the mathematical model.

The Design of Experiment performed on the brittle-brittle combination provided a significant model ($p = 0.0009$, $R^2 = 0.9693$), which described 69.92% of the data by a single principal effect, and no significant interactions were identified. The main compaction pressure was the only significant factor, and its effect on layer adhesion was independent of the rotation speed and pre-compaction pressures (Table 14). This confirmed the initial hypothesis.

Table 14. *p*-Values and parameter estimates of Emcompress-Emcompress combination.

	Pre	Main	Rtn	Pre·Main	Pre·Rtn	Main·Rtn	Pre·Main·Rtn	Pre ^{2}	Main ^{2}	Rtn ^{2}
Estimate	-8.334	95.614*	-6.256	-12.009	-5.714	-2.159	-3.796	49.568*	13.598	23.928
***p*-Value**	0.3288	<0.001*	0.456	0.220	0.539	0.814	0.681	0.017*	0.405	0.166

Pre = pre-compression pressure, Main = main compression pressure, Rtn = turret rotation speed;
"*" indicates significant factors and "2" indicates non-linear parameters

The reduction of dwell time caused by the increase in rotation speed had no significant effect on layer adhesion, due to the unresponsive nature of brittle materials to strain rate, as indicated by the surface of response for the combination Emcompress-Emcompress (Fig. 44).

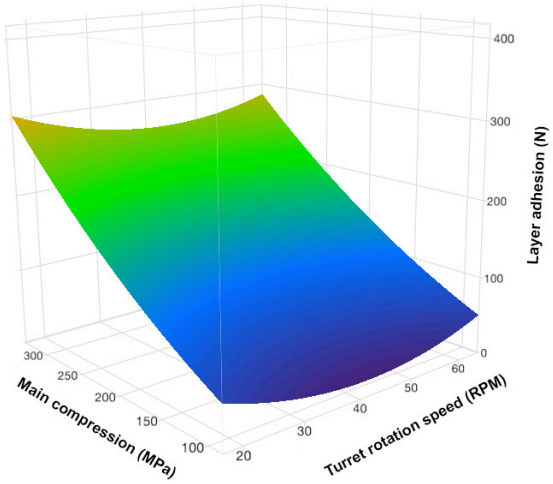

Figure 44. Effect of main compaction and turret rotation speed on layer adhesion: surface plot of Emcompress-Emcompress formulation.

Indeed, the layer adhesion increased proportionally to the increase of compaction pressure applied. Furthermore, the model identified a non-linear effect of pre-compaction pressure (Pre^2 p = 0.0171) (Table 14). Since pre-compaction had no significant effect on layer adhesion and the estimate of $pre\text{-}compaction^2$ was remarkably lower than main compaction value, the non-linearity was considered as negligible.

3.3.2.2. Effect of process parameters on layer adhesion of plastic-plastic combination

Methocel K15M and Avicel PH-112 were selected to evaluate a plastic-plastic formulation with a pronounced difference in elastic recovery between the excipients of the two layers (6.70%). Based on previous experiments concerning elastic recovery (cf. 3.3.1.2.), a strong influence of material elasticity on layer adhesion was expected with this excipients combination.

The performed Design of Experiment on bilayer tablets with the combination of Methocel K15M and Avicel PH-112 provided a significant model (p = 0.0075, R^2 = 0.9361), which described 74.96% of the data by three principal parameters (pre-compaction, main compaction and turret rotation speed) and three 2-factors interactions (pre-compaction·main compaction, pre-compaction·rotation and main compaction·rotation) (Table 15).

Table 15. *p*-Values and parameter estimates of Methocel K15M-Avicel PH-112 combination.

	Pre	Main	Rtn	Pre·Main	Pre·Rtn	Main·Rtn	Pre·Main·Rtn	Pre ²	Main ²	Rtn ²
Estimate	-12.897*	-9.415*	-12.897*	-9.739*	9.856*	-7.294*	7.336*	-10.555	25.335*	9.675
***p*-Value**	0.008*	0.029*	0.008*	0.038*	0.037*	0.095*	0.094*	0.149	0.007*	0.180

Pre = pre-compression pressure, Main = main compression pressure, Rtn = turret rotation speed;
"*" indicates significant factors and "²" indicates non-linear parameters

Among the principal factors, pre-compaction and rotation speed had the same negative effect on layer adhesion, while main compaction resulted to have a less negative impact. The interactions pre-compaction·main compaction and pre-compaction·rotation had opposite effect on layer adhesion, both to a similar extent. Based on the *p*-value higher than 0.05, all other parameters and interactions were not significant, therefore they were not considered in the following discussion and no further model optimization was performed. The negative effect of pre-compaction on layer adhesion was attributed to the reduction in surface roughness of the first layer, which resulted in less bonding area and particle interlocking, within the experimental limits. However, the extent of this effect was lower than what was reported in the literature [79], perhaps because the pre-compaction range in the present work was set to a lower value. Indeed, an excessive increase of pre-compaction would determine to a flat bonding surface, preventing the interaction with the second layer. The main compaction had a non-linear effect (Main^2 p = 0.0073), identified with a concave curvature on the surface of response obtained by applying a central composite Design of Experiment: the upper and lower boundaries represented the best conditions to obtain good layer adhesion (Fig. 45).

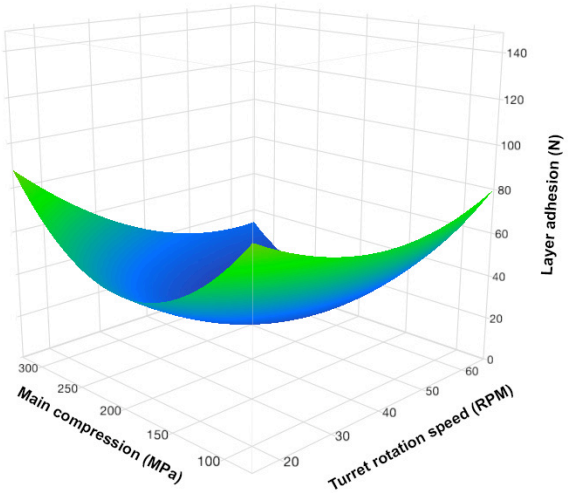

Figure 45. Effect of main compaction and turret rotation speed on layer adhesion: surface plot of Methocel K15M-Avicel PH-112 formulation.

The formation of stronger bonds occurred at high pressures due to increased plastic flowing and surface interaction. However, the increasing pressure also generated a greater elastic rebound. As previously mentioned (cf. 3.3.1.1.), the combination Methocel K15M-Avicel PH-112 was characterized by high elastic recovery difference (6.70%), and the layer adhesion was markedly influenced by the compaction pressure. Therefore, this effect could be partially counterbalanced

by the higher bonding occurring at high pressures, which justified the non-linearity of this parameter and the increase in layer adhesion at high compaction pressures.

Turret rotation speed had a negative effect on the layer adhesion due to the reduction of dwell time and simultaneous increase in strain rate (Table 15). As the speed of the tablet press increased, the extent of this negative effect increased because the plastic flowing demanded a certain time in order to determine tablet consolidation [106,120].

The interactions pre-compaction·rotation and pre-compaction·main compaction had similar extent, but with opposite effect on layer adhesion. The interactions pre-compaction·rotation had a positive impact on layer adhesion (Table 15): pre-compaction provided an initial improvement uniquely at high speed (60 RPM), but above 10-15 MPa the combination of negative effects due to rotation speed and pre-compaction prevailed and the layer adhesion value decreased below 15 N (Fig. 46).

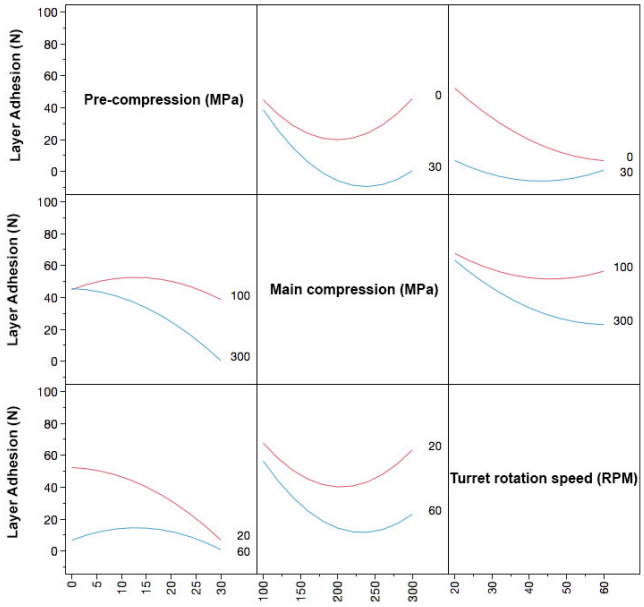

Figure 46. Methocel K15M-Avicel PH-112 formulation: interaction profile.

This interaction had no positive effect on layer adhesion at low turret rotation speed, suggesting that the high surface roughness due to lower pre-compaction pressure was counterbalanced by a higher strain rate as a result of a greater volume of the first layer when in the range 0-15 MPa. Furthermore, at high rotation speed, the high pressure could contribute to increasing the strain rate because the punches travelled deeper into the die within the same timeframe.

A layer adhesion of about 30N was considered the minimum layer adhesion required to withstand handling, production and packaging processes. Therefore, the slight improvement given by the

interaction pre-compaction pressure·turret rotation speed was considered not sufficient for a successful manufacturing.

In contrast, the interaction between pre-compaction and main compaction pressure had a remarkable negative effect on layer adhesion (Table 15). As previously discussed, the pre-compaction was responsible for the decrease in surface roughness and consequent decrease in layer adhesion, which the main compaction pressure could not compensate for. Furthermore, this negative effect was dependent on the turret rotation speed and it was particularly visible at high speeds. A layer adhesion above 30 N was obtained at any main compaction value throughout the pre-compaction range 0-20 MPa at 20 RPM (Figure 47).

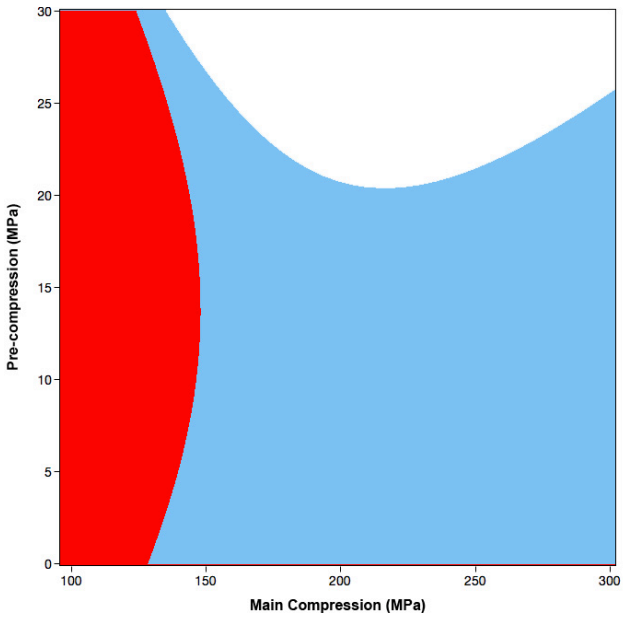

Figure 47. Methocel K15M-Avicel PH-112 formulation: contour plot of layer adhesion higher than 30 N (blue area 20 RPM and red area 60 RPM).

In contrast, a sufficient layer adhesion was only obtained at 60 RPM with the main compaction being in the range 100-150 MPa. To improve the layer adhesion at high rotation speed, an increase of main compaction pressure would be expected to compensate the negative effect of the decreased dwell time and increased strain rate. Instead, high pressure and speed conditions led to the lowest layer adhesion (Fig. 47). The higher elasticity of plastic materials was suggested as a possible cause for the effect, since at high pressures the elastic rebound was generally higher (cf. 3.3.1.2.).

3.3.2.3. Effect of process parameters on layer adhesion of plastic-brittle combination

Methocel K15M-Emcompress were selected to evaluate a plastic-brittle combination, which possessed a pronounced difference in elastic recovery (9.30%). Based on the results obtained for the elastic recovery (cf. 3.3.1.2.), a slight influence of material elasticity on layer adhesion was expected with this combination.

The Design of Experiment on bilayer tablets with the combination of Methocel K15M and Emcompress provided a significant model ($p = 0.0081$, $R^2 = 0.9343$), which described 73.59% of the data by two principal effects (Table 16), and no significant interactions were obtained.

Table 16. *p*-Values and parameter estimates of Methocel K15M-Emcompress combination.

	Pre	Main	Rtn	Pre·Main	Pre·Rtn	Main·Rtn	Pre·Main·Rtn	Pre ^{2}	Main ^{2}	Rtn ^{2}
Estimate	-3.883	-42.094*	-18.534*	-5.49	-7.634	3.544	-8.349	2.611	-16.096*	7.461
***p*-Value**	0.377	0.002*	0.007*	0.226	0.144	0.465	0.329	0.587	0.008*	0.379

Pre = pre-compression pressure, Main = main compression pressure, Rtn = turret rotation speed;
"*" indicates significant factors and "²" indicates non-linear parameters

The main compaction and turret rotation speed were identified as the most important factors. All parameters and interactions with *p*-value higher than 0.05 were not significant, therefore they were not considered in the following discussion.

As previously reported for the brittle-brittle formulation, the compaction pressure had a remarkable effect on the layer adhesion due to the presence of brittle materials. Therefore, a similar behavior was expected even for the plastic-brittle combination (cf. 3.3.2.1.). However, as the compaction pressure increased, the high elastic rebound typical of Methocel K15M, became the major effect, leading to a swift decrease in layer adhesion. This non-linear trend was detected as a concave curvature on the surface of response (Main^2 $p = 0.0075$) (Fig. 48), due to the contribution of both excipients, and up to 150-200 MPa, the behavior was similar to the brittle-brittle formulation.

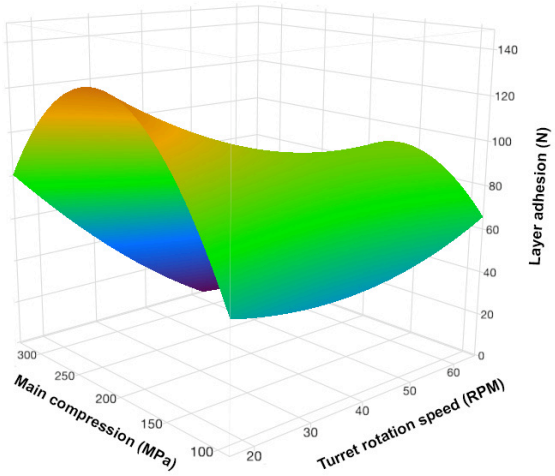

Figure 48. Effect of main compaction and turret rotation speed on layer adhesion: surface plot of Methocel K15M-Emcompress combination.

Above 250 MPa, irrespective of the turret rotation speed, the formulation acted similarly to the plastic-plastic combination, where the decrease in layer adhesion was driven by the difference in elastic recovery. This outcome was in partially contrasting other studies [58], where a direct proportion between compaction and layer adhesions was obtained, testing a formulation with a plastic material in the first layer. Probably, the change in the trend was not observed because of the experimental settings, which limited the compaction pressure to a lower level (230 MPa).

The turret rotation speed had a negative effect, which was due to the strain rate sensitivity of Methocel K15M. Indeed, the plastic flowing required a certain time to effectively create bonds, therefore, as the turret rotation speed increased, the dwell time and the bonding decreased [106,120].

3.3.2.4. Comparison of Design of Experiments with different material combinations

The consolidation mechanism of plastic (*i.e.* plastic flowing) and brittle (*i.e.* fragmentation) are well documented in literature and mainly depend on the punches dwell time, hence on the turret rotation speed [106,119,120].

As expected, the combination with brittle-brittle materials had a negligible influence of rotation speed on layer adhesion. Despite the initial brittle behavior, the excipient combination Methocel K15M-Emcompress presented a remarkable impact of the turret rotation speed on layer adhesion (Fig. 48). It was supposed that the initial adhesion was promoted by Emcompress fragmentation, causing a great increase of the bonding surface. However, the negative impact of elasticity on layer adhesion prevailed at high compaction pressures.

The evaluation of the plastic-plastic formulation demonstrated that pre-compaction had a remarkable impact on layer adhesion, in particular at high rotation speed: high pre-compaction pressures might lead to a flat layer interface, preventing the particle interlocking and the interlayer bond formation. In contrast, the layer adhesion of the brittle-brittle combination was not affected by the level of pre-compaction pressure. Therefore, it was reasonable to expect a combination of the two consolidation mechanisms for the plastic-brittle formulation. Indeed, the formulations Methocel K15M-Avicel PH-112 (Fig. 45) and Methocel K15M-Emcompress (Fig. 48) presented an opposite trend on their response surfaces: the plastic-plastic combination had a convex curvature, while the plastic-brittle combination presented a concave curvature. This was not caused by a different sequence in layer compaction, since in both formulations Methocel K15M was present in the first layer. Furthermore, the materials in each layer had similar differences in elastic recovery (Methocel K15M-Avicel PH-112 6.61% and Methocel K15M-Emcompress 9.30%). Therefore, it was suggested that the opposite trend was caused by the different material combination in use: plastic-plastic and plastic-brittle combination, respectively. Probably, the presence of a brittle material in the second layer could counterbalance the negative effect on layer adhesion given by the difference in elastic recovery. The practical outcome of this difference concerns the potential manufacturing range in which the layer adhesion is sufficiently high (>30 N). Indeed, the plastic-brittle combination offered a wide area for production, whether the plastic-brittle formulation presented a strong adhesion only at the boundary of the experimental setup.

3.3.3. Analysis of strain rate

Strain rate is defined as the change in deformation (or strain) of a material with respect of time. Depending on material properties, a different impact on the consolidation mechanism is expected [121]. In literature, plastic materials are well documented to be strain rate sensitive [17,21,122,123]. Indeed, at high rotation speed, the reduction in dwell time determines a lack of particle consolidation and low tablet hardness, while tableting plastic formulations. As previously supposed (3.3.2.2.), high pressure could contribute to increase the strain rate because the punches travelled deeper into the die within the same timeframe. The punch movement was recorded during compaction cycles at 100 and 300 MPa, both at low and high speed (20 RPM and 60 RPM, respectively) and the strain rate was calculated.

3.3.3.1. Evaluation of strain rate at 20 RPM

At low speed, as the lower punch started the movement, the strain rate profile had an initial spike (16.58 s^{-1}) (Fig. 49 B).

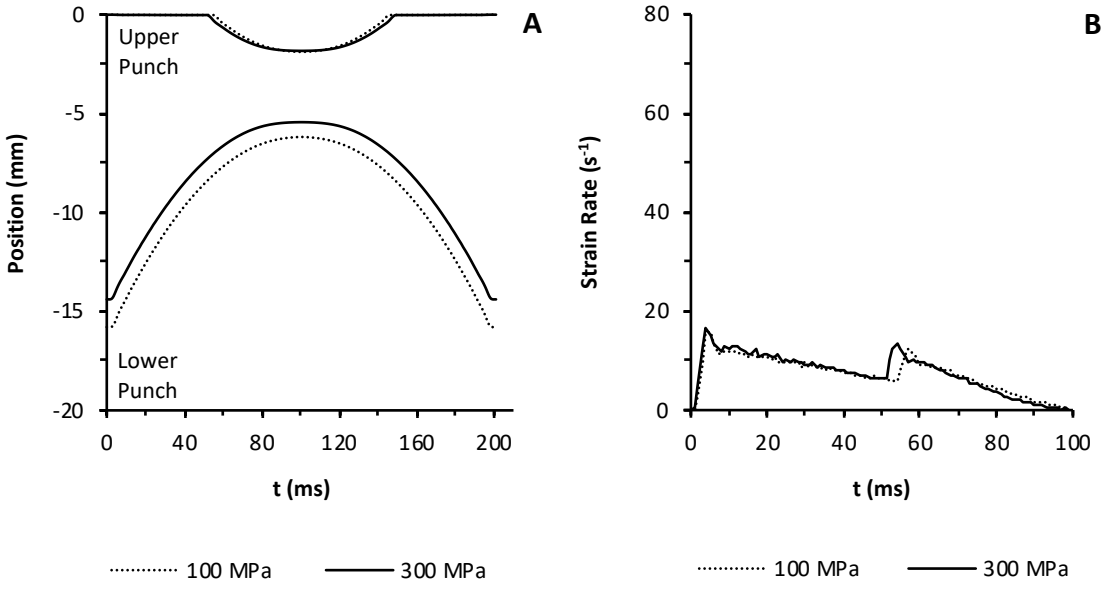

Figure 49. Compaction cycle at 20 RPM: (A) position of the punches and (B) strain rate (de-compaction not depicted).

The bell-shape movement profile of the lower punch (Fig. 49 A) determined a constant decrease in strain rate. After 56 ms, the upper punch started the downward movement, increasing two-folds strain rate value (from 5.735s^{-1} to 12.483 s^{-1}). As the punch gap reached the lowest value (after 100 ms), the strain rate decreased to zero. The shift toward right observed for the strain rate in the compaction profile at 100 MPa was determined by an initial lag of the upper punch movement (Fig. 49 A). Indeed, the change in compaction pressure caused a slightly different movement of the punches, hence slightly different strain rate profiles.

3.3.3.2. Evaluation of strain rate at 60 RPM

In contrast, the strain rate profile at 60 RPM had no spike (Fig. 50 B), because movement of the lower punch was almost constant throughout the initial part of the compaction cycle (Fig. 50 A).

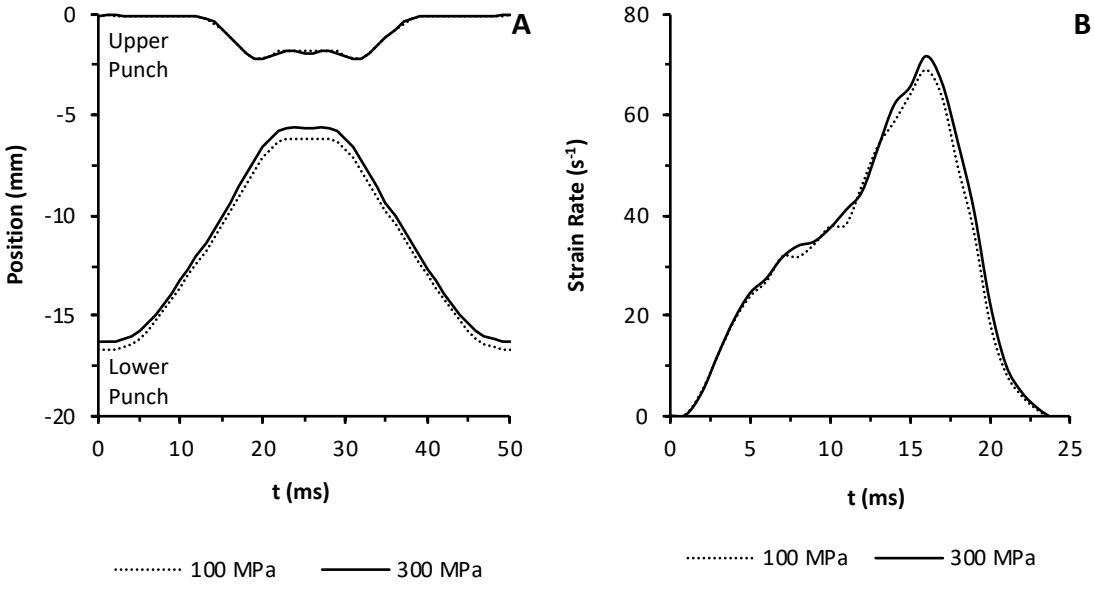

Figure 50. Compaction cycle at 60 RPM: position of the punches (A) and strain rate (B) (de-compaction not depicted).

After 13 ms, the upper punch started the downward movement, resulting in an abrupt increase of the strain rate to 71.731 s^{-1}. As the punch gap reached the lowest value (25 ms), the strain rate decreased to zero. The indentation observed on punch profiles between 20 and 30 ms was caused by punch and press elasticity (Fig. 50 A). Indeed, elasticity is a property belonging to every material, at different extents. At high pressure, metal parts of the compaction simulator and tooling are subjected to deformation, proportional to the applied load. This behavior was not present at lower compaction pressure.

3.3.3.3. Comparison of strain rates at different press speeds

Consolidation and maximum particle bonding occurred, while the punches were at the minimum gap. Therefore, the effect of compaction pressure on the strain rate was evaluated in the range 60-100 ms at 20 RPM and 15-25 ms at 60 RPM. For each time-point, the instantaneous difference in strain rate between the compaction profiles at 100 and 300 MPa were calculated and the two mean values were compared.

It was observed a difference in strain rate of 0.0567s^{-1} (0.907%) between the profiles recorded at different compaction pressure at 20 RPM. In contrast, the average difference at 60 RPM was 40-fold higher, reaching 2.435 s^{-1} (8.039%). Therefore, it was concluded that the influence of an increase in compaction pressure on the strain rate was remarkable only at high rotation speed (60 RPM). Furthermore, this confirmed the hypothesis proposed to explain the positive effect of the pre-compaction·rotation interaction with plastic-plastic excipient combinations (cf. 3.3.2.2.). Indeed, at high rotation speed, the high pressure contributed to increase the strain rate because the punches travelled deeper into the die within the same timeframe.

3.3.4. Validation of the experimental design

As expected, the results of the Design of Experiments were strongly dependent on the type and combination of materials in use. The plastic-plastic combination was affected by all process parameter and by the difference in elasticity of the excipients in use, instead the plastic-brittle formulation was not sensitive to a change in pre-compaction pressure. Despite the same first layer of Methocel K15M, the properties of the excipient in the second layer caused remarkable differences. Probably, the formulation behavior was determined by the differences plasticity/brittleness and elasticity, critical material properties to consider in multilayer tableting. To confirm this hypothesis, two supplementary Design of Experiment were performed on the same process parameters. The combinations were modified, replacing an excipient with another one to keep constant the formulation properties: Kollidon SR-Avicel PH-112 as plastic-plastic combination and Avicel PH-112-Emcompress as plastic-brittle combination.

3.3.4.1. Validation of the plastic-plastic combination

The combination Kollidon SR-Avicel PH-112 possessed a slight difference in elastic recovery (1.37%), lower than the other plastic-plastic formulation. Therefore, a negligible influence of material elasticity on layer adhesion was expected with this combination.

The Design of Experiment performed on bilayer tablets provided a significant model (p = 0.0380, R^2 = 0.9286), which described 69.97% of the data by two principal effects (Table 17), pre-compaction and turret rotation speed, and three interactions (pre-compaction·main compaction, pre-compaction·rotation and main compaction·rotation).

Table 17. *p*-Values and parameter estimates of Kollidon SR-Avicel PH-112 combination.

	Pre	Main	Rtn	Pre·Main	Pre·Rtn	Main·Rtn	Pre·Main·Rtn	Pre ^{2}	Main ^{2}	Rtn ^{2}
Estimate	61.718*	-14.936	-51.508*	40.988*	-46.798*	38.428*	31.508	44.280	-8.470	36.40
***p*-Value**	0.0034*	0.300	0.0079*	0.0318*	0.0191*	0.0401*	0.0761	0.1324	0.7505	0.2024

Pre = pre-compression pressure, Main = main compression pressure, Rtn = turret rotation speed;
"*" indicates significant factors and "^{2}" indicates non-linear parameters

The effect of pre-compaction and rotation on layer adhesion of plastic-plastic combinations have been already discussed (cf. 3.3.2.2.). It was previously proposed that a large elasticity difference between materials comprised in the two layers could be the cause of sensitivity to main compaction pressure (cf. 3.3.1.2.) and source of non-linearity. In contrast to the previous Design of Experiment with plastic-plastic combination, the layer adhesion of Kollidon SR-Avicel PH-112 formulation was not affected by the main compaction pressure (p = 0.300) and no lack of linearity on this parameter was identified (Table 17). This result confirmed the hypothesis that an increase in elasticity difference promoted a higher sensitivity to main compaction, since the difference in elasticity between Kollidon SR and Avicel PH-112 was low, compared the other investigated combinations.

The interaction pre-compaction·rotation and main compaction·rotation have been already discussed (cf. 3.3.2.2.). The latter was explained by the increase in strain rate at high tableting pressures and this effect was visible on the surface of response, as a reduction in layer adhesion at high compaction pressure and turret speed (Fig. 51).

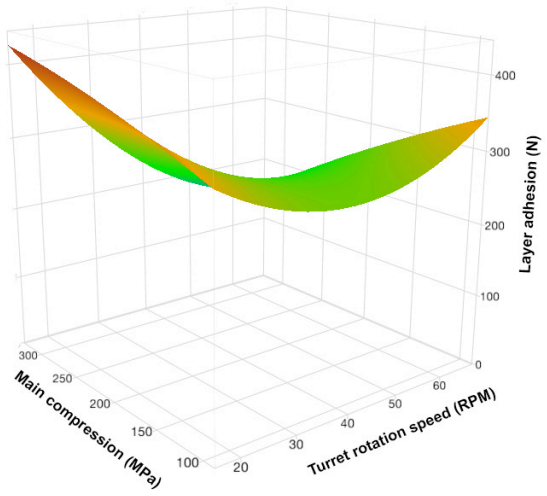

Figure 51. Effect of main compaction and turret rotation speed on layer adhesion: surface plot of Kollidon SR-Avicel PH-112 combination.

Interestingly, the shape of the surface of response for Kollidon SR-Avicel PH-112 combination was similar to the one observed for Methocel K15M- Avicel PH-112 formulation, hence these plastic-plastic combinations had a similar mathematical model (Fig. 44). However, the layer adhesion values were remarkably higher for Kollidon SR-Avicel PH-112 formulation and this difference was caused by the higher elasticity difference of the materials in use.

3.3.4.2. Validation of the plastic-brittle combination

As previously discussed (cf. 3.3.1.1.), the difference in elastic recovery between Avicel PH-112 and Emcompress was low, compared to other excipient formulations (2.60%). Therefore, a slight influence of material elasticity on layer adhesion was expected for this combination.

The Design of Experiment provided a significant model (p = 0.0066, R^2 = 0.9388), which described 94.32% of the data by two principal effects (pre-compaction and rotation) and a single two-ways interaction (main compaction·rotation) (Table 18).

Table 18. *p*-values and parameter estimates of Avicel PH-112-Emcompress combination.

	Pre	Main	Rtn	Pre·Main	Pre·Rtn	Main·Rtn	Pre·Main·Rtn	Pre ^{2}	Main ^{2}	Rtn ^{2}
Estimate	-19.13*	1.767	-18.308*	-2.0175	2.005	-19.398*	4.238	-52.17*	-72.771*	74.604*
***p*-Value**	0.0309*	0.8041	0.0363*	0.8001	0.8013	0.0438*	0.5983	0.0074*	0.0015*	0.0013*

Pre = pre-compression pressure, Main = main compression pressure, Rtn = turret rotation speed;
"*" indicates significant factors and "^{2}" indicates non-linear parameters

Moreover, it was noticed a strong non-linearity determined by pre-compaction and rotation (Pre^2 p = 0.0074 and Rtn^2 p = 0.0013), which curvature on the surface of response (Fig. 52). Main compaction was reported as well as source of a non-linearity (Main^2 p = 0.0015). Methocel K15M-Emcompress Design of Experiment already identified main compaction and rotation as significant process parameters, and no impact of pre-compaction on layer adhesion was reported (cf. 3.3.2.3.).

In contrast, the Avicel PH-112-Emcompress combination was remarkably affected by the pre-compaction and rotation. Indeed, during the pre-compaction phase the high compactability of Avicel PH-112 [78] have probably formed a smooth layer interface, which prevented a strong interaction with the material of the second layer. Moreover, no impact of main compaction was identified on Avicel PH-112-Emcompress combination, because of the low difference in elasticity of these excipients (2.60%), in comparison to Methocel K15M-Emcompress (9.30%).

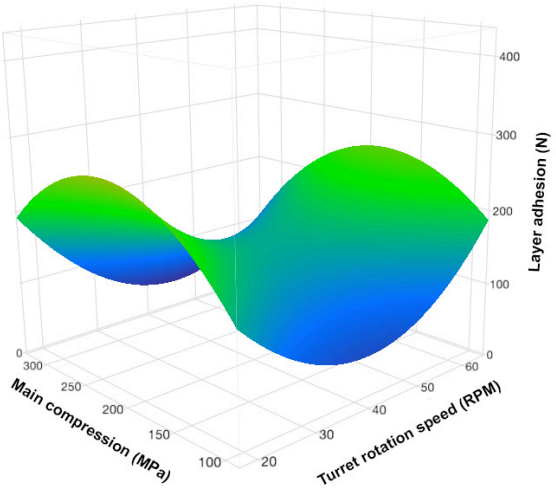

Figure 52. Effect of main compaction and turret rotation speed on layer adhesion: surface plot of Avicel PH-112-Emcompress combination.

The surface of responses obtained from the Design of Experiments of plastic-brittle combinations presented a profile with similar shape (Fig. 48 and 52), characterized by a saddle in the range 150-200 MPa with an initial increase in layer adhesion (brittle-brittle behavior) and, after 200 MPa a constant decrease as compaction pressure and press speed increase (plastic-plastic behavior). However, the turret rotation speed in the Design of Experiment Avicel PH-112-Emcompress formulation had a positive effect on the layer adhesion, especially at low values.

Despite this similar behavior, the surface of response for Avicel PH-112-Emcompress presented remarkably higher values of layer adhesion compared to the previous Design of Experiment with plastic-brittle combination. As previously discussed, the difference in elasticity of the materials constituting the layers had a remarkable impact on the layer adhesion of each formulation. In the Design of Experiment with plastic-brittle materials, Methocel K15M was replaced with Avicel PH-112, causing an increase of the difference in elastic recovery from 9.3% to 2.6%. The decrease of difference in elastic recovery was suggested to be the source of the significant difference in layer adhesion between the two Designs of Experiments.

4. Summary

Quality, safety and efficacy of single and multilayer tablets depend both on formulation and optimization of process parameters, such as press speed, pre-compaction and main compaction pressure. To date, the effect of these parameters on the final product quality have been extensively investigated, but fewer studies were focused on die filling process, which has a great impact on the content uniformity, in particular at high rotation speed. These studies have been conducted on custom model-shoe systems, which provide a good insight on the powder behavior during the process but are difficult to correlate to industrial scale process parameters. Alternatively, studies on die filling were performed on standard rotary presses to accurately replicate the filling process, at the cost of high material consumption.
To date, process parameters involved in the manufacturing of multilayer tablets have been investigated only in separated experiments. Hence, the effect of process parameters interactions on layer adhesion is still unknown and few studies evaluated the influence of material properties in bilayer tableting.

To overcome the aforementioned limitations, the die filling behavior of excipients commonly used in tableting was investigated through the replication of an industrial tablet press on a compaction simulator. The completeness of die filling for each material was correlated to the powder rheological properties to predict the effect of turret rotation speed on the filling process.
Moreover, a central composite design of experiment was performed to investigate the influence of process parameters and their interactions on delamination tendency of bilayer tablets. The layer adhesion was measured with a novel shear test, specifically developed to overcome the limitations of available methods, such as friction, elastic deformation of the test device and long setup time.

Particle properties and powder rheology are critical attributes towards the flow of each material, as they affected the filling process. Therefore, 9 excipients commonly used in tableting (Avicel PH-112, Avicel PH-200, Cellphere CP-102, Emcompress, Flowlac 90, Kollidon SR, Methocel K15M, Starch 1500 and Tablettose 80) were selected and characterized by Hausner ratio, residual moisture content, particle shape and size distribution and compared to rheological properties evaluated with a powder rheometer.
The filling process of the investigated materials was reproduced on a compaction simulator with gravity, forced and suction fill techniques. Good flowing excipients, such as Emcompress,

Cellphere CP-102, Tablettose 80 and Flowlac 90 were expected to have excellent die filling due to their optimal particle properties. In contrast, a complete die filling with gravity fill technique was observed at low press speed (15 RPM), instead at higher speeds a complete filling process was achieved only for Emcompress and Cellphere CP-102. The use of forced and suction fill techniques remarkably improved the completeness of the filling process because of the strong mechanical stresses applied on the loose powder, which prevented the formation of powder bridges and improved the powder motion in the feeder.

The die filling profiles were described with a semi-log equation and the calculated slopes were correlated to powder rheology measurements. A strong correlation was obtained between the semi-log equation slopes and Basic Flowability Energy ($R^2 = 0.902$), during die filling simulation with gravity fill. Similarly, a strong correlation was also obtained between the slopes equation slopes and the Specific Energy not normalized on sample mass ($R^2 = 0.931$). No significant correlation was identified with forced and suction fill techniques, because of the strong mechanical stresses, which promoted powder flowing of the excipients. The model was validated by predicting the behavior of Pearlitol 200 SD and confirmed by experimental values.

The Hausner Ratio was not suitable to describe the flow properties of Kollidon SR and Pearlitol SD 200. Indeed, the values for these excipients were not consistent with their die filling profiles, whereas the characterization of the rheological properties could predict the powder flowing behavior under standard conditions (*i.e.* gravity fill technique) with a good approximation. The novel technique offered the possibility to combine die filling and compaction properties evaluations on a single machine. This represents a first important step to promote a fast and efficient formulation development and scale up.

Afterwards, a novel test to measure the layer adhesion on bilayer tablets was developed to characterize tablets prepared with different compaction pressures and excipients. The device design was improved through different versions to fulfil 4 test requirements: short setup time, reproducibility, ability to differentiate tablets prepared with different excipients and compaction pressures. The device was adapted to be equipped on a compaction simulator, which ensured low elastic deformation and high data acquisition speed.

Maximal test speed (1 mm/s), compaction pressure and excipient differentiation, reproducibility and influence of tablet positioning were extensively evaluated to define the optimal test conditions. Moreover, the influence of temperature, moisture and storage time on layer adhesion were investigated both on hygroscopic and non-hygroscopic excipient combinations. Storage time and moisture were identified as critical parameters for hygroscopic materials, having a negative effect on layer adhesion. Instead, non-hygroscopic excipient combinations presented a reduction

in layer adhesion only dependent on storage time. The differential expansion of the layers due to moisture exposure was suggested as the cause of delamination or reduced layer adhesion of multilayer tablets. Moreover, 25°C and 40% RH were identified as the best condition to store multilayer tablets and reduce the layer adhesion decay during long term storage.

This novel test was used to investigate the effect of process parameters and material properties on layer adhesion of bilayer tablets. Three potential pharmaceutical formulations were selected as combinations of immediate (Emcompress and Avicel PH-112) and sustained (Emcompress and Methocel K15M) drug release. A 3-levels 3-factors central composite Design of Experiment was performed on each formulation to evaluate the effect of three process parameters (*i.e.* pre-compaction, main compaction and turret rotation speed) and their interactions towards tablet delamination. The shear test developed for this study was used to determine the tendency of the tablet to delaminate and the layer adhesion was employed as response factor in the Design of Experiments.

Main compaction pressure and turret rotation speed were the most important parameters to be optimized during bilayer tablets production. Main compaction had a positive effect on layer adhesion for the combination of brittle materials and turret speed had no significant impact due to the unresponsive nature of brittle materials to strain rate. In contrast, once plastic materials were included in the formulation, the increase of main compaction or rotation speed promoted the delamination tendency. This effect was prominent for excipient combinations with a high difference in elastic recovery. However, plastic-brittle formulation presented a non-linear effect of main compaction on layer adhesion. The excipient combination acted as a brittle-brittle combination at main compaction pressures below 200 MPa and switched to a plastic-brittle behavior at high pressures, where the decrease in layer adhesion was driven by the difference in elastic recovery

Pre-compaction had no significant impact on layer adhesion of the combination with brittle materials due to the consolidation mechanism: independently of the level of pre-compaction, the particle fragmentation caused by the main compaction pressure promoted the formation of new bonding surfaces. In contrast, high pre-compaction levels on the plastic-plastic combination generated a flat surface, which remarkably reduced the layer adhesion.

An increased delamination tendency was promoted by the interaction pre-compaction·main compaction, which was responsible for the formation of a smooth first layer surface and the low adhesion with the second layer. Similarly, the interaction main compaction·rotation presented a negative effect on layer adhesion. At high turret speed, an increase of main compression was expected to improve the layer adhesion. Instead, high pressure and speed conditions, led to tablet

delamination. In contrast, the interaction pre-compaction·rotation presented a positive effect on layer adhesion due to a decrease of strain rate, promoted by a lower powder volume to compact, as the pre-compaction pressure was increased.

To confirm the models obtained from the plastic-plastic and brittle-brittle combinations, two supplementary Design of Experiment were performed, replacing one material with an excipient of similar properties. Despite the different layer adhesion of the tested formulations, caused by the variation of one excipient in the tested formulations, the surfaces of response and the mathematical models were comparable for similar material combinations. The difference in elastic recovery of the excipients present in the two layers of the formulation was the main factor, which determined the layer adhesion value. However, the combination of plastic and brittle excipients in two different layers granted a broader range of optimal tablet manufacturing.

5. Zusammenfassung

Qualität, Sicherheit und Wirksamkeit von Einzel- und Mehrschichttabletten hängt sowohl von der Formulierung als auch von der Optimierung der Herstellungsparameter, wie Pressgeschwindigkeit, Vorkompression und Hauptkompression ab. Bislang wurde der Einfluss dieser Parameter auf die Qualität des Endprodukts intensiv untersucht, aber nur wenige Studien konzentrierten sich auf den Prozess des Füllens der Form, was sich insbesondere bei hohen Rotationsgeschwindigkeiten stark auf die Gleichförmigkeit der Masse auswirkt. Diese Studien wurden an kundenspezifischen Modell-Füllschuh-Systemen durchgeführt, die einen guten Einblick in das Verhalten der Pulver während des Prozesses bieten, aber schwer mit industriellen Prozessparametern korrelieren. Alternativ wurden Untersuchungen zur Formfüllung auf Standard-Rotationspressen durchgeführt, um den Füllprozess bei einem hohen Materialverbrauch nachzubilden.
Bislang wurden Prozessparameter bei der Herstellung von Mehrschichttabletten nur in getrennten Versuchen untersucht. Daher ist der Einfluss von Prozessparameter-Wechselwirkungen auf die Schichtadhäsion noch unbekannt und in nur wenigen Studien wurde der Einfluss von Materialeigenschaften bei der Zweischichttablettierung untersucht.

Um die oben erwähnten Einschränkungen zu überwinden, wurde das Formfüllverhalten von Hilfsstoffen, die üblicherweise beim Tablettieren verwendet werden, durch die Simulation einer industriellen Tablettenpresse auf einem „Compaction Simulator“ untersucht. Die Vollständigkeit der Formfüllung für jedes Material wurde mit den rheologischen Pulvereigenschaften korreliert, um den Effekt der Revolverdrehgeschwindigkeit auf den Füllprozess vorherzusagen.
Darüber hinaus wurde ein generell anwendbarer Versuchsaufbau angewendet, um den Einfluss von Prozessparametern und deren Wechselwirkungen auf die Delaminationsneigung von Zweischichttabletten zu untersuchen. Die Schichthaftung wurde mit einem neuartigen Schertest gemessen, der speziell entwickelt wurde, um die Einschränkungen der verfügbaren Verfahren wie Reibung, elastische Verformung der Testvorrichtung und lange Einrichtungszeiten zu überwinden.

Partikeleigenschaften und Pulverrheologie sind kritische Parameter für den Fluss jedes Materials, da sie den Füllprozess beeinflussen. Daher wurden 9 Hilfsstoffe, die üblicherweise beim Tablettieren verwendet werden (Avicel PH-112, Avicel PH-200, Cellphere CP-102, Emcompress, Flowlac 90, Kollidon SR, Methocel K15M, Starch 1500 und Tablettose 80), ausgewählt und durch den Hausner-Faktor, Restfeuchtigkeit, Partikelform und Größenverteilung charakterisiert und im Vergleich zu rheologischen Eigenschaften, die mit einem Pulverrheometer gemessen wurden, bewertet.

Der Füllprozess der untersuchten Materialien wurde auf einem „Compaction Simulator“ mit Schwerkraft-, Zwangs- und Saugfüllverfahren reproduziert. Gut fließende Hilfsstoffe, wie Emcompress, Cellphere CP-102, Tablettose 80 und Flowlac 90, wiesen aufgrund ihrer optimalen Partikeleigenschaften eine ausgezeichnete Formfüllung auf. Im Gegensatz dazu wurde eine vollständige Formfüllung mit Hilfe der Schwerkraftfülltechnik nur bei niedriger Pressegeschwindigkeit (15 U/min) beobachtet, bei höheren Geschwindigkeiten wurde ein vollständiger Füllprozess nur für Emcompress und Cellphere CP-102 erreicht. Die Verwendung von Zwangs- und Saugfülltechniken verbesserte den Füllprozess aufgrund der starken mechanischen Beanspruchungen, die auf das lose Pulver ausgeübt wurden, was die Bildung von Pulverbrücken verhinderte und die Pulverbewegung in der Zuführeinrichtung verbesserte.
Die Profile der Matrizenfüllung wurden mit einer halblogarithmischen Gleichung beschrieben und die berechneten Steigungen wurden mit Pulverrheologischen-Messungen korreliert. Es wurde eine starke Korrelation mit der Basis-Fließfähigkeitsenergie ($R2 = 0{,}902$) und mit der auf die Probenmasse nicht harmonisierten Energie ($R2 = 0{,}931$) festgestellt, während der Matrizenfüllung mit Schwerkraftfüllung. Aufgrund der starken mechanischen Spannungen, die das Fließverhalten der untersuchten Hilfsstoffe verbesserte, konnte keine signifikante Korrelation bei der erzwungenen- und der Saugfüllung festgestellt werden. Das Modell wurde validiert, indem das Verhalten von Pearlitol 200 SD vorhergesagt und durch experimentelle Werte bestätigt wurde.
Der Hausner-Faktor war nicht geeignet die Fließeigenschaften von Kollidon SR und Pearlitol SD 200 zu beschreiben. Die Werte für diese Hilfsstoffe stimmten nicht mit ihren Formfüllprofilen überein, während die Charakterisierung der rheologischen Eigenschaften das Fließverhalten der Pulver unter Standardbedingungen mit guter Näherung vorhersagen konnte (z.B. Schwerkraftfülltechnik). Diese neuartige Technik bot die Möglichkeit, die Bewertung der Matrizenfüllung und der Verdichtungseigenschaften auf einer einzigen Maschine zu kombinieren. Dies ist ein erster wichtiger Schritt, um eine schnelle und effiziente Formulierung vorherzusagen und diese auf den industriellen Maßstab zu übertragen.

Anschließend wurde ein neuartiger Test zur Messung der Schichtadhäsion an Doppelschichttabletten entwickelt, um Tabletten zu charakterisieren, die mit unterschiedlichen Pressdrücken und Hilfsstoffen hergestellt wurden. Das Gerätedesign wurde durch verschiedene Versionen verbessert, um 4 Testanforderungen zu erfüllen: kurze Einrichtungszeit, Reproduzierbarkeit, Differenzierungsfähigkeit von Tabletten, die mit verschiedenen Hilfsstoffen und Pressdrücken hergestellt wurden. Das Gerät wurde so angepasst, dass es an einem „Compaction Simulator" angebracht werden konnte, der eine geringe elastische Verformung und eine hohe Datenerfassungsgeschwindigkeit sicherstellte.
Die maximale Testgeschwindigkeit (1 mm/s), der Pressdruck, die Hilfsstoffdifferenzierung, die Reproduzierbarkeit und der Einfluss der Tablettenpositionierung wurden umfassend untersucht, um die optimalen Testbedingungen zu definieren. Darüber hinaus wurde der Einfluss von Temperatur, Feuchtigkeit und Lagerzeit auf die Schichtadhäsion sowohl an hygroskopischen als auch an nicht hygroskopischen Hilfsstoffkombinationen erforscht. Lagerzeit und Feuchtigkeit wurden als kritische Parameter für hygroskopische Materialien identifiziert, die sich negativ auf die Schichthaftung auswirkten. Stattdessen zeigten nicht-hygroskopische Hilfsstoffkombinationen eine Verringerung der Schichtadhäsion nur in Abhängigkeit von der Lagerungszeit. Die unterschiedliche Ausdehnung der Schichten aufgrund von Feuchtigkeitseinwirkung wurde als der Grund für die Delaminierung oder verringerte Schichthaftung von Mehrschichttabletten vorgeschlagen. Darüber hinaus wurden 25 ° C und 40% RH als die beste Bedingung zum Lagern von Mehrschichttabletten identifiziert da die Verringerung der Schichtadhäsion während der Langzeitlagerung hier am geringsten war.

Dieser neuartige Test wurde verwendet, um die Auswirkung von Prozessparametern und Materialeigenschaften auf die Schichtadhäsion von Zweischichttabletten zu untersuchen. Drei potentielle pharmazeutische Formulierungen wurden als Kombination von schneller (Emcompress und Avicel PH-112) und verlängerter (Emcompress und Methocel K15M) Arzneimittelfreisetzung ausgewählt. Ein 3-stufiges 3-Faktoren-Design-Experiment wurde an jeder Formulierung durchgeführt, um die Auswirkungen von drei Prozessparametern (Vorkompression, Hauptkompression und Pressegeschwindigkeit) und deren Wechselwirkungen auf die Delaminierung der Tablette zu bewerten. Der für diese Studie entwickelte Schertest wurde verwendet, um die Neigung der Tablette zum Delaminieren zu bestimmen, die Schichtadhäsion wurde als Messparameter in der Versuchsplanung angewendet.
Der Hauptverdichtungsdruck und die Pressegeschwindigkeit waren die wichtigsten Parameter zur Optimierung der Herstellung von Zweischichttabletten. Die Hauptkompression hatte einen positiven Effekt auf die Schichtadhäsion für die Kombination von spröden Materialien und die

Pressgeschwindigkeit hatte keine signifikante Auswirkung aufgrund der nicht ansprechenden Eigenschaften von spröden Materialien gegenüber der Dehnungsrate. Im Gegensatz dazu förderte die Zunahme der Hauptkompression oder der Pressegeschwindigkeit die Delaminierungsneigung, sobald plastische Materialien in die Formulierung eingeschlossen waren. Dieser Effekt war für Hilfsstoffkombinationen mit einem großen Unterschied in der elastischen Entspannung ausschlaggebend. Formulierungen mit spröden und plastischen Hilfsstoffen zeigten jedoch einen nicht-linearen Effekt der Hauptkompression auf die Schichthaftung. Es wurde vermutet, dass die Hilfsstoffkombination bei Hauptpressdrücken unter 200 MPa als spröde-spröde Kombination fungierten und bei hohen Drücken auf ein plastisch-sprödes Verhalten umschalteten, wobei die Abnahme der Schichthaftung durch den Unterschied in der elastischen Entspannung erklärt wurde.

Die Vorkompression hatte aufgrund des Verdichtungsmechanismus keinen wesentlichen Einfluss auf die Schichthaftung der Kombination mit sprödem Material: Unabhängig von der Vorkompression förderte die durch den Hauptverdichtungsdruck verursachte Partikelzerkleinerung die Bildung neuer Haftflächen. Im Gegensatz dazu erzeugten hohe Vorverdichtungspegel auf der plastisch-plastischen-Kombination eine flache Oberfläche, was die Schichthaftung merklich reduzierte.

Eine erhöhte Delaminationsneigung wurde durch die Wechselwirkung Vorkompression-Hauptkompression begünstigt, die für die Ausbildung einer glatten ersten Schichtoberfläche und die geringe Haftung mit der zweiten Schicht verantwortlich war. In ähnlicher Weise wirkte die Hauptkompression-Pressegeschwindigkeit Wechselwirkung negativ auf die Schichthaftung. Bei hoher Pressegeschwindigkeit wurde eine Zunahme der Hauptkompression erwartet, um die Schichthaftung zu verbessern. Stattdessen führten ein hoher Druck und eine hohe Geschwindigkeit zur Delaminierung der Tabletten. Im Gegensatz dazu zeigte die Wechselwirkung Vorkompression-Pressegeschwindigkeit einen positiven Effekt auf die Schichtadhäsion aufgrund einer Abnahme der Verformungsrate, begünstigt durch ein niedrigeres Pulvervolumen zum Verdichten, wenn der Vorverdichtungsdruck erhöht wurde.

Um die aus den plastisch-plastisch- und spröden-spröden-Kombinationen erhaltenen Modelle zu bestätigen, wurden zwei ergänzende Versuchspläne durchgeführt, wobei ein Material durch einen Hilfsstoff mit ähnlichen Eigenschaften ersetzt wurde. Trotz der unterschiedlichen Schichthaftung der getesteten Formulierungen, verursacht durch die Variation eines Hilfsstoffs in den getesteten Formulierungen, waren die Oberflächen des getauschten Hilfsstoffes und des konstanten Hilfsstoffes für ähnliche Materialkombinationen vergleichbar. Der Unterschied in der elastischen Rückstellung der Hilfsstoffe, die in den zwei Schichten der Formulierung vorhanden sind, war

der Hauptfaktor, der den Schichtadhäsionswert bestimmte. Die Kombination von plastischen und spröden Hilfsstoffen in zwei verschiedenen Schichten gewährleistete jedoch eine breitere Palette an optimaler Tablettenherstellung.

6. References

[1] I. Jivraj, L. Martini, C. Thomson, An overview of the different excipients useful for the direct compression of tablets., Pharm. Sci. Technolo. Today. 3 (2000) 58–63. http://www.ncbi.nlm.nih.gov/pubmed/10664574.

[2] I.C. Sinka, K.G. Pitt, Tabletting, in: A.D. Salman, M. Hounslow, J.P.K. Seville (Eds.), Handb. Powder Technol. Granulation, Elsevier, 2006: pp. 735–778.

[3] Y. Qiu, Rational Design of Oral Modified-release Drug Delivery Systems, in: L.L. and W.R.P. Yihong Qiu, Yisheng Chen, Geoff G.Z. Zhang (Ed.), Dev. Solid Oral Dos. Forms Pharm. Theory Pract., Elsevier I, 2009: pp. 469–499.

[4] R. Lewanczuk, S.W. Tobe, More medications, fewer pills: Combination medications for the treatment of hypertension, Can. J. Cardiol. 23 (2007) 573–576.

[5] Food and Drug Administration, FDA Approved Drug Products Database, (2018). https://www.accessdata.fda.gov/scripts/cder/daf/index.cfm (accessed April 18, 2018).

[6] M.H. Rubinstein, Tablets in pharmaceutics: the science of dosage form design, Churchill Livingstone, New York, USA, 1989.

[7] C. Nyström, G. Alderborn, M. Duberg, P.G. Karehill, Bonding surface area and bonding mechanism-two important factors fir the understanding of powder comparability, 1993.

[8] E.. Hiestand, Tablet bond . I . A theoretical model, Int. J. Pharm. 61 (1991) 217–229.

[9] E.N. Hiestand, Principles, tenets and notions of tablet bonding and measurements of strength, Eur. J. Pharm. Biopharm. 44 (1997) 229–242.

[10] M. Stasiak, J. Tomas, M. Molenda, R. Rusinek, P. Mueller, Uniaxial compaction behaviour and elasticity of cohesive powders, Powder Technol. 203 (2010) 482–488.

[11] A. Rankell, T. Higuchi, Physics of Tablet Compression XV: Thermodynamic and Kinetic Aspects of Adhesion Under Pressure, (1968) 574–577.

[12] N.A. Armstrong, R.F. Haines-Nutt, Elastic recovery and surface area changes in compacted powder systems, Powder Technol. 9 (1974) 287–290.

[13] F. Bassam, P. York, R.C. Rowe, R.J. Roberts, Young's modulus of powders used as pharmaceutical excipients, Int. J. Pharm. 64 (1990) 55–60.

[14] N. Rasenack, B.W. Müller, Crystal habit and tableting behavior, Int. J. Pharm. 244 (2002) 45–57.

[15] M. Çelik, Pharmaceutical Powder Compaction Technology, CRC Press, 2016.

[16] F.P. Beer, R. Johnston, J. DeWolf, D. Mazurek, Mechanics of materials, McGraw-Hil, New York, 2012.

[17] A. Nokhodchi, J.L. Ford, P.H. Rowe, M.H. Rubinstein, The effects of compression rate and force on the compaction properties of different viscosity grades of hydroxypropylmethylcellulose 2208, Intenational J. Pharm. 129 (1996) 21–31.

[18] M. Šantl, I. Ilić, F. Vrečer, S. Baumgartner, A compressibility and compactibility study of real tableting mixtures: the effect of granule particle size., Acta Pharm. 62 (2012) 325–40.

[19] B. Van Veen, K.V.D.V. Maarschalk, G.K. Bolhuis, K. Zuurman, H.W. Frijlink, Tensile strength of tablets containing two materials with a different compaction behaviour, Int. J. Pharm. 203 (2000) 71–79.

[20] R.W. Heckel, Density-Pressure Relationships in Powder Compaction, Trans. Metall. Soc. AIME. 221 (1961) 671–675.

[21] S. Jain, Mechanical properties of powders for compaction and tableting: an overview, Pharm. Sci. Technolo. Today. 2 (1999) 20–31.

[22] R.J. Roberts, R.C. Rowe, Mechanical Properties, Pharmaceut, Taylor & Francis, 1995.

[23] M. Asgharnejad, D.E. Storey, Application of a Compaction Simulator to the Design of a High-Dose Tablet Formulation. Part I, Drug Dev. Ind. Pharm. 22 (1996) 967–975.

[24] M. Peleg, Flowability of Food Powders and Methods for Its Evaluation — a Review, J. Food Process Eng. 1 (1977) 303–328.

[25] E. Aulton, K. Taylor, Particle Science and Powder Technology, in: Elsevier Health Sciences (Ed.), Aulton's Pharm. Des. Manuf. Med., 2013: pp. 187–198.

[26] M.P. Mullarney, B.C. Hancock, G.T. Carlson, D.D. Ladipo, B.A. Langdon, The powder

flow and compact mechanical properties of sucrose and three high-intensity sweeteners used in chewable tablets, Int. J. Pharm. 257 (2003) 227–236.

[27] N.-O. Lindberg, M. Pålsson, A.-C. Pihl, R. Freeman, T. Freeman, H. Zetzener, G. Enstad, Flowability measurements of pharmaceutical powder mixtures with poor flow using five different techniques., Drug Dev. Ind. Pharm. 30 (2004) 785–91.

[28] G.E. Amidon, M.E. Houghton, The Effect of Moisture on the Mechanical and Powder Flow Properties of Microcrystalline Cellulose, Pharm. Res. An Off. J. Am. Assoc. Pharm. Sci. 12 (1995) 923–929.

[29] Q. Li, V. Rudolph, B. Weigl, A. Earl, Interparticle van der Waals force in powder flowability and compactibility., Int. J. Pharm. 280 (2004) 77–93.

[30] G. Gold, R.N. Duvall, B.T. Palermo, J.G. Slater, Powder flow studies II. Effect of glidants on flow rate and angle of repose, J. Pharm. Sci. 55 (1966) 1291–1295.

[31] H.H. Hausner, Friction conditions in a mass of metal powder, Int. J. Powder Metall. 3 (1967) 7–13.

[32] A.W. Jenike, Storage and flow of solids, Bull. No. 123, Utah State Univ. (1964).

[33] R. Freeman, Measuring the flow properties of consolidated, conditioned and aerated powders — A comparative study using a powder rheometer and a rotational shear cell, Powder Technol. 174 (2007) 25–33.

[34] K. Thalberg, D. Lindholm, A. Axelsson, Comparison of different flowability tests for powders for inhalation, Powder Technol. 146 (2004) 206–213.

[35] F. Lavoie, L. Cartilier, R. Thibert, New methods characterizing avalanche behavior to determine powder flow, Pharm. Res. 19 (2002) 887–893.

[36] Y.S. Lee, R. Poynter, F. Podczeck, J.M. Newton, Development of a dual approach to assess powder flow from avalanching behavior., AAPS PharmSciTech. 1 (2000) E21.

[37] Y. Yaginuma, Y. Ozeki, M. Kakizawa, S.I. Gomi, Y. Watanabe, Effects of powder flowability on die-fill properties in rotary compression, J. Drug Deliv. Sci. Technol. 17 (2007) 205–210.

[38] M. Levin, Tablet Press Instrumentation, Encycl. Pharm. Technol. (2002) 1–26.

[39] Fette GmbH, 3200i Brochure, (2018).

[40] Korsch AG, XL800 Brochure, (2018).

[41] X. Xie, V.M. Puri, Uniformity of powder die filling using a feed shoe: A review, Part. Sci. Technol. 24 (2006) 411–426.

[42] S. Jackson, I.C. Sinka, A.C.F. Cocks, The effect of suction during die fill on a rotary tablet press, Eur. J. Pharm. Biopharm. 65 (2007) 253–256.

[43] A.S. Narang, V.M. Rao, H. Guo, J. Lu, D.S. Desai, Effect of force feeder on tablet strength during compression, Int. J. Pharm. 401 (2010) 7–15.

[44] R. Mendez, F. Muzzio, C. Velazquez, Study of the effects of feed frames on powder blend properties during the filling of tablet press dies, Powder Technol. 200 (2010) 105–116.

[45] L.C.R. Schneider, I.C. Sinka, A.C.F. Cocks, Characterisation of the flow behaviour of pharmaceutical powders using a model die-shoe filling system, Powder Technol. 173 (2007) 59–71.

[46] G.F. Palmieri, E. Joiris, G. Bonacucina, M. Cespi, A. Mercuri, Differences between eccentric and rotary tablet machines in the evaluation of powder densification behaviour, Int. J. Pharm. 298 (2005) 164–175.

[47] S.P. Li, M.G. Karth, K.M. Feld, L.C. Di Paolo, C.M. Pendharkad, R. Williams, Evaluation of Bilayer Tablet Machines - A Case Study, Drug Dev. Ind. Pharm. 21 (1995) 571–590.

[48] L. Benkerrour, O. Galley, F. Quinet, A. Abebe, P. Timmins, Multilayered tablet containing Prevastatin and Aspirin and method. US 2004/0115265 A1, 2004.

[49] S.R. Vaithiyalingam, V.A. Sayeed, Critical factors in manufacturing multilayer tablets-assessing material attributes, in-process controls, manufacturing process and product performance., Int. J. Pharm. 398 (2010) 9–13. doi:10.1016/j.ijpharm.2010.07.025.

[50] C. LaForce, D.A. Gentile, D.P. Skoner, A randomized, double-blind, parallel-group, multicenter, placebo-controlled study of the safety and efficacy of extended-release guaifenesin/ pseudoephedrine hydrochloride for symptom relief as an adjunctive therapy to antibiotic treatment of acute respir, Postgrad. Med. 120 (2008) 53–59.

[51] M. Ruzicka, F.H.H. Leenen, Monotherapy versus combination therapy as first line treatment of uncomplicated arterial hypertension, Drugs. 61 (2001) 943–954.

[52] Zerbe H.G., M. Krumme, Smartrix; Design characteristics and release properties of a novel erosion-controlled oral delivery system, CRC Press, 2002.

[53] J. Nirmal, S. Saisivam, C. Peddanna, S. Muralidharan, S. Godwinkumar, M. Nagarajan, Bilayer tablets of atorvastatin calcium and nicotinic acid: formulation and evaluation., Chem. Pharm. Bull. (Tokyo). 56 (2008) 1455–1458.

[54] B. Shiyani, S. Gattani, S. Surana, Formulation and evaluation of bi-layer tablet of metoclopramide hydrochloride and ibuprofen., AAPS PharmSciTech. 9 (2008) 818–827.

[55] S. Abdul, S.S. Poddar, A flexible technology for modified release of drugs: multi layered tablets., J. Control. Release. 97 (2004) 393–405.

[56] R.K. Verma, S. Garg, Current Status of Drug Delivery Technologies and Future Directions, Pharm. Technol. 25 (2001) 1–14.

[57] I. Akseli, D. Dey, C. Cetinkaya, Mechanical property characterization of bilayered tablets using nondestructive air-coupled acoustics., AAPS PharmSciTech. 11 (2010) 90–102.

[58] N. Kottala, A. Abebe, O. Sprockel, J. Bergum, F. Nikfar, A.M. Cuitiño, Evaluation of the performance characteristics of bilayer tablets: Part I. Impact of material properties and process parameters on the strength of bilayer tablets., AAPS PharmSciTech. 13 (2012) 1236–42.

[59] P.G. Karehill, M. Glazer, C. Nystrom, Studies on direct compression of tablets. XXIII. The importance of surface roughness for the compactability of some directly compressible materials with different bonding and volume reduction properties, Int. J. Pharm. 64 (1990) 35–43.

[60] S.J. Inman, B.J. Briscoe, K.G. Pitt, Topographic Characterization of Cellulose Bilayered Tablets Interfaces, Chem. Eng. Res. Des. 85 (2007) 1005–1012.

[61] A. Abebe, I. Akseli, O. Sprockel, N. Kottala, A.M. Cuitiño, Review of bilayer tablet technology., Int. J. Pharm. 461 (2013) 549–58.

[62] H. Diarra, V. Mazel, V. Busignies, P. Tchoreloff, Investigating the effect of tablet thickness and punch curvature on density distribution using finite elements method, Int. J. Pharm. 493 (2015) 121–128.

[63] C.-Y. Wu, J.P.K. Seville, A comparative study of compaction properties of binary and bilayer tablets, Powder Technol. 189 (2009) 285–294.

[64] F. Podczeck, Theoretical and experimental investigations into the delamination tendencies of bilayer tablets., Int. J. Pharm. 408 (2011) 102–12.

[65] R. Cazes, A QbD Approach to Shorten Tablet Development Time, Pharm. Technol. Solid Dos. Drug Dev. Manuf. Suppl. 42 (2018) 16–20.

[66] I. Akseli, S. Iyer, H.P. Lee, A.M. Cuitiño, A Quantitative Correlation of the Effect of Density Distributions in Roller-Compacted Ribbons on the Mechanical Properties of Tablets Using Ultrasonics and X-ray Tomography, AAPS PharmSciTech. 12 (2011) 834–853.

[67] I. Akseli, N. Ladyzhynsky, J. Katz, X. He, Development of predictive tools to assess capping tendency of tablet formulations, Powder Technol. 236 (2013) 139–148.

[68] V. Mazel, V. Busignies, H. Diarra, P. Tchoreloff, Lamination of pharmaceutical tablets due to air entrapment: Direct visualization and influence of the compact thickness, Int. J. Pharm. 478 (2015) 702–704.

[69] J.S.M. Garr, M.H. Rubinstein, An investigation into the capping of paracetamol at increasing speeds of compression, Int. J. Pharm. 72 (1991) 117–122.

[70] T. Higuchi, A.N. R, W. Busse, J. Swintosky, Physics of tablet compression. II The Influence of Degree of Compression on Properties of Tablets, J. Am. Pharm. Assoc. 42 (1953) 194–200.

[71] S.T. David, L.L. Augsburger, Plastic flow during compression of directly compressible fillers and its effect on tablet strength., J. Pharm. Sci. 66 (1977) 155–159.

[72] R. Ishino, H. Yoshino, Y. Hirakawa, K. Noda, Influence of tabletting speed on compactibility and compressibility of two direct compressible powders under high speed compression., Chem. Pharm. Bull. (Tokyo). 38 (1990) 1987–1992.

[73] A.R. Fassihi, I. Kanfer, Effect of compressibility and powder flow properties on tablet weight variation, Drug Dev. Ind. Pharm. 12 (1986) 1947–1966.

[74] C.Y. Wu, L. Dihoru, A.C.F. Cocks, The flow of powder into simple and stepped dies, Powder Technol. 134 (2003) 24–39.

[75] M. Çelik, K. Marshall, Use of a compaction simulator system in tabletting research, Drug Dev. Ind. Pharm. 15 (1989) 759–800.

[76] S.J. Inman, B.J. Briscoe, K.G. Pitt, C. Shiu, The non-uniformity of microcrystalline cellulose bilayer tablets, Powder Technol. 188 (2009) 283–294.

[77] N. Kottala, A. Abebe, O. Sprockel, I. Akseli, F. Nikfar, A.M. Cuitiño, Influence of

compaction properties and interfacial topography on the performance of bilayer tablets., Int. J. Pharm. 436 (2012) 171–8.

[78] C.K. Tye, C.C. Sun, G.E. Amidon, Evaluation of the effects of tableting speed on the relationships between compaction pressure, tablet tensile strength, and tablet solid fraction., J. Pharm. Sci. 94 (2005) 465–72.

[79] I. Akseli, A. Abebe, O. Sprockel, A. Cuitiño, Mechanistic characterization of bilayer tablet formulations, Powder Technol. 236 (2013) 30–36.

[80] A. Abebe, J.D. Petty, J.N. Huckins, A. David, Patent Application Publication US 2002/0187020 A1, 2012.

[81] B. Eiliazadeh, B.J. Briscoe, Y. Sheng, K. Pitt, Investigating Density Distributions for Tablets of Different Geometry During the Compaction of Pharmaceuticals, Part. Sci. Technol. 21 (2003) 303–316.

[82] I.C. Sinka, F. Motazedian, A.C.F. Cocks, K.G. Pitt, The effect of processing parameters on pharmaceutical tablet properties, Powder Technol. 189 (2009) 276–284.

[83] S.Y. Chang, J. xin Li, C.C. Sun, Tensile and shear methods for measuring strength of bilayer tablets, Int. J. Pharm. 523 (2017) 121–126.

[84] P. Dietrich, a Bauer-Brandl, R. Schubert, Influence of tableting forces and lubricant concentration on the adhesion strength in complex layer tablets., Drug Dev. Ind. Pharm. 26 (2000) 745–754.

[85] G. Klinzing, A. Zavaliangos, Understanding the effect of environmental history on bilayer tablet interfacial shear strength., Pharm. Res. 30 (2013) 1300–10.

[86] V. Busignies, V. Mazel, H. Diarra, P. Tchoreloff, Development of a new test for the easy characterization of the adhesion at the interface of bilayer tablets: Proof-of-concept study by experimental design, Int. J. Pharm. 477 (2014) 476–484.

[87] F. Podczeck, E. Al-Muti, The tensile strength of bilayered tablets made from different grades of microcrystalline cellulose., Eur. J. Pharm. Sci. 41 (2010) 483–8.

[88] V. Busignies, V. Mazel, H. Diarra, P. Tchoreloff, Role of the elasticity of pharmaceutical materials on the interfacial mechanical strength of bilayer tablets., Int. J. Pharm. 457 (2013) 260–7.

[89] M. Niwa, Y. Hiraishi, N. Iwasaki, K. Terada, Quantitative analysis of the layer separation

risk in bilayer tablets using terahertz pulsed imaging, Int. J. Pharm. 452 (2013) 249–256.

[90] S. Wang, X.C. Zhang, Pulsed terahertz tomography, J. Phys. D. Appl. Phys. 37 (2004).

[91] J.A. Zeitler, L.F. Gladden, In-vitro tomography and non-destructive imaging at depth of pharmaceutical solid dosage forms, Eur. J. Pharm. Biopharm. 71 (2009) 2–22.

[92] V. Busignies, B. Leclerc, P. Porion, P. Evesque, G. Couarraze, P. Tchoreloff, Investigation and modelling approach of the mechanical properties of compacts made with binary mixtures of pharmaceutical excipients, Eur. J. Pharm. Biopharm. 64 (2006) 51–65.

[93] I.C. Sinka, K.G. Pitt, A.C.F. Cocks, The strength of pharmaceutical tablets, in: A.D. Salman, M. Ghadiri, M. Hounslow (Eds.), Handb. Powder Technol. Part. Break., Elsevier, 2007: pp. 941–970.

[94] E.G. Rippie, D.W. Danielson, Viscoelastic stress/strain behavior of pharmaceutical tablets: analysis during unloading and postcompression periods., J. Pharm. Sci. 70 (1980) 476–82.

[95] L. Yang, G. Venkatesh, R. Fassihi, Characterization of compressibility and compactibility of poly(ethylene oxide) polymers for modified release application by compaction simulator., J. Pharm. Sci. 85 (1996) 1085–90.

[96] M. Celik, K. Marshall, S. Kline, F. Laboratories, K. Prussia, Use of a compaction simulator system in tableting research, Drug Dev. Ind. Pharm. 5 (1989) 759–800.

[97] SKF, Hydraulic cylinders, (2017). http://www.skf.com/it/products/seals/industrial-seals/hydraulic-seals/general-technical-information/introduction-to-fluid-power/hydraulic-cylinders/index.html (accessed April 4, 2018).

[98] D. Collins, Roller screw actuators: Design and applications, (2017). https://www.linearmotiontips.com/roller-screw-actuators-design-and-applications/ (accessed April 4, 2018).

[99] Council of Europe, Bulk density and tapped density of powders, in: Eur. Pharmacopoeia, 8th Ed., 2013: pp. 343–346.

[100] R. Freeman, X. Fu, Characterisation of powder bulk, dynamic flow and shear properties in relation to die filling, Powder Metall. 51 (2008) 196–201.

[101] C. Hare, U. Zafar, M. Ghadiri, T. Freeman, J. Clayton, M.J. Murtagh, Analysis of the dynamics of the FT4 powder rheometer, Powder Technol. 285 (2015) 123–127.

[102] M. Leturia, M. Benali, S. Lagarde, I. Ronga, K. Saleh, Characterization of flow properties of cohesive powders: A comparative study of traditional and new testing methods, Powder Technol. 253 (2014) 406–423.

[103] P. Paronen, Heckel plots as indicators of elastic properties of pharmaceuticals, Drug Dev. Ind. Pharm. 12 (1986) 1903–1912.

[104] J.S.M. Garr, M.H. Rubinstein, Direct Compression Characteristics of Vitamin-a-Acetate, Drug Dev. Ind. Pharm. 18 (1990) 1111–1116.

[105] J. Goole, K. Amighi, 3D printing in pharmaceutics: A new tool for designing customized drug delivery systems, Int. J. Pharm. 499 (2016) 376–394.

[106] W.R. Vezin, H.M. Pang, K.A.K.& S. Malkowska, The effect of precompression in a rotary machine on tablet strength, Drug Dev. Ind. Pharm. 9 (1983) 1465–1474.

[107] C.-Y. Wu, a.C.F. Cocks, a. C.F. Cocks, Flow behaviour of powders during die filling, Powder Metall. 47 (2004) 127–136.

[108] F. Podczeck, Y. Miah, The influence of particle size and shape on the angle of internal friction and the flow factor of unlubricated and lubricated powders, Int. J. Pharm. 144 (1996) 187–194.

[109] R.P. Zou, A.B. Yu, Evaluation of the packing characteristics of mono-sized non-spherical particles, Powder Technol. 88 (1996) 71–79.

[110] E. Abdullah, D. Geldart, The use of bulk density measurments as a flowability indicators, Powder Technol. 102 (1999) 151–165.

[111] D. Geldart, E.C. Abdullah, A. Hassanpour, L.C. Nwoke, I. Wouters, Characterization of powder flowability using measurement of angle of repose, China Particuology. 4 (2006) 104–107.

[112] N. Kottala, A. Abebe, O. Sprockel, I. Akseli, F. Nikfar, A.M. Cuitiño, Characterization of interfacial strength of layered powder compacted solids, Powder Technol. 239 (2013) 300–307.

[113] J.C. Callahan, G.W. Cleary, M. Elefant, G. Kaplan, T. Kensler, R.A. Nash, Equilibrium moisture content of pharmaceutical excipients, Drug Dev. Ind. Pharm. 8 (1982) 355–369.

[114] C.C. Sun, Mechanism of moisture induced variations in true density and compaction properties of microcrystalline cellulose, Int. J. Pharm. 346 (2008) 93–101.

[115] Y. Okuda, Y. Irisawa, K. Okimoto, T. Osawa, S. Yamashita, Further improvement of orally disintegrating tablets using micronized ethylcellulose, Int. J. Pharm. 423 (2012) 351–359.

[116] K. Nidhi, S. Indrajeet, M. Khushboo, K. Gauri, D.J. Sen, Hydrotropy: A promising tool for solubility enhancement: A review, Int. J. Drug Dev. Res. 3 (2011) 26–33.

[117] M.S. Anuar, B.J. Briscoe, Interfacial elastic relaxation during the ejection of bilayered tablets., Int. J. Pharm. 387 (2010) 42–7.

[118] F. Podczeck, K.R. Drake, J.M. Newton, I. Haririan, The strength of bilayered tablets., Eur. J. Pharm. Sci. 29 (2006) 361–6.

[119] H. Mohammed, B.J. Briscoe, K.G. Pitt, The interrelationship between the compaction behaviour and the mechanical strength of pure pharmaceutical tablets, Chem. Eng. Sci. 60 (2005) 3941–3947.

[120] S.T. David, L.L. Augsburger, Flexure test for determination of tablet tensile strength, J. Pharm. Sci. 63 (1974) 933–936.

[121] J.M. Katz, I.S. Buckner, Characterization of strain rate sensitivity in pharmaceutical materials using indentation creep analysis, Int. J. Pharm. 442 (2013) 13–19.

[122] R.J. Roberts, R.C. Rowe, Brittle/ductile behaviour in pharmaceutical materials used in tabletting, Int. J. Pharm. 36 (1987) 205–209.

[123] N. Armstrong, Time-dependent factors involved in powder compression and tablet manufacture, Int. J. Pharm. 49 (1989) 1–13.

7. List of publications and presentations resulting from this work

Bellini, M., Bodmeier, R. Evaluation of manufacturing process parameters causing multilayer tablets delamination. *Under submission.*

Bellini, M., Bodmeier, R. Establishment of a new model to predict die filling on a compaction simulator through powder rheological properties. *Under submission.*

Bellini, M., "Manufacturing process parameters leading to bilayer tablet failure", *Compaction Simulation Forum 2017*, Ghent (Belgium), 20 June 2017

Bellini, M., "Evaluation of bilayer tablets interfacial adhesion via shear stress test", *Compaction Simulation Forum 2016*, Boston (MA), 22 June 2016

Bellini, M., "Prediction of die filling at different turret rotation speed", Poster T1087 *AAPS Annual Meeting and Exposition,* San Diego (CA), 14-19 November 2017

Bellini, M., Bodmeier, R. Poster Evaluation of bilayer tablets interfacial adhesion via shear stress test. Poster *Compaction Simulation Forum 2016*, Boston (MA), 21-22 June 2016

8. Curriculum vitae

For reasons of data protection, the curriculum vitae is not published in the electronic version.